

University of Mississippi

eGrove

---

Electronic Theses and Dissertations

Graduate School

---

1-1-2019

## Magnetic amphiphiles and their potential applications for low energy separations processes

Alexander Fortenberry

Follow this and additional works at: <https://egrove.olemiss.edu/etd>



Part of the [Chemical Engineering Commons](#)

---

### Recommended Citation

Fortenberry, Alexander, "Magnetic amphiphiles and their potential applications for low energy separations processes" (2019). *Electronic Theses and Dissertations*. 1735.

<https://egrove.olemiss.edu/etd/1735>

This Thesis is brought to you for free and open access by the Graduate School at eGrove. It has been accepted for inclusion in Electronic Theses and Dissertations by an authorized administrator of eGrove. For more information, please contact [egrove@olemiss.edu](mailto:egrove@olemiss.edu).

MAGNETIC AMPHIPHILES  
AND THEIR POTENTIAL APPLICATIONS FOR LOW  
ENERGY SEPARATIONS PROCESSES

A Thesis

Presented for the Degree of  
Master of Science in Engineering Science  
Department of Chemical Engineering  
The University of Mississippi

Alex Fortenberry

August 2019

Copyright © 2019 by Alex Fortenberry

All rights reserved

## ABSTRACT

To address the growing energy demands of our society, we investigated magnetic surfactants and their potential application to low energy separations processes. The research described in this work details our investigation of the stability of unimeric magnetic surfactants in aqueous solution and our investigation of magnetically enhancing the solubilization capacity of magnetic amphiphilic polymers for low energy separations processes. We believe that this work is critical to the growing body of research that involves magnetic amphiphiles.

Predicting the behavior of magnetic surfactants in magnetic fields is critical for designing magnetically driven processes such as chemical separations or the tuning of surface tensions. Our work supports the hypothesis that the ability of magnetic fields to alter the interfacial properties of magnetic surfactant solutions depends on the strength of association between the magnetic and surfactant moieties of the surfactant molecules. Our research shows that the stability of a magnetic surfactant in an aqueous environment is dependent upon the type of complex that contains the paramagnetic element, and these findings provide valuable insight for the design of magnetic surfactants for applications in aqueous media. The surfactants investigated were ionic surfactants, which contained paramagnetic counterions. This investigation looked at both anionic and cationic surfactants and utilized solution conductivity, cyclic voltammetry (CV), sampled current voltammetry (SCV), and solution pH measurements to qualitatively evaluate the stability of the magnetic counterions in aqueous solution. In addition, solution conductivity was used to quantify the degree of binding between the paramagnetic ions and surfactant micelles in solution.

These results indicate metal halide-based cationic surfactants are unstable in aqueous solutions. We hypothesize that this instability results in the difference in the magnetic response of anionic vs. cationic surfactants examined in this study.

To our knowledge, increasing the solubilization capacity of magnetically responsive amphiphiles by exposing them to parallel magnetic fields has not been investigated before. If this were possible, it could be exploited in the design of a low energy separation process. Herein, we report the synthesis of two kinds of magnetic polymeric amphiphiles which form micelles in water, and we investigated their relative solubilization capacities in aqueous solutions inside and outside of parallel magnetic fields for three organic contaminants. The organic contaminants were: toluene, naphthalene and anthracene. We utilized UV-VIS spectroscopy as our method of detection of the relative concentrations of the contaminants. We did not detect an increase in the solubilization capacity of the polymers for toluene or anthracene when they were placed inside of a parallel magnetic field, although our results indicated that the solubilization capacity of the polymers for naphthalene increases when the samples are exposed to a parallel magnetic field of approx. 0.6 Tesla.

Using our results, we speculate about the future design of magnetic amphiphiles and we believe that our work contributes to the growing body of research in this field.

## LIST OF ABBREVIATIONS

CMC	Critical Micelle Concentration
UV-VIS	Ultraviolet-visible
SCV	Sampled Current Voltammetry
DLS	Dynamic Light Scattering

## ACKNOWLEDGEMENTS

I would like to thank my committee members; Dr. Adam Smith, Dr. Paul Scovazzo and Dr. John O'Haver for their help and support during the course of my research.

I would also like to thank the NSF, Award CBET 1605894 for making this research possible.

## TABLE OF CONTENTS

ABSTRACT.....	ii
LIST OF ABBREVIATIONS.....	iv
ACKNOWLEDGEMENTS.....	v
LIST OF TABLES.....	ix
LIST OF FIGURES.....	x
CHAPTER I.....	1
1. Motivation and Background.....	1
1.1 Project Background and Overview.....	1
1.2 Magnetic Unimeric Surfactants.....	2
1.3 Magnetic Polymeric Surfactants.....	3
CHAPTER II.....	5
2 Literature Review.....	5
2.1 Introduction to Surfactants.....	5
2.2 Stimuli-Responsive Surfactants.....	10
CHAPTER III.....	23
3 Stability of Magnetic Surfactants in Aqueous Solutions: Measurement Techniques and Impact on Magnetic Processes.....	23
3.1 Abstract.....	23



3.2	Introduction .....	24
3.3	Methods and Materials .....	25
3.4	Results and Discussion .....	29
3.5	Conclusions .....	42
CHAPTER IV .....		44
4	The Investigation of Various Other Magnetic Surfactants .....	44
4.1	Introduction .....	44
4.2	Methods and Materials .....	44
4.3	Results and Discussion .....	46
CHAPTER V .....		50
5	Magnetic Polymer Solubilization Experiments .....	50
5.1	Introduction .....	50
5.2	Experimental/Methodology .....	51
5.3	Results and Discussion .....	54
5.4	Conclusion and Outlook .....	62
CHAPTER VI .....		63
6	Looking to the Future .....	63
6.1	Magnetic Unimeric Surfactants .....	63
6.2	Magnetic Polymeric Surfactants .....	64
LIST OF REFERENCES .....		68

LIST OF APPENDICES.....75

## LIST OF TABLES

Table 2.1: Typical Type I Magnetic Surfactants .....	15
Table 2.2: Properties of some Type I magnetic cationic surfactants at 25°C .....	17
Table 3.1: CMC and Degree of Counterion Binding Data for MnDDS and C <sub>16</sub> TABr.....	32
Table 3.2: The half wave potentials of Fe <sup>3+</sup> ions in solution obtained from the SCV results.....	37
Table 3.3: The approximate pH values of an aqueous solution of C <sub>16</sub> TAF <sub>3</sub> Br as well as FeCl <sub>3</sub> and C <sub>16</sub> TABr for comparison.....	42
Table 4.1: Failed Redoxable Magnetic Surfactants .....	47
Table 4.2: Failed Type I magnetic anionic surfactants .....	48
Table 4.3: Type IIa Surfactants.....	49
Table 5.1: The wavelengths of the baseline and organic contaminant absorbances for MagPolySurfA and MagPolySurfB .....	53
Table 5.2: MagPolySurfA Toluene Solubilization Results.....	57
Table 5.3: MagPolySurfB Toluene Solubilization Results.....	57
Table 5.4: MagPolySurfA Naphthalene Solubilization Results .....	59
Table 5.5: MagPolySurfB Naphthalene Solubilization Results.....	59
Table 5.6: MagPolySurfA Anthracene Solubilization Results .....	61
Table 5.7: MagPolySurfB Anthracene Solubilization Results .....	62

## LIST OF FIGURES

Figure 1.1: Organic contaminant capture and removal.....	2
Figure 1.2: A hypothetical magnetically driven separations process involving a magnetic polymeric surfactant.....	4
Figure 2.1: Cetyltrimethylammonium Bromide (C16TABr).....	6
Figure 2.2: A surfactant being added to water with increasing surfactant concentration from left to right.....	7
Figure 2.3: A generic drawing of an ionic micelle. The hydrocarbon tails comprise the core of the micelle.....	8
Figure 2.4: An oil-in-water emulsion stabilized by surfactants.....	9
Figure 2.5: An amphiphilic block copolymer.....	10
Figure 2.6: A cationic redoxable surfactant unimer undergoing a redox reaction.....	12
Figure 2.7: The reversible formation and disruption of micelles formed from a redoxable surfactant.....	12
Figure 2.8: Different types of magnetic surfactants.....	13
Figure 2.9: A type IIa surfactant example: DyC <sub>10</sub> DOTA.....	20
Figure 2.10: A depiction of C <sub>n</sub> DOTA coordinated to a divalent metal (M <sup>2+</sup> ).....	21
Figure 3.1: The magnetic surfactants investigated. ....	25
Figure 3.2: Emulsions formed from magnetic surfactants.....	30
Figure 3.3: Specific conductivity vs. reduced concentration measurements of MnDDS and C16TABr in deionized water.....	33

Figure 3.5: [C <sub>16</sub> TA] <sub>2</sub> CoCl <sub>2</sub> Br <sub>2</sub> . In its' solid form (a) and when it is mixed with water (b). .....	35
Figure 3.6: The results of the sampled current voltammetry (SCV) experiments with FeCl <sub>3</sub> / LiCl solutions. ....	37
Figure 3.7: Specific conductivity vs. concentration of aqueous iron(III) trichloride solutions at constant concentration as sodium acetate is added. ....	38
Figure 3.8: Specific conductivity vs. C <sub>14</sub> TABr concentration for three constant solution concentrations of aqueous iron(III) trichloride. ....	39
Figure 3.9: Specific conductivity vs. C <sub>14</sub> TABr concentration for three constant solution concentrations of aqueous gadolinium(III) trichloride. ....	39
Figure 3.10: The specific conductivity of C <sub>16</sub> TAF <sub>2</sub> FeCl <sub>3</sub> Br, C <sub>16</sub> TABr + 2 molar equivalents of NaCl, and C <sub>16</sub> TABr in aqueous solution.....	41
Figure 4.1: A magnetic redoxable surfactant.....	46
Figure 5.1: The magnetic polymers used in the solubilization experiments.....	52
Figure 5.2: The organic contaminants used in the polymer solubilization experiments. ....	53
Figure 5.3: The UV-Vis absorbance spectrum of MagPolySurfA in water.....	55
Figure 5.4: The UV-Vis absorbance spectrum of MagPolySurfB in water.....	55
Figure 5.5: The UV-Vis absorbance spectrum of water saturated with toluene.....	56
Figure 5.6: The UV-Vis absorbance spectrum of MagPolySurfA samples in water saturated with toluene.....	56
Figure 5.7: The UV-Vis absorbance spectrum of MagPolySurfB samples in water saturated with toluene.....	56

Figure 5.8: The UV-Vis absorbance spectrum of water saturated with naphthalene .....	58
Figure 5.9: The UV-Vis absorbance spectrum of MagPolySurfA samples in water saturated with naphthalene. ....	58
Figure 5.10: The UV-Vis absorbance spectrum of MagPolySurfB samples in water saturated with naphthalene. ....	58
Figure 5.11: The absorbance spectrum of anthracene saturated water (blue line) and MagPolySurfA in water saturated with anthracene (red line) .....	60
Figure 5.12: The UV-Vis absorbance spectrum of MagPolySurfA samples in water saturated with anthracene. ....	60
Figure 5.13: The UV-Vis absorbance spectrum of MagPolySurfB samples in water saturated with anthracene. ....	61
Figure 6.1: A divalent metal coordinated to EDTA forming an anionic complex. ....	64
Figure 6.2: (Top) Water contaminated with organic molecules enters on the shell side of the membrane and partitions into the polymer composite contained inside of the tubes. (Bottom) When the magnets are removed, the super saturated polymer composite spits the organic contaminants out. ....	66

## CHAPTER I

### 1. Motivation and Background

#### 1.1 Project Background and Overview

Due to the growing energy demands in our economy, there is high demand for low energy separations processes [1]. As the primary investigator (PI) of this research project calculated, a magnetically driven separation process utilizing a “magnetic swing” versus a conventional “pressure swing” or “temperature swing” could result in dramatic energy savings and in certain instances utilizing as little as 2% of an alternative thermally driven separation process. Our overall research goal is devoted to utilizing the unique properties of magnetic amphiphiles to develop such a process. Since approx. 15% of the global energy demand is for separation processes [2], society will benefit greatly from separations processes that result in dramatic energy savings.

Magnetic amphiphiles, otherwise known as magnetic surfactants, are magnetic on the molecular level. This is in contrast to standard paramagnetic solutions, which contain suspensions of nanometer to micrometer sized magnets. Since magnetic surfactants form micelles in aqueous solution like ordinary surfactants, we set out to investigate if we could magnetically control the mass transfer of hydrophobic contaminants into the micelles and/ or remove the compounds from aqueous feed solution.

This manuscript is not intended to be a comprehensive review of all of the work involved in this project, but instead will describe work related to specific areas of the project. It will discuss some of our work involved in the development and characterization of some of the magnetic amphiphiles, in addition our work that investigated the magnetically-driven organic contaminant solubilization into micelles formed from magnetic polymeric amphiphiles.

## 1.2 Magnetic Unimeric Surfactants

One of the topics covered in this work involves the development of single-molecule magnetic amphiphiles. This is important in the larger context of the project since it will allow for the determination of if contaminant filled micelles formed from these materials can be attracted to a magnet and removed from solution as depicted in Figure 1.1.

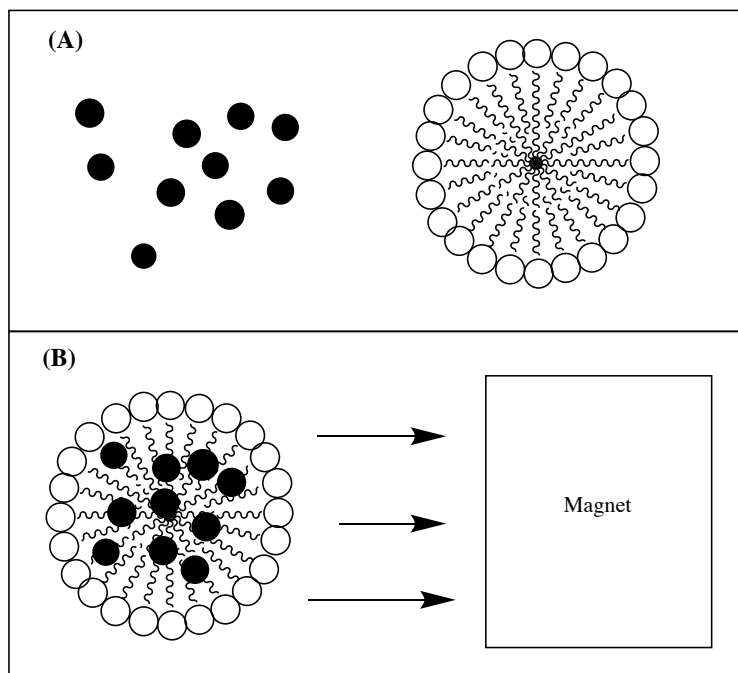


Figure 1.1: Organic contaminant capture and removal. (A) An organic contaminant in water being solubilized in a micelle. (B) The contaminant filled micelle migrating to an external magnet.



We investigated a range of magnetic surfactants for their suitability for such a separation process by examining existing magnetic surfactants found in the literature, as well as novel magnetic surfactants which we synthesized. We investigated magnetic surfactants that were cationic or anionic. We intended to synthesize a variety of magnetic surfactants to expand the existing catalog of magnetic surfactants and to apply unique types to specific separations processes. The current work investigated the solubility and stability in aqueous solution of these compounds. The information gained from these studies is intended to guide future work in utilizing these materials for magnetically driven separations.

One special class of surfactants we investigated possessed a redoxable moiety that has been demonstrated to allow the formed micelles to be electrochemically broken and re-formed [3]. By adding a magnetic moiety to such a surfactant, they can be envisioned to act as carriers for organic contaminants in aqueous solution that could migrate to a magnetic surface and then be destroyed in a controllable manner upon oxidation to release the contaminants. Following the recovery of the contaminants, the micelles could then be re-formed via reduction, and then the magnetism turned off allowing the surfactants to migrate back to the bulk solution to recover more contaminants and the process repeated. Figure 1.2 depicts this hypothetical process.

### 1.3 Magnetic Polymeric Surfactants

The other main topic covered in this work examined the synthesis of polymeric magnetic surfactants and their performance in achieving magnetically-enhanced solubilization of organic contaminants. The synthesis of these magnetic polymers was informed from the synthesis of the single molecule magnetic surfactants.

In his modeling, Zubarev [4] showed that passing an organic phase with imbedded magnetic centers through a magnetic field will alter its molar volume and thus potentially

increase the free volume of the organic phase. If this occurs with a magnetic polymeric surfactant, it could theoretically allow for a larger solubilization capacity of the surfactant while inside of a magnetic field. This could be exploited for designing a magnetically driven separation device that would separate a mixture of components that differ in their capacity to be solubilized in the micelles as depicted in Figure 1.2. In this work, our intention was only to perform preliminary investigations into the possibility of “magnetically tuning” solubilization capacity of these compounds.

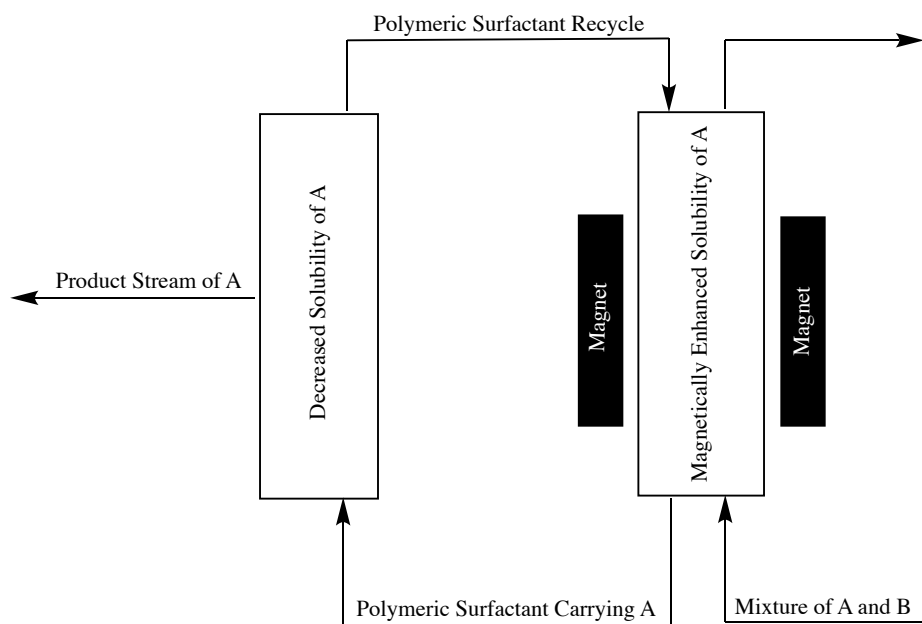


Figure 1.2: A hypothetical magnetically driven separations process involving a magnetic polymeric surfactant.

## CHAPTER II

### 2 Literature Review

#### 2.1 Introduction to Surfactants

Surfactants, a contraction of the phrase “surface active agents”, are organic compounds with amphiphilic properties, which means that they possess both lyophilic (solvent loving) and lyophobic (solvent hating) groups. Hence surfactants exhibit a tendency to migrate to interfaces while in solution and form aggregates called micelles above a certain concentration called the critical micelle concentration (CMC). This tendency to transition to interfaces and form micelles is entropically driven and caused by the amphiphilic nature of the surfactant molecules and their interaction with the surrounding solvent. Surfactant molecules (called “unimers”) are soluble owing largely to the lyophilic groups, while the lyophobic groups disrupt the orientation of the surrounding solvent molecules, which increases the free energy of the system. This increase in free energy drives the migration of surfactants to interfaces where the lyophobic groups can at least partially escape the solvent molecules and thus minimize the free energy of the system. This migration to the interface tends to have the effect of lowering the surface tension between the solvent and the surrounding fluid. Eventually, interfaces become saturated with surfactants, and as more surfactants are added to the system, they begin to aggregate in solution to form micelles. Thus the three characteristics of surfactants are that they:

transition to interfaces, lower the interfacial tension, and form aggregates (micelles) above a certain concentration.

Surfactants are utilized in various commercial and industrial applications including: emulsifiers, detergents, additives in pharmaceutical medicines, and chemical aides in environmental remediation operations. The common theme in most of these applications is the ability of surfactants to form stable organic/ water interfaces and enhance the solubility of organic components in water.

### 2.1.1 Unimeric Surfactants

An example of a common surfactant is cetyltrimethylammonium bromide ( $C_{16}TABr$ ) and is depicted in Figure 2.1. This surfactant unimer is composed of a hydrophilic ionic headgroup and a hydrophobic hydrocarbon tailgroup. Surfactants can be cationic, anionic, nonionic or even zwitterionic. In this manuscript, only ionic surfactants are discussed.



Figure 2.1: Cetyltrimethylammonium Bromide ( $C_{16}TABr$ )

As depicted in Figure 2.2, when a surfactant dissolves in water, the unimers migrate to the solution interface where the hydrophobic tailgroups escape from the water and the hydrophilic headgroups remain in solution. Usually, the longer the hydrocarbon tail, the more “surface active” the surfactant is (up until a tail length of approx. 16 carbons in length). As more surfactant is added to solution, the surface tension drops continuously until the surface is

completely saturated with surfactant. Once this happens, as more unimers are added to the system, their hydrophobic tailgroups will begin to aggregate together to form micelles in the bulk solution. The exact CMC of a surfactant is dependent upon several factors including: temperature, hydrocarbon tail length, the ionic strength of the solution, and the presence of solution impurities, among many others [5].

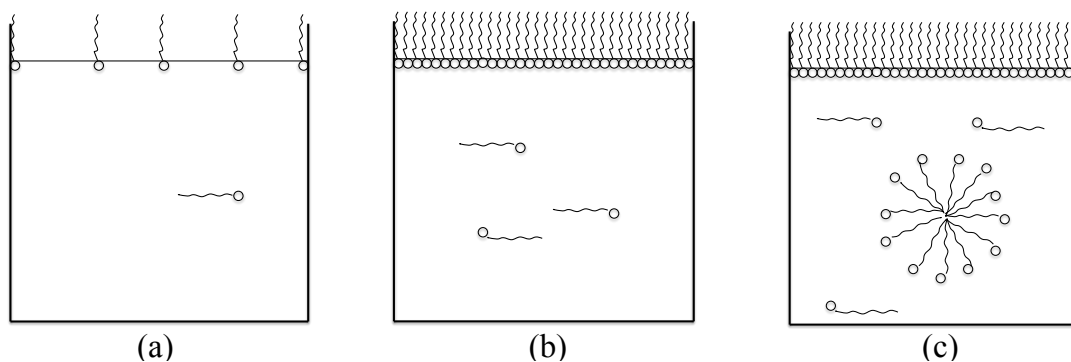


Figure 2.2: A surfactant being added to water with increasing surfactant concentration from left to right. a) low concentration of the surfactant with migration to the interface b) the interface has become saturated with surfactant c) micelles begin to form in solution.

Figure 2.3 depicts a generic drawing of an ionic micelle in an aqueous solution. For an ionic surfactant, a micelle is an aggregation of about 50-100 surfactant unimers [5]. The hydrophobic tailgroups are directed inward to the micelle core and the hydrophilic groups directed outward towards the water. For ionic surfactants, some of the counterions will be bound to the micellar surface, while others remain electrostatically attracted to the surface in a diffuse layer surrounding the micelle [5]. Since the micelle core is composed of hydrophobic lipid tails, it is able to solubilize hydrophobic organic molecules.

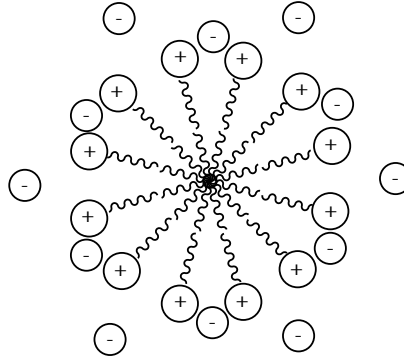


Figure 2.3: A generic drawing of an ionic micelle. The hydrocarbon tails comprise the core of the micelle.

The ability of surfactants to transition to interfaces and form micelles makes them excellent emulsifiers. Emulsions are dispersions of two immiscible fluids stabilized by surfactants or particles. An example would be an oil-in-water emulsion depicted in Figure 2.4 in which a hydrophobic liquid (such as a kind of oil) is suspended as fine droplets in a bulk fluid of water. Surfactants adsorb onto the surface of the oil droplets (with their tails pointing inward contacting the oil) and their hydrophilic heads pointing outward (contacting the water). This provides enhanced stability for the oil droplets to remain suspended in the aqueous solution. Emulsions can either be microemulsions, which are thermodynamically stable colloids consisting of droplets less than 100 nm in size, or they can be ordinary emulsions which are nonstable colloidal systems consisting of droplets in excess of about 100 nm [5].

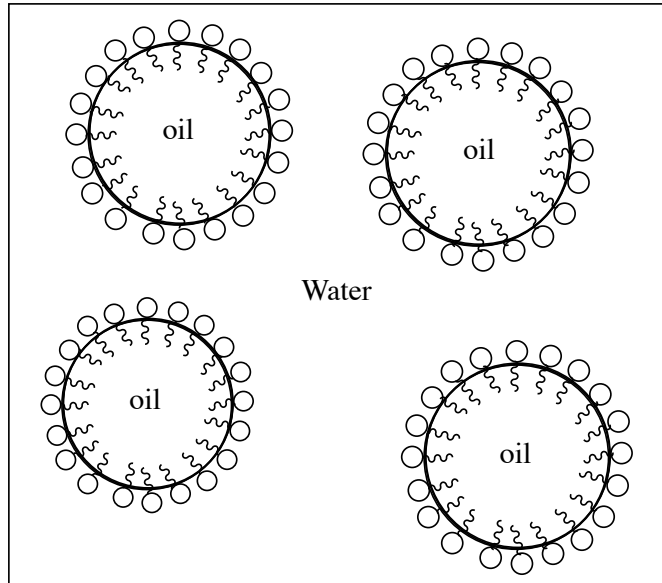


Figure 2.4: An oil-in-water emulsion stabilized by surfactants.

### 2.1.2 Polymeric Surfactants

In addition to being unimeric molecules, surfactants can also be polymeric. A polymer is a molecule composed of many repeating units called monomers. Polymeric surfactants are block copolymers, which means that they are composed of different sections called blocks where each block is comprised of a different type of monomer unit. The amphiphilic properties of these macromolecules arise from the molecule possessing both hydrophilic and hydrophobic blocks. The simplest example is a diblock copolymer and is depicted in Figure 2.5.

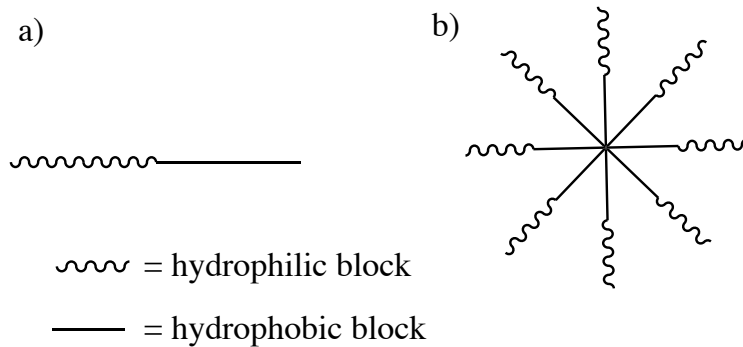


Figure 2.5: An amphiphilic block copolymer. a) a polymeric surfactant unimer and b) a polymeric surfactant micelle.

Polymeric surfactants have the same basic qualities as traditional surfactants; i.e. they transition to interfaces, reduce interfacial tension and form micelles above a CMC. The CMCs of polymeric surfactants tend to be much lower than those of traditional surfactants, and they can form aggregates that are much larger and thus often have high solubilization capacities. Because of these qualities, polymeric surfactants are commonly investigated in the literature as drug delivery vehicles to carry solubilized hydrophobic drugs to targeted locations in vivo [6].

## 2.2 Stimuli-Responsive Surfactants

Due to their inherent chemistry, surfactant properties and self-assembly behavior can be manipulated by changing solution temperature, pH, and ionic strength. For example, nonionic surfactants precipitate out of solution above a certain temperature called the “cloud point” and the addition of an electrolyte to a solution containing ionic surfactants decreases the CMC due to decreases in electrostatic repulsions between surfactant headgroups [5]. These are fundamental characteristics of surfactants and are well documented. Surfactants that respond to external stimuli in ways outside of the ordinary responses are often called “stimuli responsive surfactants” and have attracted much attention in materials science research. There are several excellent and comprehensive reviews of these surfactants [7] [8] [9] and the reader is directed



there for further information. Among the stimuli responsive surfactants that are most relevant to the present work include electrochemically responsive (redoxable) surfactants and magnetic surfactants.

### 2.2.1 Redoxable Surfactants

Redoxable surfactants are surfactants that respond to a change in electrochemical potential. Many of these types of surfactants are reviewed elsewhere [9] but there is one type in particular that is especially relevant to the present work. First reported by Saji et al. in 1985 [3], these cationic surfactants contain an electrochemically active ferrocene-based redox moiety in the headgroup. This redoxable moiety allows for the reversible manipulation of surfactant unimer charge, which can vary from +1 to +2, by oxidizing or reducing the ferrocene moiety. A schematic of this is depicted in Figure 2.6. The charge manipulation of the surfactant headgroup allows for the reversible formation and disruption of micelles in solution since micelles that form with a surfactant unimer charge of +1, can be “blown apart” by oxidizing the unimers to a charge of +2, which increases the electrostatic repulsion between the surfactant headgroups. This is intriguing since it allows hydrophobic compounds to be reversibly solubilized and released in solution by simply oxidizing and reducing the surfactant unimer. A drawing of this process is depicted in Figure 2.7. Several interesting studies have been reported with these surfactants and related compounds and they involve: selectively depositing hydrophobic compounds at electrode surfaces [10], the disruption of emulsions [11], controlled drug release [12], and separating hydrophobic compounds in a microchannel via an electrochemically generated surfactant concentration gradient [13].

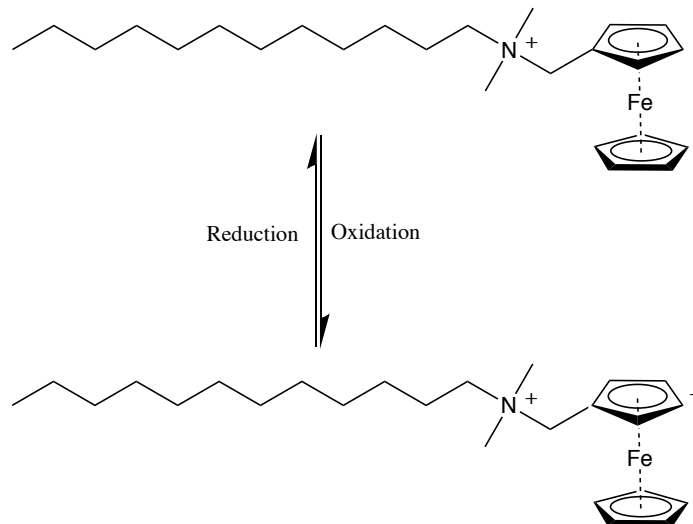


Figure 2.6: A cationic redoxable surfactant unimer undergoing a redox reaction. Note: counterions are not depicted.

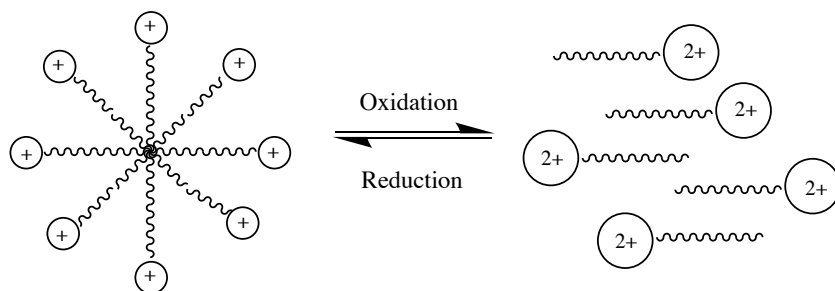


Figure 2.7: The reversible formation and disruption of micelles formed from a redoxable surfactant.

### 2.2.2 Magnetic Surfactants

Magnetic surfactants combine the amphiphilic properties of ordinary surfactants with paramagnetic properties. These paramagnetic properties allow the magnetic response of the surfactant to be turned “on” or “off” by the simple addition or removal of an external magnet. These magnetic moieties are on the molecular level in the form of either paramagnetic metal ions or organic free radicals. This distinguishes them from magnetic nanocomposites in which magnetic nanoparticles are combined with organic molecules to endow the composite material

with magnetic properties. Since the most common type of magnetic moieties are paramagnetic ions, only these kinds of magnetic surfactants will be discussed in this work.

Polarz et al. [14], divided magnetic surfactants into three categories, or types, based on how the magnetic moiety is associated with the unimer. Type I magnetic surfactants poses paramagnetic counterions that are electrostatically attracted to the unimers while in solution. Type IIa magnetic surfactants possess magnetic moieties that are chelated directly in the surfactant headgroup. Type IIb magnetic surfactants possess inorganic paramagnetic headgroups. All three of these types of surfactants are depicted in Figure 2.8.

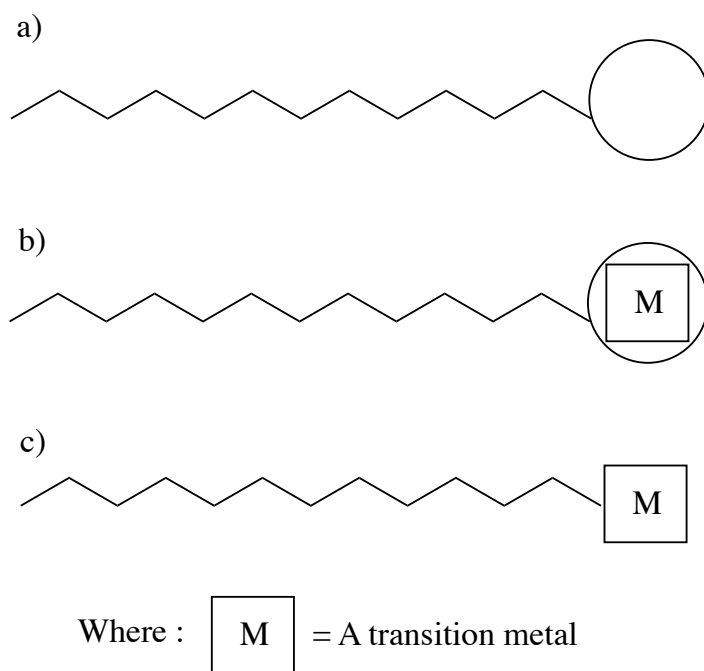
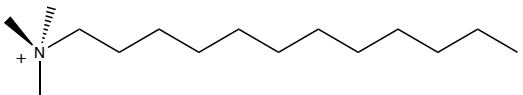
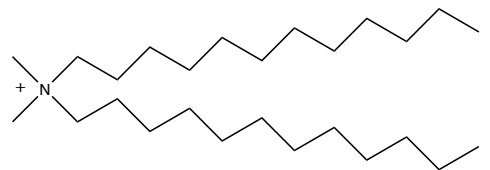
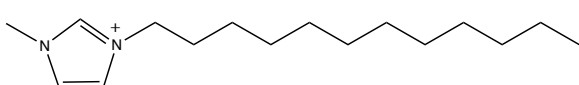
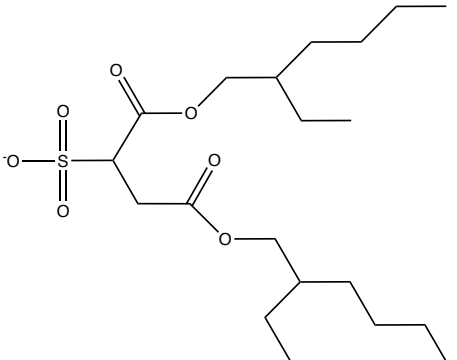
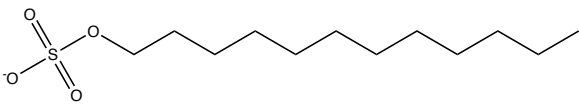


Figure 2.8: Different types of magnetic surfactants. a) Type I magnetic surfactants, b) Type IIa magnetic surfactants and c) Type IIb magnetic surfactants. [14]

### 2.2.2.1 Type I Magnetic Surfactants

Examples of Type I magnetic surfactants are in Table 2.1 The literature on these materials is scarce prior to 2012 [15]. The earliest report of Type I magnetic surfactants occurred in 1960 and describes the synthesis of various metal dodecyl sulfates (some of them containing paramagnetic counterions such as  $\text{Mn}^{2+}$  and  $\text{Co}^{2+}$ ), but their magnetic properties were not investigated [16]. In 1994, Shaikh et al. reported the enhanced recovery of calcite and barite particles by coating them with thin films of magnetic surfactants possessing  $\text{Mn}^{2+}$  counterions followed by exposing the particles to a magnetic field [17].

Table 2.1: Typical Type I Magnetic Surfactants

Counterion	Unimer
[FeCl <sub>3</sub> Br] <sup>-</sup>	
[GdCl <sub>3</sub> Br] <sup>-</sup>	
[CeCl <sub>3</sub> Br] <sup>-</sup>	
[HoCl <sub>3</sub> Br] <sup>-</sup>	
Co <sup>2+</sup> Mn <sup>2+</sup> Ce <sup>3+</sup> Ho <sup>3+</sup>	
Co <sup>2+</sup> Mn <sup>2+</sup>	

The year 2012 marked the beginning of a surge of publications and research interest involving magnetic surfactants when Brown et al. introduced a new class of magnetic surfactants derived from magnetic ionic liquids [18]. These surfactants attracted attention due to their simple and easy synthesis which could be completed via a one step reaction to produce surfactants comprised of cationic unimers and that possessed Fe(III) tetrahalide counterions. These compounds exhibit paramagnetic behavior and were shown to form micelles when dissolved in

water. Brown et al. followed this work by introducing other Type I cationic magnetic surfactants which possess lanthanide tetrahalide counterions based on Gd(III) [19], Ho(III) [19] and Ce(III) [20]. These surfactants are structurally similar to the previously synthesized surfactants with the Fe(III) tetrahalide counterions [18] and were also prepared via simple one-step reactions. The paramagnetic counterion catalog was expanded to include these f-block metals since they exhibit higher magnetic moments than Fe(III) and possess different characteristics [20]. When dilute aqueous solutions of these surfactants were investigated by electrical conductivity measurements, the CMCs of these compounds were usually found to decrease slightly when their halide counterions were exchanged for the metal tetrahalide counterions, and their surfactant ionization constants (measures of how dissociated the counterions are from the micellar surfaces) were found to increase. Brown et al. explained that the decrease in CMC was surprising since larger anions should be less effective in screening electrostatic head-to-head repulsions, which should increase the CMC [18]. The authors explained these results by stating that the counterions may be transitioning into the micellar core of the surfactant micelles [18]. An alternative explanation, which we argue in Chapter III, is that the metal halide counterions are ionizing into their constituent ionic species and increasing the ionic strength of the solution, which causes the CMC of the surfactant to decrease. A summary of the reported CMCs and the degrees of counterion binding ( $1-\beta$ ) of these surfactants with some comparisons to their nonmagnetic counterparts are in Table 2.2.

Table 2.2: Properties of some Type I magnetic cationic surfactants at 25°C

Unimer	Counterion	CMC (mM)	$\beta$	Reference
DTA <sup>+</sup>	Br <sup>-</sup>	15.5	0.26	[20]
DTA <sup>+</sup>	[FeCl <sub>3</sub> Br] <sup>-</sup>	13.6	0.81	[18]
DTA <sup>+</sup>	[GdCl <sub>3</sub> Br] <sup>-</sup>	11.9	0.59	[20]
DTA <sup>+</sup>	[CeCl <sub>3</sub> Br] <sup>-</sup>	10.9	0.82	[20]
DTA <sup>+</sup>	[HoCl <sub>3</sub> Br] <sup>-</sup>	11.6	0.76	[20]
C10mim <sup>+</sup>	Cl <sup>-</sup>	37.0	0.55	[20]
C10mim <sup>+</sup>	[FeCl <sub>4</sub> ] <sup>-</sup>	40.6	0.73	[18]
C10mim <sup>+</sup>	[GdCl <sub>4</sub> ] <sup>-</sup>	30.0	0.82	[20]
C10mim <sup>+</sup>	[CeCl <sub>4</sub> ] <sup>-</sup>	27.6	0.75	[20]
C10mim <sup>+</sup>	[HoCl <sub>4</sub> ] <sup>-</sup>	31.3	0.74	[20]
DDA <sup>+</sup>	Br <sup>-</sup>	0.05	0.53	[18]
DDA <sup>+</sup>	[FeCl <sub>3</sub> Br] <sup>-</sup>	0.06	0.87	[18]
CTA <sup>+</sup>	Br <sup>-</sup>	0.97	0.31	[21]
CTA <sup>+</sup>	[FeCl <sub>3</sub> Br] <sup>-</sup>	0.42	-	[22]
CTA <sup>+</sup>	[GdCl <sub>3</sub> Br] <sup>-</sup>	0.73	0.83	[19]

Abbreviations: CMC: Critical Micelle Concentration;  $\beta$ : degree of counterion dissociation; DTA<sup>+</sup>: dodecyltrimethylammonium; C<sub>10</sub>mim<sup>+</sup>: 1-Decyl-3-methyl imidazolium; DDA<sup>+</sup>: didodecyltrimethylammonium; CTA<sup>+</sup>: cetyltrimethylammonium

Brown et al. reported that these surfactants exhibit bulk paramagnetic properties, can lower the surface tension of aqueous solutions to a greater extent than an equivalent amount of their non-magnetic counterparts [18] [20]. They also showed that magnetically responsive oil-in-water emulsions could be formed from the Gd(III) and Fe(III) based surfactants and that these emulsions could magnetically levitated or pulled through a layer of dodecane [23]. They hypothesized that these materials could be utilized in applications including environmental cleanup and enhanced oil recovery [23]. This possibility is intriguing and has even garnered

widespread attention for these materials outside of the scientific community [24] [25] since these surfactants could hypothetically be used as “recoverable soap” that would capture oil and then magnetically remove it from the surface of water after oil spills. As exciting as these results were, this work was not without criticism. In 2014 Degen et al. investigated the behavior of surfactants with paramagnetic Fe(III) tetrahalide counterions and [26] demonstrated the behavior of the surfactants can be explained by the combination of bulk paramagnetic fluid properties and the interfacial tension reducing surface activity of surfactants. They concluded their work by stating that there is nothing inherently special about these types of magnetic surfactants.

Cationic Type I surfactants were also investigated for their use in applications involving the magnetic transport or migration of particles and molecules in solution. In 2012, Brown et al. demonstrated that these surfactants can bind to proteins and DNA and concentrate them when exposed to a low strength external magnetic field [19]. Later in 2015, McCoy et al. showed that these surfactants can coagulate graphene oxide particles at acidic pH in water and magnetically concentrate them [27]. In 2016, Brown et al. [21] demonstrated that these surfactants can bind to proteins and separate them in the presence of a low strength magnetic field. These surfactants have also been investigated in other research areas including: biomedicine [28], materials fabrication [29] [30], low toxicity antimicrobial agents [31], DNA delivery [32], and forming worm-like micelles with magnetic properties [33].

It is also worth mentioning that in addition to the cationic Type I magnetic surfactants, Brown et al. also reported the synthesis of a novel Type I anionic magnetic surfactant in 2012 [34] derived from the commercial surfactant Aerosol-OT (AOT). This surfactant is comprised of anionic unimers with single ion paramagnetic transition d- or f- block metals. The surfactants were dissolved in an organic solvent, n-heptane to form reverse micelles and then water was



added to form water-in-oil microemulsions. The micelles formed were spherical and the emulsions exhibited effective magnetic moments that were greater than those of the pure surfactants. Brown et al. described these as the first example of stable nanoparticle-free ferrofluids and speculated that they could have potential applications in biomedicine.

This present work is not intended to be a comprehensive review of Type I magnetic surfactants and the interested reader can find two such excellent reviews in the references [35] [36]. It should be emphasized that the bulk of the research performed with these materials focused on the cationic versions with metal halide counterions due to their ease of synthesis, paramagnetic properties, and water solubility.

#### 2.2.2.2 Type IIa Magnetic Surfactants

In contrast to Type I magnetic surfactants, Type IIa magnetic surfactants contain paramagnetic metal ions that are chelated directly into the surfactant headgroup. Surfactants that are able to chelate metals into their headgroup were first reported in 1980 [37] and were composed of polar macrocyclic headgroups with paraffinic tails. These surfactants were able to create ordered metal ion structures in solution by chelating alkaline earth metals. In 1999 Macke et al. [38] reported the synthesis of a paramagnetic surfactant that consists of a seven-donor macrocyclic complex headgroup that can chelate  $Gd^{3+}$  ions. This surfactant was shown to form micelles in solution and was intended to act as a potential MRI contrast agent since it also demonstrated high proton relaxivities comparable to other macrocyclic contrast agents.

More recently in 2013, Polarz et al. reported the synthesis of a novel Type IIa surfactant that contained  $Dy^{3+}$  chelated into the headgroup [39]. This surfactant was a decyl-modified 1,4,7,10-tetraazacyclododecane-1,4,7,10-tetraacetic acid ( $C_{10}DOTA$ ) with  $Dy^{3+}$  coordinated into the headgroup and is depicted in Figure 2.9.  $Dy^{3+}$  was selected as the magnetic moiety due to its

magnetic moment which is highest among paramagnetic ions. Polarz demonstrated that the solubility of these surfactants in water is low and is pH dependent. They showed that these compounds form micelles in water, and upon a temperature increase, grow into larger structures. Upon cooling the solution back to room temperature large dumbbell-shaped macroscopic objects formed within two days. When the same C<sub>10</sub>DOTA surfactant ligand was coordinated to diamagnetic Lu<sup>3+</sup> instead of paramagnetic Dy<sup>3+</sup>, large- structure precipitates were not observed at room temperature even after heating the solution, which provides evidence that magnetic interaction played a crucial role in the self-organization process of the DyC<sub>10</sub>DOTA.

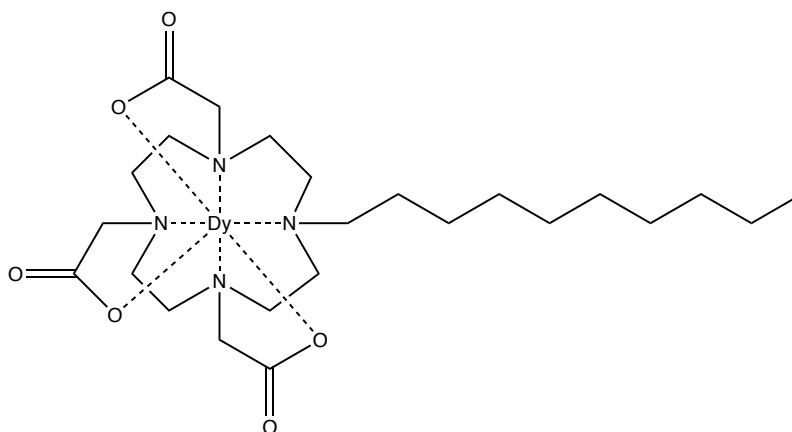


Figure 2.9: A type IIa surfactant example: DyC<sub>10</sub>DOTA. Synthesized by Polarz et al. [39].

Motivated by Degen et al.'s criticisms of the Type I magnetic cationic surfactants with metal halide counterions, Hermann et al. [40] decided to investigate the possibility of preparing surfactants in which the paramagnetic transition metal species is coordinated directly in the headgroup. To improve the water solubility of these compounds, they selected divalent transition metal ions such as Mn<sup>2+</sup> as the magnetic moiety, which would give the MC<sub>n</sub>DOTA a total charge of -1 and thus make it more water soluble and more surfactant-like than the previously investigated DyC<sub>10</sub>DOTA. In this work, they also manipulated the length of the hydrocarbon tail.

A drawing of these kinds of surfactants is depicted in Figure 2.10. Their findings were intriguing. For example, they found that the magnetic behavior of  $\text{MnC}_{16}\text{DOTA}$  increases with increasing temperature and that the micelles transition from spherical to rod-like when the temperature increases above 287 K. They also performed experiments with paramagnetic  $\text{MnC}_{16}\text{DOTA}$  and diamagnetic  $\text{ZnC}_{16}\text{DOTA}$  and showed that the surface tension of the fluid decreases when the  $\text{MnC}_{16}\text{DOTA}$  solution is exposed to an external magnetic field. They did not observe the same reduction in surface tension for the  $\text{ZnC}_{16}\text{DOTA}$  system even when an equal amount of paramagnetic  $\text{Mn}^{2+}$  ions were added to solution, indicating that the reduction in surface tension of the  $\text{MnC}_{16}\text{DOTA}$  system was due to the coordination of  $\text{Mn}^{2+}$  to the surfactant headgroup. They also showed that these surfactants could act as stabilizers for the formation of organic-in-water emulsions.

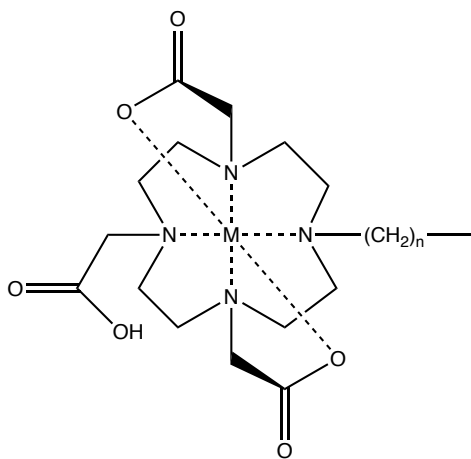


Figure 2.10: A depiction of  $\text{C}_n\text{DOTA}$  coordinated to a divalent metal ( $\text{M}^{2+}$ ). Synthesized by Hermann et al. [40].

Certain Type IIa magnetic surfactants may provide at least a couple key advantages over the Type I magnetic cationic surfactants that have attracted so much attention in the literature. First, the incorporation of the paramagnetic ion directly into a high donor macrocyclic headgroup

may allow for greater stability of the surfactant. Also as Hermann et al. [40] pointed out, when the magnetic moiety is chelated directly in the surfactant headgroup, it may also allow a magnetic field to generate a torque in the surfactant molecule. However, the downside of using these materials is that the synthesis tends to be more involved than the simple one-step procedure required to synthesize the Type I metal-halide based cationic surfactants. Although initial reports of these materials are encouraging, to our knowledge, these materials have not yet been studied in magnetically-driven separation processes.

### 2.2.2.3 Type IIb Magnetic Surfactants

Type IIb magnetic surfactants are surfactants that possess paramagnetic inorganic headgroups with organic hydrocarbon tailgroups. Most examples of these types of surfactants found in the literature possess headgroups comprised of polyoxometallate (POM) clusters. Since Type IIb surfactants largely fall outside of the scope of the current work, the reader is referred to two review papers covering the topic [35] [14]. However, there is at least one type that is worth mentioning here. In 2012, Polarz et al. introduced a Type IIb surfactant possessing a ruthenium containing POM headgroup. This surfactant could undergo reversible electrochemically induced charge manipulation from -1 to -4, and exhibited paramagnetic properties depending on the charge of the headgroup [41].

## CHAPTER III

### 3 Stability of Magnetic Surfactants in Aqueous Solutions: Measurement Techniques and Impact on Magnetic Processes

#### 3.1 Abstract

Predicting the behavior of magnetic surfactants in magnetic fields is critical for designing magnetically driven processes such as chemical separations or the tuning of surface tensions. The ability of magnetic fields to alter the interfacial properties of magnetic surfactant solutions may be dependent upon the strength of association between the magnetic and surfactant moieties of the surfactant molecules. This research shows that the stability of a magnetic surfactant in an aqueous environment is dependent upon the type of complex that contains the paramagnetic ion, and these findings provide valuable insight for the design of magnetic surfactants for applications in aqueous media. The surfactants investigated were ionic surfactants, which contained paramagnetic counterions. This investigation looked at both anionic and cationic surfactants and utilized solution conductivity, cyclic voltammetry (CV), sampled current voltammetry (SCV), and solution pH measurements to qualitatively evaluate the stability of the magnetic counterions in aqueous solution. In addition, solution conductivity was used to quantify the degree of binding between the paramagnetic ions and surfactant micelles in solution. These results indicate metal halide-based cationic surfactants are unstable in aqueous solutions. We

hypothesize that this instability results in the difference in the magnetic response of anionic vs. cationic surfactants examined in this study.

### 3.2 Introduction

Magnetic surfactants are a class of amphiphiles that possess the characteristics of traditional amphiphiles, but incorporate magnetically responsive moieties. The magnetic moieties can either be the surfactant's counterion, or they can be incorporated directly into the surfactant unimer via a chelation complex [14]. As previous research has shown, these magnetic moieties endow the surfactant solutions with the ability to respond to external magnetic fields [18] [35]. While further research is needed, these results indicate that these surfactants could potentially be used in certain applications such as low-energy separations or drug delivery.

The motivation for the present work is to explain the inconsistencies in the reported response of metal halide-based cationic magnetic surfactants in magnetic fields. For example, Brown et al. reported that a magnetic field can move metal halide-based cationic magnetic surfactants in solution and change the solution's surface tension [18]. While Brown's hypothesis that the changes in surface tension were due to alteration of the surfactant properties, Degen et al. [26] offer an alternative explanation that did not require magnetic alteration of the surfactant unimer. Degen states that the behavior of magnetic surfactants in aqueous solution could be explained by the combination of decreased surface tension due to the surfactant unimers in conjunction with the magnetic properties of a bulk fluid that contains paramagnetic ions.

We hypothesize that the inconsistency in magnetic manipulation of emulsions and solution surface tensions are a function of the strength of association of the magnetic counterion with the ionic surfactant's head group. To test this hypothesis this report utilized solution conductivity to evaluate the strength of association between the paramagnetic metals and the

amphiphile components. The report further utilized Sampled Current Voltammetry (SCV) to examine counterion instability. For clarity, we will refer to “dissociation” as a magnetic counterion having a weak association with the surfactant amphiphile, while “instability” will refer to the magnetic counterion being chemically altered, resulting in decreased interaction with the surfactant amphiphile. SCV provides information about the equilibrium constants of the chemical alteration of the magnetic counterion, while solution conductivity measurements can determine the association of magnetic counterions with the surfactant micelles. Measurements of solution pH complemented the aforementioned electrochemical techniques by providing information about hydrolysis reactions occurring with iron-containing metal halide surfactants.

### 3.3 Methods and Materials

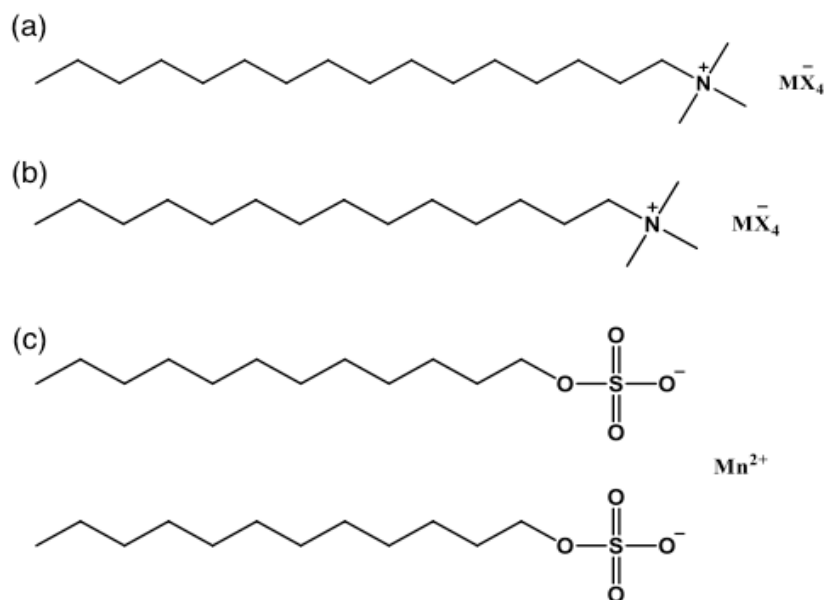


Figure 3.1: The magnetic surfactants investigated. (a) and (b) The metal halide-based cationic surfactants studied in this manuscript. (c) Manganese di-dodecyl sulfate (MnDDS)- the magnetic anionic surfactant studied in this manuscript

Note: in this manuscript, the alkyltrimethylammonium surfactants used are depicted with the notation:  $\text{C}_y\text{TAMX}_4$  and are drawn generically in Figure 3.1a, where:  $\text{MX}_4^-$  represents the

metal halide counterion and  $y$  is either 14 or 16 and represents the linear saturated hydrocarbon tail. Specifically,  $M$  represents the type of metal contained in the counterion (either  $\text{Fe}^{3+}$ ,  $\text{Gd}^{3+}$  or  $\text{Co}^{2+}$ ),  $X$  represents the type of halide ion coordinated to the metal (either  $\text{Cl}^-$  or  $\text{Br}^-$ ). For the nonmagnetic cationic alkyltrimethylammonium surfactants described in this manuscript, the counterion is always  $\text{Br}^-$ . The magnetic anionic surfactant described is manganese di-dodecyl sulfate (MnDDS) (Figure 3.1c).

### 3.3.1 Chemicals and Materials

Iron (III) trichloride hexahydrate 98%, tetradecyltrimethylammonium bromide (99%  $\text{C}_{14}\text{TABr}$ ), cetyltrimethylammonium bromide (99%  $\text{C}_{16}\text{TABr}$ ), Oil Blue N, 96%, and gadolinium chloride hexahydrate 99% were purchased from Sigma Aldrich. Lithium chloride 99%, sodium dodecyl sulfate (ACROS Organics) 99%, dodecane (ACROS Organics) 98%, anhydrous sodium acetate 99%, saturated KCl, and FisherBrand pH strips were purchased from Fisher Scientific. Anhydrous manganese (II) chloride, 99% was purchased from American Elements. Cobalt (II) chloride hexahydrate 98% was purchased from Alfa Aesar. Deionized water with a resistivity at 25C of  $18.2 \text{ M}\Omega\cdot\text{cm}$  was used for all experiments unless otherwise specified. The Great Value Brand distilled water was used in the Sampled Current Voltammetry (SCV) experiments.

The electrochemical cell was constructed using a CH Instruments Ag/AgCl reference electrode (part number: CHI111) filled with 1 M KCl, a CH Instruments platinum disk (diameter approx. 3/32 inch) working electrode (part number: CHI102) and a platinum counter electrode. The counter electrode was constructed in house out of a single platinum wire of approx. 14 inches in length and 1/64 inch in diameter by twisting and weaving the wire in such a way that it formed a lollipop shape with the flat round end portion of about 3/8 inch diameter.



### 3.3.2 Synthesis and Solution Preparation

$C_{16}TAFeCl_3Br$  was synthesized by following a modified literature procedure [18]. Briefly,  $C_{16}TABr$  was dissolved in methanol at room temperature to form a concentrated solution of 1 g/ml.  $FeCl_3$  hexahydrate was dissolved in methanol to form a 0.25 g/ml solution and added to the  $C_{16}TABr$  solution to form a yellow crystalline solid precipitate. This solution was then placed in a freezer at  $-20^\circ C$  overnight and filtered over a vacuum filter to collect the solid product. The product was recrystallized from methanol three more times.  $C_{16}TAGdCl_3Br$  was prepared following a method described previously in the literature [19].  $[C_{16}TA]CoCl_2Br_2$  was synthesized by dissolving  $C_{16}TABr$  in methanol to form a 1 g/ml solution and then adding a 0.5 molar equivalent of a 0.25 g/ml solution of  $CoCl_2$  hexahydrate in methanol. Blue crystals formed and were collected by vacuum filtration. The blue product was recrystallized from methanol two more times. Manganese didodecyl sulfate (MnDDS) was synthesized by modifying a previously reported literature method [16]. Briefly, sodium dodecyl sulfate was dissolved into deionized water to form a concentrated solution and then an excess of concentrated aqueous manganese chloride solution was added. The solution was then placed in a refrigerator until crystals formed. The crystals were recovered by vacuum filtration and then purified by recrystallization three times in pure deionized water.  $C_{16}TAGdCl_3Br$  and MnDDS emulsions were prepared by dissolving 5 mM of surfactant into  $\sim 10$  mL of deionized water, then adding  $\sim 2$  mL of dodecane dyed with the hydrophobic dye "Oil Blue N". Then a high shear mixer was used to mix the solutions for  $\sim 1$  minute until uniform blue emulsions formed. These emulsions were allowed to phase separate forming an oil rich top phase and a transparent blue colored bottom layer. This transparent blue bottom layer was extracted and used in the emulsion experiments (Fig. 3.2).

### 3.3.3 Characterization

The SCV experiments were performed using a “Princeton Applied Research Potentiostat/Galvanostat Model 273A” potentiostat. The procedure followed in this experiment was based on a previously published procedure [42]. Briefly, the transition metal halide/lithium chloride solutions were prepared and nitrogen was bubbled through them for at least 15 minutes. Next, cyclic voltammetry measurements were performed on the solutions to obtain the potential ranges for operating the SCV scans. SCV was conducted by selecting a potential about 250 mV above the redox potential of the metal complex in solution as the working electrode potential at  $t = -0.1$  seconds, and then at  $t = 0$  seconds, the potential was immediately decreased to a value within the vicinity of the redox reaction and the current was allowed to decay for 2 seconds. After this, the SCV procedure was repeated with the same working electrode potential at  $t = -0.1$  seconds followed by lower potential at  $t = 0$  seconds than the measurement prior to it. This process was repeated until the value of the potential at  $t = 0$  covered the whole range of the potentials obtained from the CV graphs. Then, at a certain time  $\tau$ , the value of the current was obtained for each scan and then plotted in a graph of normalized current ( $i/i_d$ ) vs. potential (E/V vs. Ag/AgCl) and a third order polynomial curve fit was applied to obtain the half wave potential ( $E_{1/2}$ ) of the metal complex by selecting the point on the curve that was halfway between the maximum and minimum current. The experiments were completed within an hour after solution preparation, and at room temperature under an inert nitrogen atmosphere with nitrogen bubbling in solution before and in between measurements. In between each experiment, the electrochemical cell and the electrodes were rinsed with DI water, and the platinum counter electrode was heated under a flame until red-hot. The working electrode was cleaned with HCl in between experiments or as needed to remove any contaminants that may have been adhering to

the surface. The 1 M KCl solution contained inside of the reference electrode was replaced periodically as needed.

The degree of micelle counterion binding was determined by an electrical conductivity method using a Thermo Scientific Orion Star A215 pH/ Conductivity Meter. The ionic dissociation constant ( $\beta$ ) was determined by the ratio of the slopes above and below the CMC of the specific conductivity vs. concentration graphs. The degree of counterion binding of the surfactant micelles was determined by  $1-\beta$ .

Solution pH measurements were also determined by using the Thermo Scientific Orion Star A215 pH/Conductivity Meter. Critical micelle concentrations (CMCs) were determined by surface tension measurements with a Sigma 700/701 Biolin Scientific Force Tensiometer.

### 3.4 Results and Discussion

#### 3.4.1 Oil-In-Water Emulsion Stability

The inspiration for the current manuscript derives from the following observation shown in Figure 3.2. This figure shows the behavior of dyed oil-in-water emulsions formed from anionic and cationic magnetic surfactants placed at the pole of a magnet that is submerged in water. The anionic surfactant was MnDDS (Figure 3.1c) and the cationic surfactant was  $C_{16}TAGdCl_3Br$ . The cationic magnetic surfactant emulsion appears to almost completely disperse after several minutes; while the anionic magnetic surfactant emulsion is stable for  $\approx 1$  hr.

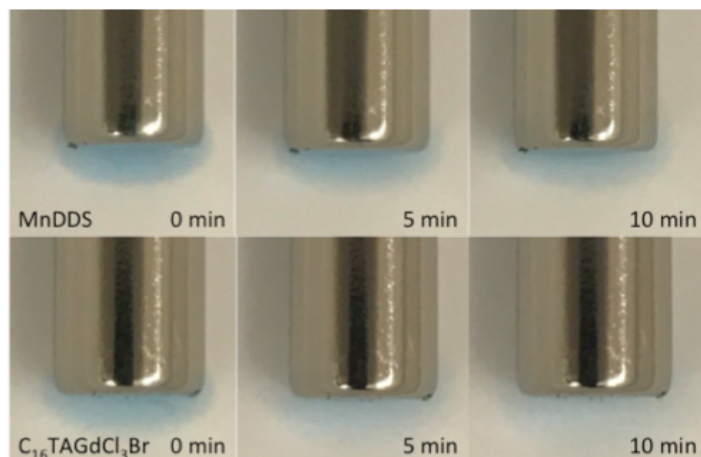


Figure 3.2: Emulsions formed from magnetic surfactants. Five mL of dyed dodecane-in-water emulsions formed from dodecane and 5mM ionic magnetic surfactants (top - anionic magnetic surfactant and bottom - cationic magnetic surfactant) dispensed at the pole of a 0.7 T magnet submerged in a solution of deionized water. From left to right, time lapsed photos of the ability of the magnetic field to hold on to these emulsions in 5 minutes intervals from 0 to 10 minutes. After 10 minutes, the cationic emulsion had mostly dispersed into the bulk solution while the anionic surfactant took  $\approx$  1 hour to achieve an equivalent dispersion.

Since  $Gd^{3+}$  has a higher calculated magnetic moment than  $Mn^{2+}$  (7.94 bohr magnetons versus 5.92 bohr magnetons) [43], it is reasonable to assume that the  $C_{16}TAGdCl_3Br$  system should have shown a greater magnetic response than the MnDDS system. But since the MnDDS emulsion showed a greater magnetic response, we hypothesized that the reason for this observation was due to differences in association of the magnetic counterions with the surfactant micelles in solution.

### 3.4.2 The Association of Magnetic Counterions with Surfactant Micelles

Manganese didodecyl sulfate (MnDDS) is a previously studied anionic surfactant [16] whose magnetic properties, to the best of our knowledge, are reported here for the first time. This anionic surfactant is composed of two dodecyl sulfate amphiphiles and one divalent paramagnetic manganese counterion (Figure 3.1c). Since the MnDDS counter ion is a single atom and not contained in a metal halide complex (which might dissociate in water), we believe that it is

inherently stable in solution and interacts strongly with the surfactant micelles. The properties of MnDDS are summarized in Table 3.1 and in the Supporting Information found in Appendix A.

Assuming the only species in solution are ionic surfactants, solution conductivity can quantify the strength of association, reported as degree of counterion binding, between the counterion and the ionic surfactant micelles by using the “ratio of the slopes” method [5]. A plot of the specific conductivity of a solution ( $\kappa$ ) versus the ionic surfactant’s concentration is linear below the critical micelle concentration (CMC) with a sharp decrease in slope at the CMC producing a new linear relationship above the CMC (Fig. 3). Defining the linear slope below the CMC as  $s_1$  and the linear slope above the CMC as  $s_2$ , the ionic dissociation constant ( $\beta$ ) is defined as  $s_2/s_1$ . The degree of counterion binding to the micellar surface can be obtained by the following equation:  $1-\beta$  [5]. For example, we determined that the degree of counterion binding of bromide ions to the surface of  $C_{16}TABr$  micelles is 0.73 as illustrated in Figure 3.3 and Table 3.1.

The CMC of both MnDDS and  $C_{16}TABr$  were determined from surface tension measurements (Figures A.1 and A.2) and agreed with the specific conductivity vs. concentration graphs (Figure A.6 and A.7). Figure 3 shows the ratio of slope method for MnDDS and the non-magnetic  $C_{16}TABr$  surfactant in deionized water. (Note: reduced concentration = concentration/CMC). Assuming complete ionization below the CMC, the degree of counterion binding of the manganese ions to the MnDDS micelles is 0.92 (Figure 3.3 and Table 3.1). This value is higher than the typical value of the degree of counterion binding of surfactants with univalent counterions. For example, we calculated the degree of counterion binding of sodium dodecyl sulfate (SDS) to be 0.65 (Table 3.1). We believe the high degree of counterion binding of

MnDDS is due to stronger binding of the divalent ions to the micellar surface than univalent ions.

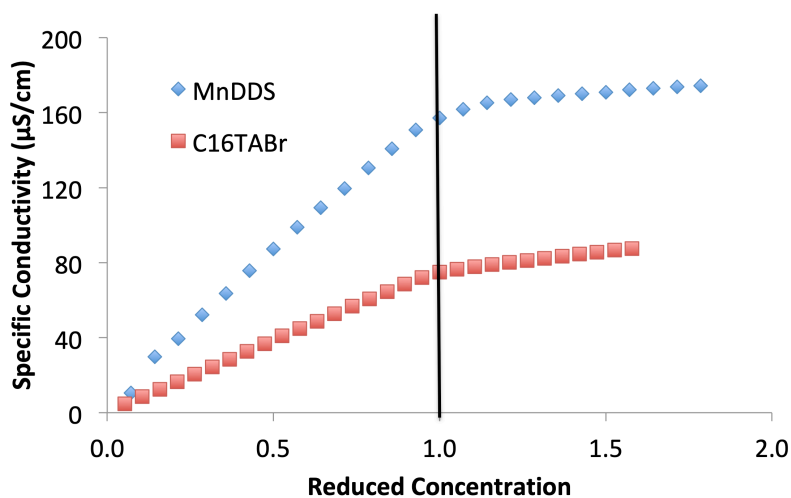


Figure 3.3: Specific conductivity vs. reduced concentration measurements of MnDDS and C16TABr in deionized water. The reduced concentration is concentration/CMC. The black vertical line represents the CMC obtained from surface tension measurements. These plots clearly indicate degrees of association between the counterions and the surfactant amphiphiles.

Table 3.1: CMC and Degree of Counterion Binding Data for MnDDS and C<sub>16</sub>TABr

Surfactant	CMC (mM)*	Degree of Counterion Binding		
		S <sub>1</sub>	S <sub>2</sub>	Binding
MnDDS	1.4	122.1	9.3	0.92
C16TABr	0.95	80.4	22	0.73
SDS	8.2	59.8	21.2	0.65

\*The CMCs were determined by surface tension measurements and can be found in Appendix A.

Figure 3.4 contains the specific conductivity vs. reduced concentration measurements of solutions of, C<sub>16</sub>TAGdCl<sub>3</sub>Br and C<sub>16</sub>TAFcCl<sub>3</sub>Br in deionized water. Both surfactants' CMCs were determined from surface tension measurements and found to be 0.8 and 0.6 mM respectively (Figures A.3 and A.4). There is no significant change in the specific conductivity versus concentration slope above and below the CMCs in Fig. 3.4, in sharp contrast to the observed changed in Fig. 3.3. Potential explanations for the behavior in Fig. 3.4 include

minimum counterion binding and/or a mixture of counterion species due to possible ionization of the metal halide ions, which could create a “swamping out” effect of the CMC due to the additional ionic species in solution. We believe that the latter hypothesis is more reasonable and provides a better explanation for the experimental results since it would also explain the high specific conductivity of the metal halide surfactant solutions. The instability of many kinds of metal halide ions in aqueous solution is well documented. For example, complex anions such as  $\text{FeCl}_4^-$  may not exist in room temperature aqueous solutions unless the concentration of  $\text{Cl}^-$  anions are several orders of magnitude higher than the concentration of  $\text{Fe}^{3+}$  cations [44]. This may indicate that paramagnetic metal halide counterions of surfactant amphiphiles containing iron, cobalt, etc. may not be stable under all test conditions.

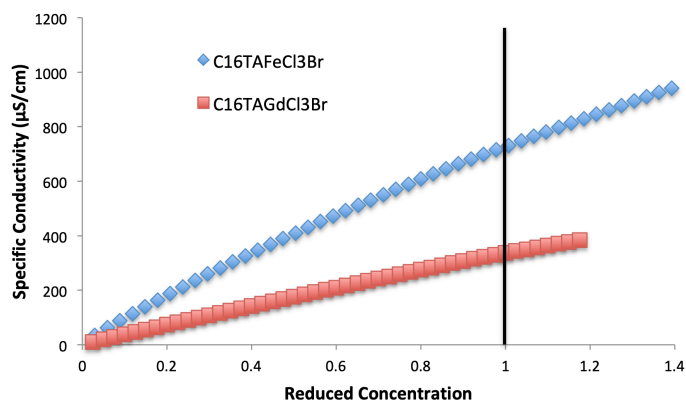


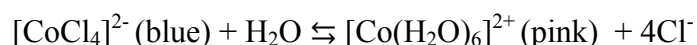
Figure 3.4: Specific conductivity vs. reduced concentration of C16TAFECl3Br and C16TAGdCl3Br in aqueous solution. Where reduced concentration = concentration/CMC. The black vertical line represents the CMC obtained from surface tension measurements. There is no discernable counterion association in these plots.

### 3.4.3 Magnetic Metal Complex Stabilities

The following stability investigations consider the common assumption found in the magnetic surfactant literature [18] [20] that the following reaction results in an aqueous stable ion:  $X^- + MCl_3 \rightarrow MCl_3X^-$  where M is a paramagnetic metal and  $X^-$  is a halide ion. Solution conductivity experiments of magnetic surfactants with both anionic counterions ( $FeCl_3X^-$  or  $GdCl_3Br^-$ ) and cationic counterions ( $Mn^{2+}$ ) measured the strength of association between the magnetic counterions and the surfactant amphiphiles. SCV and solution conductivity experiments measured the strength of association of the paramagnetic metal ions and halide ions in solution.

#### 3.4.3.1 $[C_{16}TA]_2CoCl_2Br_2$ Color Change Reaction

Some cobalt-containing complexes are known to undergo characteristic color change reactions. Specifically, cobalt tetrachloride is well documented to be a blue compound that turns pink as water molecules begin to outcompete the chloride ions to coordinate with the cobalt ions in solution according to the following equation:



To investigate the stability of a surfactant with a metal tetrahalide counterion, we synthesized the surfactant  $[C_{16}TA]_2CoCl_2Br_2$  which contained two cetyltrimethylammonium amphiphiles and one divalent paramagnetic  $CoCl_2Br_2^{2-}$  counterion. When the surfactant was synthesized, we recovered a blue crystalline solid, indicating to us that the counterion for this surfactant was indeed a cobalt tetrahalide complex (Figure 3.5). When mixed with water, this blue solid immediately turned pink, indicating that the cobalt ions were coordinating with water molecules in solution instead of halide anions (Figure 3.5). Since the cobalt appeared to exist in



solution in its hydrated cationic form, we concluded that it is probably not interacting very strongly with cationic micelles existing in solution.

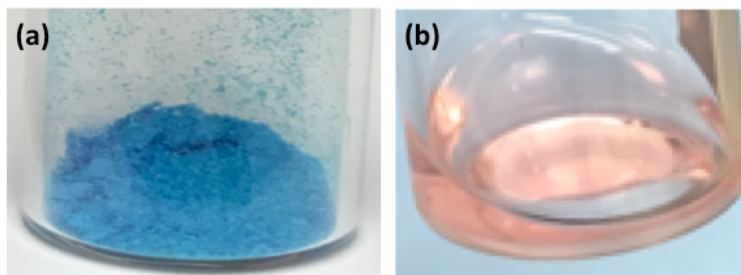


Figure 3.5:  $[C_{16}TA]_2CoCl_2Br_2$ . In its' solid form (a) and when it is mixed with water (b). The color change indicates that the cobalt tetrahalide complex anion is unstable in aqueous solution.

### 3.4.3.2 Sampled Current Voltammetry Indication of Metal Complex Stabilities

Sampled Current Voltammetry (SCV) is an electrochemical method used to determine the half-wave potential ( $E_{1/2}$ ) of metal complexes in solution [42]. The following equation is the relationship between the half-wave potentials of the complexed and uncomplexed species in solution, the equilibrium constant ( $K_C$ ), and the number of ligands associated with the metal ( $p$ ):

$$E_{1/2}^C - E_{1/2}^M = -\frac{RT}{nF} \ln K_C - \frac{RT}{nF} p \ln C_X^* + \frac{RT}{nF} \ln \frac{m_M}{m_C}$$

Where:  $E_{1/2}^C$  is the half wave potential of the metal complex in solution in V,  $E_{1/2}^M$  is the half wave potential of the uncomplexed metal in solution in V, R is the ideal gas constant, n is the stoichiometric number of electrons involved in the electrode reaction, F is Faraday's constant, T is temperature,  $K_C$  is the equilibrium constant of the metal complex, p is the number of ligands coordinating with the metal complex,  $C_X^*$  is the concentration of the ligand in the bulk solution in M,  $m_M$  and  $m_C$  are the mass transfer coefficients in cm/s to and from the working electrode surface for the uncomplexed and the complexed metal species in solution respectively. By

assuming that  $m_M$  and  $m_C$  are equal and then constructing a plot of  $-nF(E_{1/2}^C - E_{1/2}^M)/RT$  versus  $\ln C_X^*$  at different ligand concentrations, a graph is obtained where the slope of the line is equal to  $p$  and the intercept is equal to  $\ln K_c$ .

We performed SCV to examine the stability of Iron(III) halide complexes in aqueous solution. The experiments were performed by forming 0.5 mM solutions of  $\text{FeCl}_3$  and then adding certain amounts of  $\text{LiCl}$  up to 1 M. Our reason for choosing  $\text{LiCl}$  instead of a surfactant like  $\text{C}_{16}\text{TABr}$  was because we were strictly interested in the formation of magnetic counterion complexes, which should not be impacted by the presence of a cationic surfactant unimer instead of  $\text{Li}^+$ . We reasoned that the presence of a surfactant unimer could introduce an error in these experiments since it would form an adsorbed layer on the electrode surfaces and impact the surface chemistry of the system.

Figure 3.6 and Table 3.2 show the results of the SCV tests for four concentrations of  $\text{LiCl}$  mixed with a solution of 5mM  $\text{FeCl}_3$ . The  $E_{1/2}$  of the 5 mM  $\text{FeCl}_3$  solution was 0.46 V vs.  $\text{Ag}/\text{AgCl}$ . The values of the half-wave potentials vs.  $\text{Ag}/\text{AgCl}$  for solutions of 0.5 mM  $\text{FeCl}_3$  in the presence of 0.1, 0.5 and 1.0 M  $\text{LiCl}$  were 0.46 V, 0.47 V and 0.44 V respectively. Since the half-wave potential of the  $\text{Fe}^{3+}$  species reduction reaction did not change until the concentration of  $\text{Cl}^-$  ions in solution was over two orders of magnitude higher than the concentration of  $\text{Fe}^{3+}$ , we concluded that the  $\text{FeCl}_4^-$  is not the dominant iron (III) species in solution (and may not even be present in solution) when the concentrations of chloride ions are equal to or less than 1.0 M. We hypothesize that this would also apply to any iron halide; such as the  $\text{FeCl}_3\text{Br}^-$  anion that is the counterion of  $\text{C}_x\text{TAFCl}_3\text{Br}$  magnetic surfactants. Therefore, the SCV data demonstrates the instability of magnetic metal halide complex anions in room temperature aqueous solutions and

because of this, we do not believe that they act as counterions to cationic surfactants, at least for solutions containing halide ions at concentrations less than or equal to 1 M.

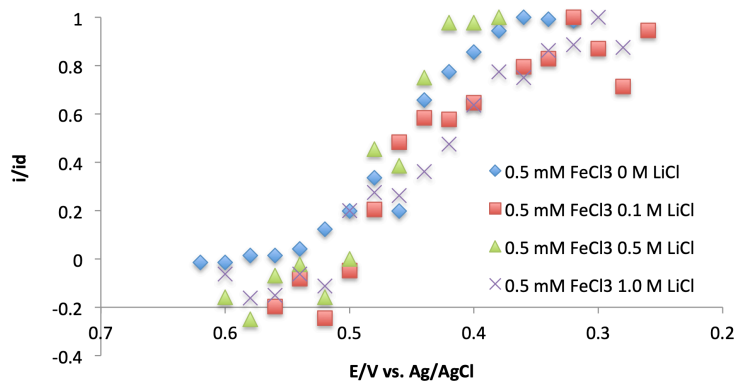


Figure 3.6: The results of the sampled current voltammetry (SCV) experiments with  $\text{FeCl}_3$  /  $\text{LiCl}$  solutions. Shows no significant shift in  $E_{1/2}$  is with increasing  $\text{Cl}^-$  ion concentration.

Table 3.2: The half wave potentials of  $\text{Fe}^{3+}$  ions in solution obtained from the SCV results.

Solution	Half Wave Potential (V vs. Ag/AgCl)
5 mM $\text{FeCl}_3$	0.46
0.5 mM $\text{FeCl}_3$ 0.1 M $\text{LiCl}$	0.46
0.5 mM $\text{FeCl}_3$ 0.5 M $\text{LiCl}$	0.47
0.5 mM $\text{FeCl}_3$ 1.0 M $\text{LiCl}$	0.44

### 3.4.3.3 Solution Conductivity Indications of Anion Stability

Since the electrical conductivity of a solution is generally dependent upon the concentration of ions in solution, conductivity measurements can often be used to detect the complexation of ions in solution. For example, previous research has shown that when sodium dodecyl sulfate (SDS) is added to a solution containing trivalent lanthanide ions, a plot of solution conductivity vs. SDS concentration shows the complexation between the lanthanide ions and dodecyl sulfate ions in the graphed plateaus and changes in the slope [45]. To illustrate this concept for iron ions, we measured changes in the iron solution conductivity with increasing

acetate anions, Figure 3.7. As iron (III) acetate complexes form in solution, the total number of ions appear to decrease, leading to the observed decrease in solution conductivity vs. acetate ligand concentration. Figure 3.7 illustrates how strong complexations between metal cations and acetate anions are detectable via solution conductivity measurements. In the presence of  $\text{Fe}^{3+}$  ions, complexation between the metal and acetate anions can be detected by changes in the slope of the lines.

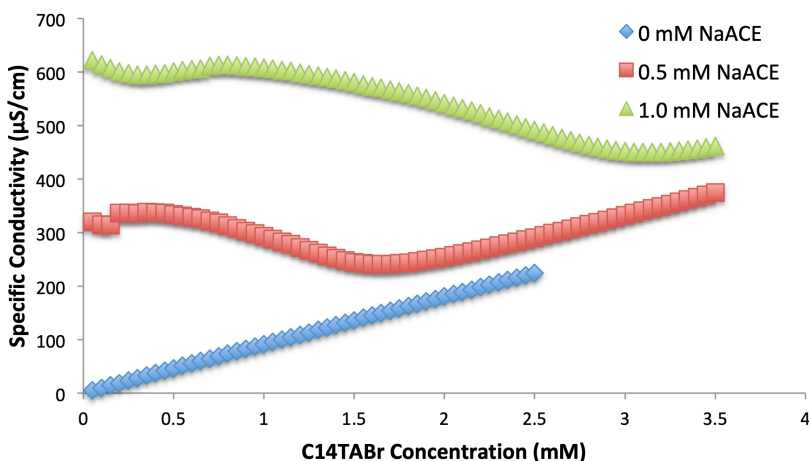


Figure 3.7: Specific conductivity vs. concentration of aqueous iron(III) trichloride solutions at constant concentration as sodium acetate is added. This figure indicates that complexation occurs between the iron(III) cations and the acetate anions.

To examine what influence a cationic surfactant would have on the complex formation of a metal halide, we also performed conductivity measurements of tetradecyltrimethylammonium bromide ( $\text{C}_{14}\text{TABr}$ ) in aqueous solution in the presence of two metal halides,  $\text{FeCl}_3$  and  $\text{GdCl}_3$ . The results shown in Figures 8 and 9 do not appear to indicate any noticeable complexation between metal halides ( $\text{Fe}^{3+}$  and  $\text{Gd}^{3+}$ ) and  $\text{C}_{14}\text{TABr}$  in the aqueous solutions due to their linearity. The sudden decrease in the slope of conductivity vs.  $\text{C}_{14}\text{TABr}$  concentration at a  $\text{C}_{14}\text{TABr}$  concentration of 4 mM is attributable to the critical micelle concentration (CMC) of the surfactant [5].

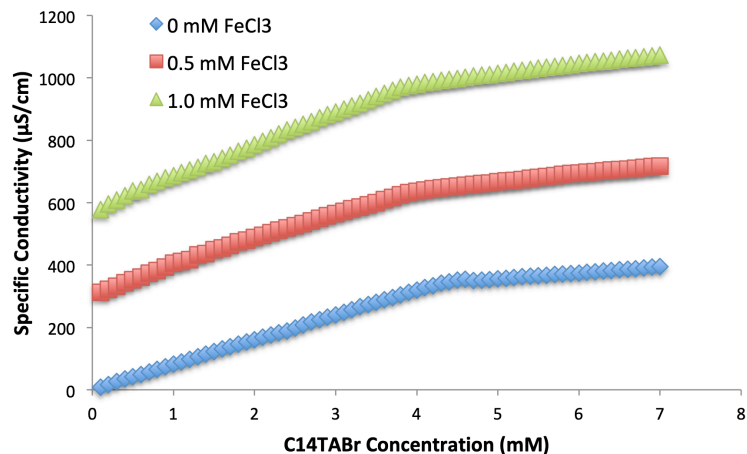


Figure 3.8: Specific conductivity vs.  $C_{14}TABr$  concentration for three constant solution concentrations of aqueous iron(III) trichloride. There does not appear to be ionic complexation occurring outside of the formation of micelles in solution.

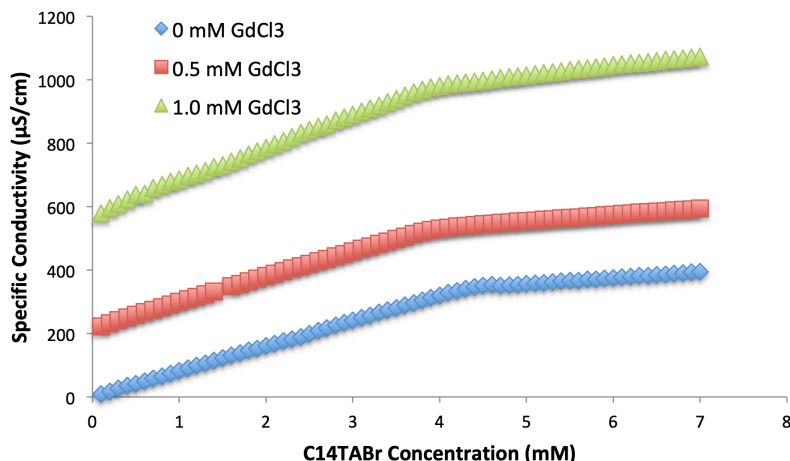


Figure 3.9: Specific conductivity vs.  $C_{14}TABr$  concentration for three constant solution concentrations of aqueous gadolinium(III) trichloride. There does not appear to be ionic complexation occurring outside of the formation of micelles in solution.

To test this latter explanation, we performed aqueous solution conductivity measurements of  $C_{16}TAFECl_3Br$ ,  $C_{16}TABr$  and  $C_{16}TABr + 2$  molar equivalents of  $NaCl$  to compare the results. Our hypothesis behind this test was if the ion  $FeCl_3Br^-$  is unstable in aqueous solution, and if for simplicity we ignore hydrolysis and the formation of  $Fe(OH)_x$  species, then each addition of

$C_{16}TAF_{e}Cl_{3}Br$  below the CMC would yield approximately 6 ionic species per  $C_{16}TAF_{e}Cl_{3}Br$  molecule ( $C_{16}TA^{+}$ ,  $Fe^{3+}$ ,  $Br^{-}$ , and three  $Cl^{-}$ 's), and the solution conductivity would, therefore, be much higher than that of  $C_{16}TABr$ . We included  $C_{16}TABr + 2$  molar equivalents of  $NaCl$  for comparison in this experiment since there should be little to no complexation occurring between these species in solution and each addition of surfactant would yield six ionic species per  $C_{16}TABr$  molecule. Therefore, if the complex ion  $FeCl_{3}Br^{-}$  is stable in aqueous solution, the solution conductivity of  $C_{16}TAF_{e}Cl_{3}Br$  should look more similar to that of  $C_{16}TABr$  than  $C_{16}TABr + 2$  molar equivalents of  $NaCl$ . As the results in Figure 10 show, the solution conductivity of  $C_{16}TAF_{e}Cl_{3}Br$  was more comparable to that of  $C_{16}TABr + 2$  molar equivalents of  $NaCl$  than it was to  $C_{16}TABr$ . These results indicate to us that there are  $\approx 6$  ionic species in solution per molecule of  $C_{16}TAF_{e}Cl_{3}Br$  and, hence, the anion  $FeCl_{3}Br^{-}$  may be breaking up in aqueous solution into its constituent ionic species. Figure 10 also shows that the CMC of  $C_{16}TABr + 2$  molar equivalents of  $NaCl$  is not as easy to determine as a solution of pure  $C_{16}TABr$  in water, and thus the increased ionic strength due to the  $NaCl$  ions appear to be “swamping out” the CMC. Therefore, we believe that the high solution conductivity, of the magnetic surfactants are actually indicative of the instability of their metal halide counterions while in aqueous solution (As can be seen from comparing Figure 3.4 with Figure 3.10).

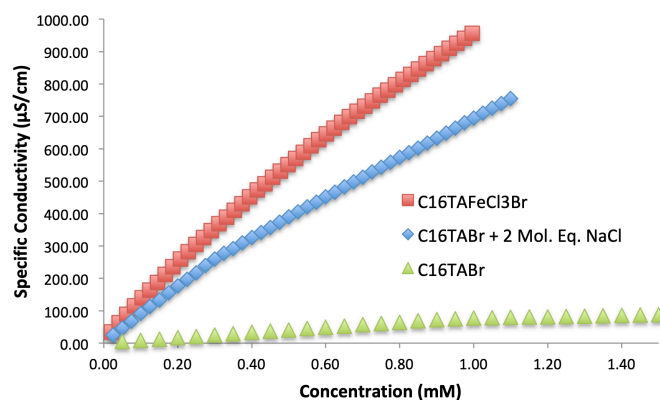


Figure 3.10: The specific conductivity of  $C_{16}TAFECl_3Br$ ,  $C_{16}TABr + 2$  molar equivalents of  $NaCl$ , and  $C_{16}TABr$  in aqueous solution. The high conductivity of the iron(III) containing surfactant seems to indicate instability of the metal halide counterions.

#### 3.4.3.4 $C_{16}TAFECl_3Br$ Solution pH Indication of Anion Stability

Iron(III) cations are known to undergo hydrolysis when dissolved in aqueous solutions and form various iron(III) hydroxide species [46]. Because of this, aqueous solutions containing iron(III) cations typically have acidic pH values. We hypothesized that if there is a decrease in solution pH of an aqueous iron(III) tetrahalide based cationic surfactant solution, then that would indicate that the  $Fe^{3+}$  ions are coordinating with  $OH^-$  anions, and hence the metal tetrahalide complex ion is dissociating when exposed to an aqueous solution. To test this hypothesis, we measured the pH of 5 mM aqueous solutions of  $C_{16}TAFECl_3Br$ ,  $FeCl_3$  and  $C_{16}TABr$ . Our experimental results are summarized in Table 3.3 and demonstrate that there is indeed a greater drop in solution pH when the magnetic surfactant  $C_{16}TAFECl_3Br$  is dissolved into water. The pH value is approximately the same as that of an equimolar solution of  $FeCl_3$  in water and much less than that of the surfactants nonmagnetic counterpart  $C_{16}TABr$ . We believe this is further evidence of the instability of metal halide-based cationic surfactants in aqueous solution.

Table 3.3: The approximate pH values of an aqueous solution of  $C_{16}TAF_{e}Cl_{3}Br$  as well as  $FeCl_{3}$  and  $C_{16}TABr$  for comparison. The magnetic surfactant solution is clearly undergoing hydrolysis much like the metal halide solution, which is evidence of the instability of the complex anion  $FeCl_{3}Br^{-}$  in aqueous solution.

Solution	Concentration (mM)	pH
$C_{16}TAF_{e}Cl_{3}Br$	5	2.39
$FeCl_{3}$	5	2.48
$C_{16}TABr$	5	5.92

#### 3.4.4 Proposed Nature of Metal Halide Based Cationic Surfactants in Aqueous Solution Based on Anion Stability Measurements

In order to unify some of the observed phenomena of these magnetic Type 1 cationic surfactants with the results of the investigation of their stability, we propose that metal-halide based Type 1 cationic surfactants almost completely ionize in aqueous solution leaving single halide anions to act as the counterions to the surfactant micelles, while the metal cations exist almost entirely in the bulk solution and interact very little with the micelles. Therefore, these surfactants should not be considered “magnetic surfactants” while existing in aqueous solution, but instead, they should be considered ordinary cationic surfactants that are suspended in a paramagnetic bulk fluid where the paramagnetic ions do not seem to be constituent parts of the surfactant amphiphiles or micellar complexes. We believe this conclusion echoes the conclusion of Degen et al [26].

### 3.5 Conclusions

While metal halide-based magnetic cationic surfactants may be stable in certain non-aqueous media, our electrochemical and pH investigations indicate that they are unstable in aqueous media. We propose the following alternative explanation for their behavior in water; some or all of their complex metal halide anions break up into constituent ions with halide anions



acting as the surfactant counterions to the surfactant amphiphiles and micelles while the paramagnetic ions do not associate with the surfactants. Therefore these surfactants do not truly act like magnetic surfactants while in water. Instead, they should be considered ordinary cationic surfactants that are suspended in a paramagnetic bulk fluid. A single drop of a paramagnetic fluid could still be moved by a magnet and not be an indication of a magnetic alteration of surfactant properties. We believe that this last point is in agreement with the conclusion of Degen et al. [26].

For our study we defined magnetic surfactants as a system where the paramagnetic ion ( $\text{Fe}^{3+}$ ,  $\text{Co}^{2+}$ ,  $\text{Mn}^{2+}$ , etc.) is strongly associated with the surfactant micelles. In our future work, we will look for magnetic surfactants that are anionic with single-atom paramagnetic counterions and for surfactants that contain ferromagnetic metals chelated directly with the unimer headgroup. We will no longer look for cationic magnetic surfactants with metal-halide counterions.

## CHAPTER IV

### 4 The Investigation of Various Other Magnetic Surfactants

#### 4.1 Introduction

As discussed in Chapter I, one of the goals of this project is to investigate single-molecule surfactants for their use in low energy separations. To accomplish this, these surfactants must first be synthesized, and their properties in aqueous solution (stability, solubility, etc.) investigated to determine their suitability for the proposed separations processes. This chapter is a continuation of Chapter III, and provides a review of the rest of the magnetic surfactants that were synthesized during the course of the work described in this thesis. This chapter covers other Type I ionic and Type IIa surfactants that we synthesized. For the most part, these surfactants were found to be unsuitable for further investigation involving low energy separations processes for a few reasons usually involving either instability in aqueous solution or low solubility.

#### 4.2 Methods and Materials

##### 4.2.1 Cationic magnetic redoxable surfactant synthesis

The non-magnetic redoxable surfactant precursor was first synthesized according to a method found in the literature [3]. Then the bromide counterion was exchanged for a paramagnetic metal tetrahalide ion according to procedures described elsewhere in the literature [20].

#### 4.2.2 Anionic magnetic surfactant synthesis

These surfactants were synthesized by forming aqueous solutions of nonmagnetic precursors (such as sodium stearate or sodium dodecyl sulfate) and then adding an aqueous metal chloride solution (such as  $\text{FeCl}_3$  or  $\text{MnCl}_2$ ). The magnetic surfactant precipitates were then collected via filtration and purified by either washing three times with DI water, or recrystallization in DI water three times. The solid products were then dried under vacuum overnight.

#### 4.2.3 Type IIa magnetic surfactant synthesis

The Gemini EDTA surfactant was synthesized according to a method found in the literature [47]. The coordination to paramagnetic ions was achieved by mixing aqueous solutions of the surfactant with aqueous solutions of metal chlorides. The magnetic surfactant precipitate was recovered via vacuum filtration and then washed three times with DI water followed by drying overnight at  $40^\circ\text{C}$  under reduced pressure. The triamine surfactant was synthesized and coordinated to paramagnetic ions according to a previous literature method [48].

#### 4.2.4 Characterization

Dynamic light scattering characterization was performed with the  $\text{Co}^{2+}$  Gemini EDTA surfactant at 90 degrees with an LSI Instruments 3D LS spectrometer.

## 4.3 Results and Discussion

### 4.3.1 Type I magnetic cationic surfactants: redoxable magnetic surfactants

As mentioned in Chapter III, the cationic metal-halide based magnetic Type I surfactants are not stable in aqueous solution. These surfactants are omitted from this chapter since they were adequately discussed in that chapter. This section discusses a similar class of surfactants that this project set out to investigate- the Type I cationic magnetic redoxable surfactants.

The first step in designing such a process involves the synthesis of magnetic redoxable surfactants. Our hypothesis was that we could synthesize the cationic ferrocene-based redoxable surfactants developed by Saji et al. [3] [49] and then exchange the  $\text{Br}^-$  counterion for a paramagnetic metal tetrahalide anion such as  $[\text{GdCl}_3\text{Br}]^-$  following the simple synthesis procedure proposed by Eastoe et al. in their synthesis of cationic Type I magnetic surfactants [18] [20]. This type of surfactant is depicted in Figure 3.1 with a generic paramagnetic counterion.

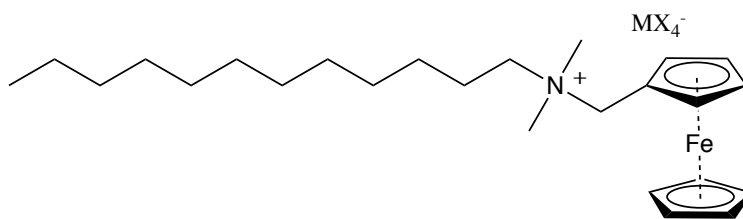
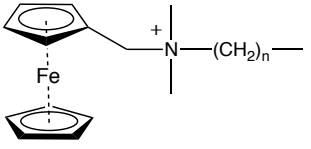


Figure 4.1: A magnetic redoxable surfactant

The first issue we encountered with this kind of surfactant was when we were attempting to exchange the halide counterion with a iron(III) containing counterion such as  $[\text{FeCl}_3\text{Br}]^-$ . When a solution containing iron(III) contacted a solution containing the ferrocene surfactant, oxidation of the ferrocene moiety occurred. This is unsurprising since  $\text{FeCl}_3$  solutions can be used to oxidize similar ferrocene-containing surfactants [11]. After this, we decided to limit the

potential counterions to  $\text{Gd}^{3+}$  and  $\text{Co}^{2+}$  based species. The conductivity vs. concentration of one particular species of this type of surfactant appeared to be similar to the conductivity vs. concentration data of typical cationic metal halide based Type I surfactants. These results are unsurprising since the paramagnetic counterions of the redoxable surfactants are also metal halide complexes, and as discussed in Chapter III, cationic metal halide based Type I magnetic surfactants' counterions appear to be ionizing while in aqueous solution. Therefore, we decided to abandon this particular class of surfactant due to the instability of the paramagnetic moiety. A summary of the different cationic Type I redoxable magnetic surfactants that were synthesized is depicted in Table 3.1.

Table 4.1: Failed Redoxable Magnetic Surfactants

Surfactant	Tail Length (n+1)	Counterion	Observations
	12	$[\text{FeCl}_3\text{Br}]^-$	Not Stable. $\text{Fe}^{3+}$ oxidizes ferrocene.
	14	$[\text{GdCl}_3\text{Br}]^-$	Counterion not stable in water.
	16	$[\text{CoCl}_2\text{Br}_2]^{2-}$	Counterion not stable in water.

The nonmagnetic surfactant precursor was synthesized from [49].

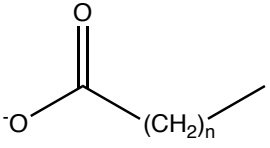
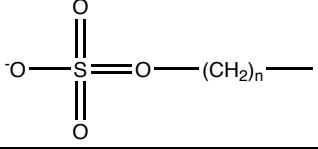
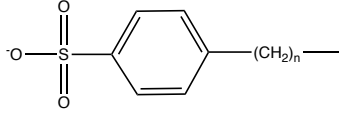
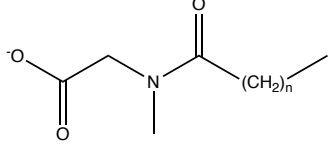
#### 4.3.2 Anionic Type I Magnetic Surfactants

Due to the instability of the cationic metal halide based Type I magnetic surfactants, we decided to synthesize Type I magnetic anionic surfactants, which contain single atom paramagnetic counterions. Our hypothesis was that these surfactants should be inherently stable in water since their magnetic moieties cannot break apart and will associate with micelles in solution.

We examined various kinds of potential Type I magnetic anionic surfactants as depicted in Table 3.2. Most of our attempts to synthesize a suitable anionic magnetic surfactant were

unsuccessful due to water solubility issues, which is not surprising. Paramagnetic ions tend to be divalent or trivalent, and anionic surfactants are often susceptible to precipitation when encountering multivalent ions in solution. The only successful example of this class was manganese didodecyl sulfate (MnDDS), which was discussed in Chapter III.

Table 4.2: Failed Type I magnetic anionic surfactants

Surfactant	Tail Length (n+1)	Counterion	Observations
	8	Dy <sup>3+</sup>	Low water solubility
	16	Fe <sup>3+</sup>	
	18	Co <sup>2+</sup> Mn <sup>2+</sup>	
	12	Dy <sup>3+</sup> Co <sup>2+</sup>	Low water solubility
	12	Co <sup>2+</sup> Mn <sup>2+</sup>	Low water solubility
	11	Mn <sup>2+</sup>	Low water solubility

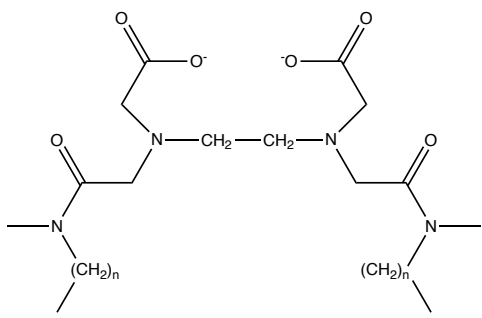
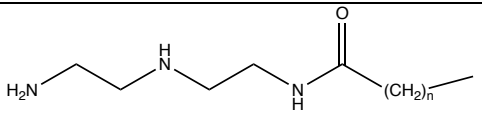
The Co<sup>2+</sup> dodecyl sulfate surfactant has been reported previously in the literature [16].

#### 4.3.3 Type IIa Magnetic Surfactants

To expand our magnetic surfactant catalog beyond MnDDS, we also attempted to synthesize two kinds of Type IIa magnetic surfactants, which contained paramagnetic elements chelated to the headgroups based on similar surfactants found in the literature [48] [47]. The surfactants formed with the triamine headgroup were observed to be unstable in aqueous

solution. Surfactants formed from the EDTA-based Gemini surfactant were either insoluble directly in water or dissolved very slowly. The  $\text{Co}^{2+}$  based surfactant was dissolved in water by first dissolving it in methanol and then dialyzing it in water with 1000 MWCO dialysis tubing. The resulting colloid was a cloudy pink solution. The aggregates formed from this compound were investigated by dynamic light scattering and were found to be  $130.9 \text{ nm} \pm 17.5 \text{ nm}$ . The results for this type of surfactant are summarized in Table 3.3. Note: stable Type IIa surfactants described in Chapter II are being investigated as potential magnetic surfactants in a different part of this project and were not investigated in this work.

Table 4.3: Type IIa Surfactants

Surfactant	Tail Length (n+1)	Counterion	Observations
	12	$\text{Gd}^{3+}$ $\text{Co}^{2+}$ $\text{Mn}^{2+}$	Low water solubility. The $\text{Co}^{2+}$ version had to be dissolved in methanol and then dialyzed into water.
	16 18	$\text{Fe}^{3+}$ $\text{Co}^{2+}$	Unstable in water

These surfactants were synthesized according to the literature methods found in the following references: [47] [48].

## CHAPTER V

### 5 Magnetic Polymer Solubilization Experiments

#### 5.1 Introduction

In addition to our previous work involving magnetic unimeric surfactants described in Chapters III and IV, we set about to investigate the synthesis and the feasibility of magnetic polymeric surfactants to separate an organic compound from water via a magnetic swing. According to Zubarev [4], organic polymer molecules with embedded magnetic centers should undergo a change in free volume as they are exposed to an external magnetic field. This increase in free volume translates into an increase in the molar volume of the polymer. Thus, we hypothesized that if we synthesized magnetic polymeric micelles capable of solubilizing hydrophobic molecules then these species may exhibit an increased solubilization capacity while inside of a parallel magnetic field versus when outside of a magnetic field. If this hypothesis were correct, then this could allow for the construction of a magnetic separation device, which would rely on a magnetic swing as the mode of separation to separate dissolved organic compounds from a contaminated aqueous feed solution.



## 5.2 Experimental/Methodology

### 5.2.1 Materials

Polystyrene-block-poly(acrylic acid), DDMAT terminated (PS:PAA 3,000:5,000, PDI  $\leq$  1.1) (PS<sub>29</sub>-b-PAA<sub>69</sub>) and Anthracene 98% were purchased from Sigma Aldrich. Polystyrene-block-poly(acrylic acid) Mn\*10<sup>3</sup> (g/mol): 28-b-70 was purchased from Polymer Source, NaOH, Toluene, and Naphthalene 99% were purchased from Fisher Scientific. MnCl<sub>2</sub> anhydrous was purchased from American Elements. DI water was used throughout the course of the experiments.

### 5.2.2 Polymer Synthesis

The magnetic polymers used in this experiment were PS<sub>29</sub>-b-P(NaA<sub>0.6</sub>-co-Mn(A<sub>2</sub>)<sub>0.4</sub>)<sub>69</sub> (hereby denoted “MagPolySurfA”) and PS<sub>268</sub>-b-P(NaA<sub>0.75</sub>-co-Mn(A<sub>2</sub>)<sub>0.25</sub>)<sub>967</sub> (hereby denoted “MagPolySurfB”). The numbers denote the number of repeating units in each block. The first steps in the synthesis procedure were to deprotonate the acrylic acid groups on the polymer and to dissolve it in an aqueous solution. This was accomplished by mixing the polymer into DI water, and adding NaOH in a 1:1 molar ratio to acrylic acid groups on the polymer. Then the next step of the synthesis involved coordinating Mn<sup>2+</sup> ions to the acrylate groups on the polymer. This was accomplished by adding a 0.1M aqueous solution of MnCl<sub>2</sub> to solution drop wise under vigorous stirring until the Mn<sup>2+</sup> Acrylate/Na<sup>+</sup> Acrylate ratio was equal to 0.4 (an estimated 40% of the acrylate groups were coordinated to manganese) for MagPolySurfA, and 0.25 for MagPolySurfB. Figure 5.1 is a depiction of both polymers used in the experiments. For MagPolySurfA, m = 29, n = 69, x = 28, and y = 41. For MagPolySurfB, m = 268, n = 967, x = 242, and y = 726.

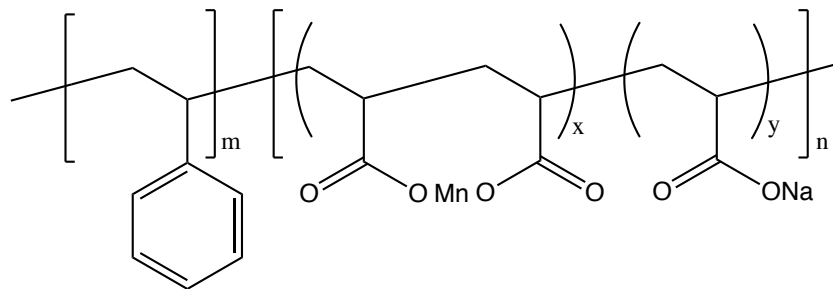


Figure 5.1: The magnetic polymers used in the solubilization experiments.  $PS_{29}\text{-}b\text{-}P(\text{NaA}_{0.6}\text{-co-Mn}(\text{A}_2)_{0.4})_{69}$  (MagPolySurfA) and  $PS_{268}\text{-}b\text{-}P(\text{NaA}_{0.75}\text{-co-Mn}(\text{A}_2)_{0.25})_{967}$  (MagPolySurfB).

### 5.2.3 Dynamic Light Scattering

Dynamic light scattering measurements were performed on dilute samples of MagPolySurfA and MagPolySurfB in water with an LSI Instruments 3D LS Spectrometer. Each sample was sonicated in warm water for 30 minutes prior to measurement at a 90 degree angle.

### 5.2.4 Solubilization Experiments

The solubilization experiments consisted of adding an excess of an organic contaminant (2 ml of toluene, 20 mg of naphthalene or 20 mg of anthracene) to two separate vials containing several ml aqueous solution of MagPolySurfA at a concentration of 1 mg/ml or MagPolySurfB at a concentration of 0.5 mg/ml. One of the vials was then placed inside of parallel magnetic fields at 30°C and the other vial was left outside of the field at 30°C. After equilibrating for several days, both solutions were extracted and placed into a 0.5 cm quartz UV-Vis cuvette. The toluene samples were extracted with a syringe inserted below the excess toluene layer and the naphthalene and anthracene samples were extracted with a syringe and then dispensed through a 0.22  $\mu\text{m}$  or a 0.45 $\mu\text{m}$  syringe filter. These solutions were then subjected to a UV-Vis scan to determine the relative amounts of dissolved contaminant. The samples were placed back inside

of their respective vials and then left alone for another 24 hours and another UV-Vis scan was taken for comparison. Each experiment was then repeated two more times. For the toluene and naphthalene samples, scans were performed from 400 nm to 240 nm and for the anthracene samples scans were performed from 410 nm to 355 nm.

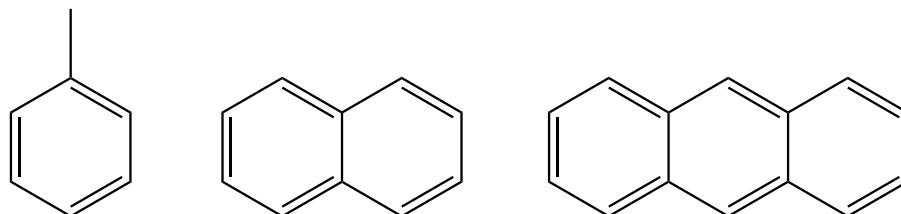


Figure 5.2: The organic contaminants used in the polymer solubilization experiments. From left to right: toluene, naphthalene and anthracene.

### 5.2.5 Calculations

For all scans, a baseline absorbance and an organic peak absorbance were selected. The baseline absorbance was selected as an absorbance of the polymer that was outside of the organic contaminant absorbance, and the organic peak absorbance was selected as the absorbance of the organic contaminant at its' highest value. The specific wavelengths of these absorbances are stated in Table 5.1.

Table 5.1: The wavelengths of the baseline and organic contaminant absorbances for MagPolySurfA and MagPolySurfB

	MagPolySurfA		MagPolySurfB	
	Organic	Baseline	Organic	Baseline
Toluene	260	310	260	310
Naphthalene	269	310	266	310
Anthracene	381	400	381	400

The following formula was used to determine the relative amounts of organic contaminant in the magnet and nonmagnet samples:

$$(M_1 - NM_1) - Y(M_2 - NM_2) = Z$$

Where:  $M_1$  is the absorbance of the organic contaminant peak for the magnet sample,  $NM_1$  is the absorbance of the organic contaminant peak for the nonmagnet sample, and  $Y$  is the ratio of the absorbance at the organic contaminant peak wavelength to the absorbance at the baseline wavelength of a polymer sample without organic contaminants. For the anthracene runs,  $Y$  was assumed to be 1.  $M_2$  is the absorbance of the baseline for the magnet sample,  $NM_2$  is the absorbance of the baseline for the nonmagnet sample, and  $Z$  is a number used to determine the relative amounts of organic contaminant concentration.  $Z$  is a positive number if there is more organic contaminant in the magnet sample, and is a negative number if there is less organic contaminant in the magnet sample. When an error analysis was performed and if  $Z$  was found to be either positive or negative, the results were determined to be inconclusive. An example calculation for MagPolySurfA samples saturated with toluene can be found in Appendix B.

## 5.3 Results and Discussion

### 5.3.1 Polymer Characterization

The aggregate diameters of MagPolySurfA and MagPolySurfB were investigated via dynamic light scattering. Both samples demonstrated inter-aggregate aggregation in solution and required sonication prior to measuring. The MagPolySurfA sample was sonicated for 2 hours in warm water prior to DLS analysis, and consisted of a monodisperse population of aggregates with diameters of  $23.9 \pm 11.2$  nm. The MagPolySurfB sample was sonicated in warm water for 30 minutes prior to DLS analysis and displayed various aggregate size distributions with the average being  $725.34 \pm 302$  nm. The large aggregate size is probably a result of the

agglomeration of smaller aggregates.

The UV-Vis absorbance spectrums for MagPolySurfA and MagPolySurfB in water are displayed in Figures 5.2 and 5.3.

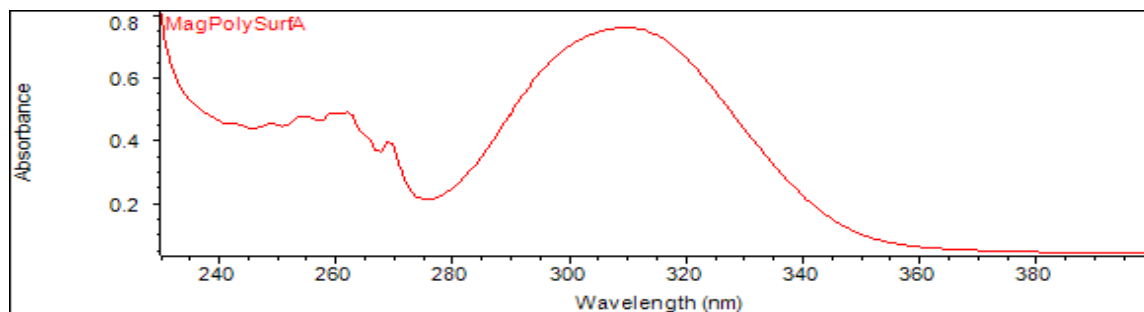


Figure 5.3: The UV-Vis absorbance spectrum of MagPolySurfA in water.

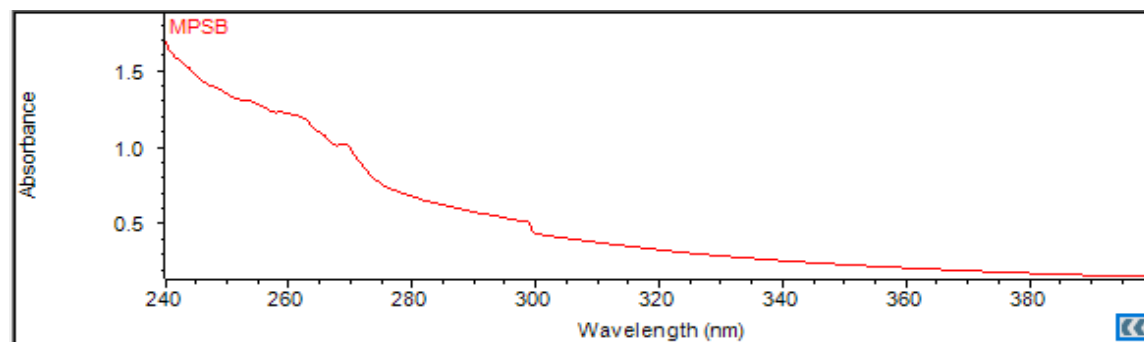


Figure 5.4: The UV-Vis absorbance spectrum of MagPolySurfB in water.

### 5.3.2 Toluene Solubilization

The UV-Vis absorbance spectrum for toluene in water is shown in Figure 5.4 and the absorbance spectrum for MagPolySurfA and MagPolySurfB samples saturated with toluene that were placed inside and outside of a magnetic field are shown in Figures 5.5 and 5.6 respectively. The magnetic field strength for the MagPolySurfA samples was 0.68 T and the magnetic field strength for the MagPolySurfB samples was 0.52 T. When toluene is solubilized into the polymer aggregates, it displays a prominent UV-Vis absorbance peak around 260 nm. The

absorbance spectrum images corresponding to some of the experiments are displayed in Appendix B.

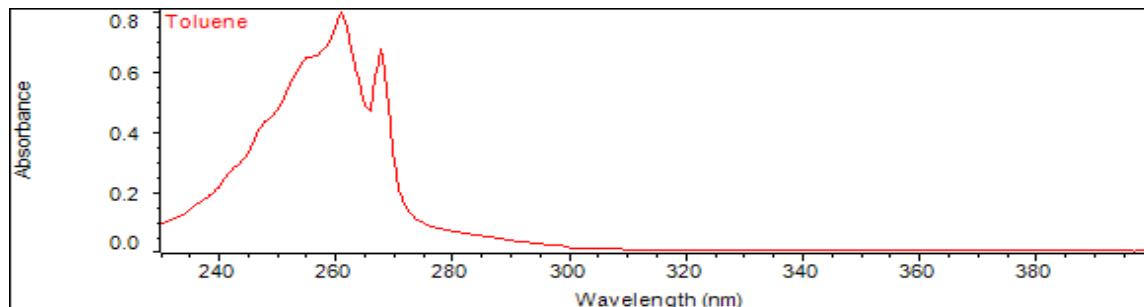


Figure 5.5: The UV-Vis absorbance spectrum of water saturated with toluene.

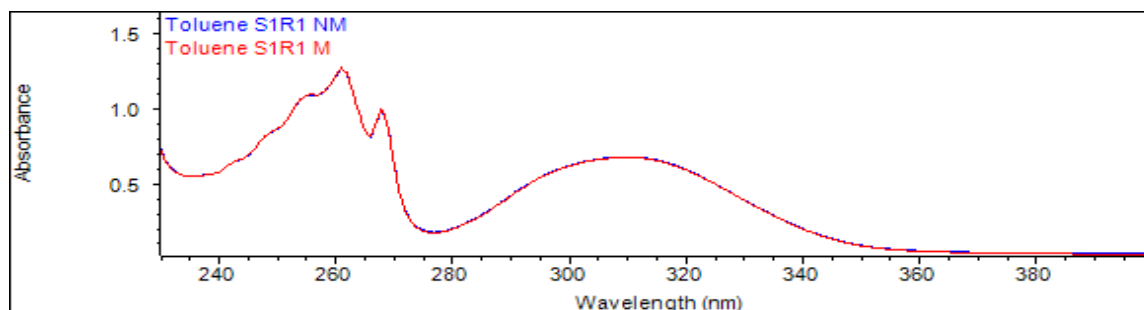


Figure 5.6: The UV-Vis absorbance spectrum of MagPolySurfA samples in water saturated with toluene. Where “M” represents the sample placed inside of a parallel magnetic field, and “NM” represents the sample placed outside of a parallel magnetic field.

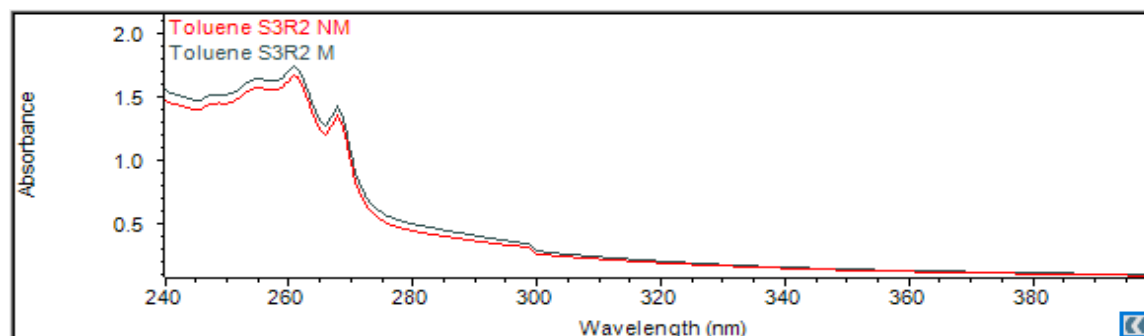


Figure 5.7: The UV-Vis absorbance spectrum of MagPolySurfB samples in water saturated with toluene. Where “M” represents the sample placed inside of a parallel magnetic field, and “NM” represents the sample placed outside of a parallel magnetic field.

The results for MagPolySurfA and MagPolySurfB are displayed in Tables 5.2 and 5.3.

For MagPolySurfA, there was 1 positive result showing more toluene present in the sample that

was placed inside of the magnetic field, 1 negative result showing less toluene present in the magnetic field and 4 neutral results showing inconclusive results about the relative amounts of toluene in the samples. For MagPolySurfB, there were 1 positive run and 5 neutral runs. Overall, the results did not demonstrate an increase in toluene concentration in a polymer sample that was placed inside of a parallel magnetic field.

Table 5.2: MagPolySurfA Toluene Solubilization Results

	Run #	Sample	Organic ABS	Baseline ABS	Z	Results
Solution 1	1	M	1.276 ± 0.007	0.673 ± 0.0047	0.0114 ± 0.0235	Neutral
		NM	1.264 ± 0.007	0.672 ± 0.0047		
	2	M	1.252 ± 0.007	0.659 ± 0.0046	-0.0054 ± 0.0233	Neutral
		NM	1.258 ± 0.007	0.66 ± 0.0046		
Solution 2	1	M	1.241 ± 0.007	0.561 ± 0.0042	-0.0709 ± 0.0224	Negative
		NM	1.28 ± 0.007	0.51 ± 0.0040		
	2	M	1.328 ± 0.007	0.556 ± 0.0042	-0.0164 ± 0.0228	Neutral
		NM	1.315 ± 0.007	0.509 ± 0.0040		
Solution 3	1	M	1.386 ± 0.008	0.578 ± 0.0043	0.0296 ± 0.0234	Positive
		NM	1.342 ± 0.007	0.555 ± 0.0042		
	2	M	1.378 ± 0.008	0.566 ± 0.0043	-0.0035 ± 0.0236	Neutral
		NM	1.389 ± 0.008	0.578 ± 0.0043		

Table 5.3: MagPolySurfB Toluene Solubilization Results

	Run #	Sample	Organic ABS	Baseline ABS	Z	Results
Solution 1	1	M	1.536 ± 0.0081	0.175 ± 0.0027	-0.0007 ± 0.0215	Neutral
		NM	1.5 ± 0.0080	0.166 ± 0.0027		
	2	M	1.574 ± 0.0083	0.175 ± 0.0027	-0.0059 ± 0.0221	Neutral
		NM	1.588 ± 0.0084	0.177 ± 0.0027		
Solution 2	1	M	1.716 ± 0.0089	0.203 ± 0.0028	0.0187 ± 0.0232	Neutral
		NM	1.681 ± 0.0087	0.199 ± 0.0028		
	2	M	1.783 ± 0.0091	0.213 ± 0.0029	0.0507 ± 0.0237	Positive
		NM	1.716 ± 0.0089	0.209 ± 0.0028		
Solution 3	1	M	1.483 ± 0.0079	0.162 ± 0.0026	0.0014 ± 0.0213	Neutral
		NM	1.506 ± 0.0080	0.168 ± 0.0027		
	2	M	1.737 ± 0.0089	0.22 ± 0.0029	0.0150 ± 0.0233	Neutral
		NM	1.665 ± 0.0087	0.206 ± 0.0028		

### 5.3.3 Naphthalene Solubilization

The UV-Vis absorbance spectrum for naphthalene in water is shown in Figure 5.7 and the absorbance spectrum for MagPolySurfA and MagPolySurfB samples saturated with naphthalene that were placed inside and outside of a magnetic field are shown in Figures 5.8 and 5.9

respectively. The magnetic field strength for the MagPolySurfA and MagPolySurfB samples was 0.6 T. When Naphthalene is solubilized into the polymer aggregates, it displays a prominent UV-Vis absorbance peak around 266 nm. The absorbance spectrum images corresponding to some of the experiments are displayed in Appendix B.

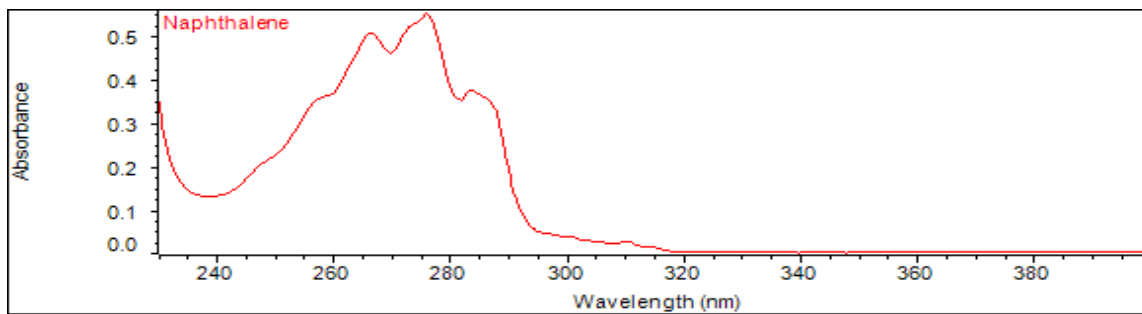


Figure 5.8: The UV-Vis absorbance spectrum of water saturated with naphthalene

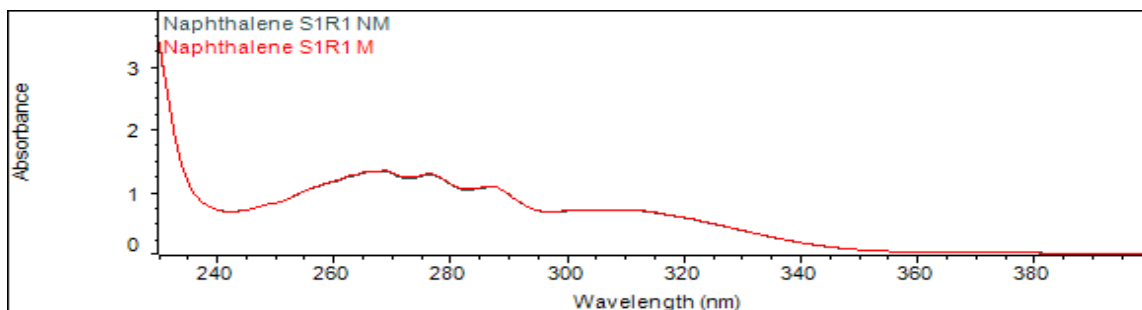


Figure 5.9: The UV-Vis absorbance spectrum of MagPolySurfA samples in water saturated with naphthalene. Where “M” represents the sample placed inside of a parallel magnetic field, and “NM” represents the sample placed outside of a parallel magnetic field.

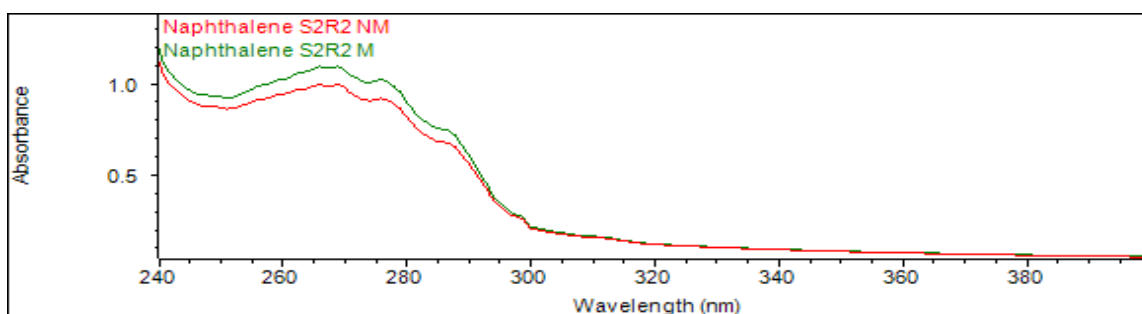


Figure 5.10: The UV-Vis absorbance spectrum of MagPolySurfB samples in water saturated with naphthalene. Where “M” represents the sample placed inside of a parallel magnetic field, and “NM” represents the sample placed outside of a parallel magnetic field.



The solubilization results for MagPolySurfA and MagPolySurfB are displayed in Tables 5.4 and 5.5. For MagPolySurfA, the results were: 3 positive runs, 2 negative runs and 1 neutral run. For MagPolySurfB, the results showed 4 positive runs, 1 negative run, and 1 neutral run. Overall, these results suggest that the presence of the parallel magnetic field may have increased the solubilization capacity for naphthalene of the polymer aggregates.

Table 5.4: MagPolySurfA Naphthalene Solubilization Results

	Run #	Sample	Organic ABS	Baseline ABS	Z	Results
<b>Solution 1</b>	1	M	1.339 ± 0.0074	0.705 ± 0.0048	0.0160 ± 0.0243	Neutral
		NM	1.324 ± 0.0073	0.707 ± 0.0048		
	2	M	1.335 ± 0.0073	0.703 ± 0.0048	0.0930 ± 0.0239	Positive
		NM	1.242 ± 0.0070	0.703 ± 0.0048		
<b>Solution 2</b>	1	M	1.059 ± 0.0062	0.666 ± 0.004664	-0.0495 ± 0.0220	Negative
		NM	1.112 ± 0.0064	0.673 ± 0.004692		
	2	M	1.042 ± 0.0062	0.655 ± 0.00462	-0.0255 ± 0.0217	Negative
		NM	1.068 ± 0.0063	0.656 ± 0.004624		
<b>Solution 3</b>	1	M	1.12 ± 0.0065	0.632 ± 0.004528	0.0350 ± 0.0220	Positive
		NM	1.096 ± 0.0064	0.654 ± 0.004616		
	2	M	1.101 ± 0.0064	0.618 ± 0.004472	0.0240 ± 0.0216	Positive
		NM	1.076 ± 0.0063	0.616 ± 0.004464		

Table 5.5: MagPolySurfB Naphthalene Solubilization Results

	Run #	Sample	Organic ABS	Baseline ABS	Z	Results
<b>Solution 1</b>	1	M	1.193 ± 0.0068	0.172 ± 0.0027	-0.0220 ± 0.0190	Negative
		NM	1.215 ± 0.0069	0.172 ± 0.0027		
	2	M	0.971 ± 0.0059	0.152 ± 0.0026	0.1124 ± 0.0165	Positive
		NM	0.843 ± 0.0054	0.147 ± 0.0026		
<b>Solution 2</b>	1	M	1.168 ± 0.0067	0.158 ± 0.0026	-0.0052 ± 0.0187	Neutral
		NM	1.192 ± 0.0068	0.164 ± 0.0027		
	2	M	1.234 ± 0.0069	0.17 ± 0.0027	0.1079 ± 0.0188	Positive
		NM	1.123 ± 0.0065	0.169 ± 0.0027		
<b>Solution 3</b>	1	M	1.203 ± 0.0068	0.173 ± 0.0027	0.1296 ± 0.0183	Positive
		NM	1.039 ± 0.0062	0.162 ± 0.0026		
	2	M	1.086 ± 0.0063	0.162 ± 0.0026	0.0669 ± 0.0176	Positive
		NM	0.991 ± 0.0060	0.153 ± 0.0026		

#### 5.3.4 Anthracene Solubilization

Water saturated with anthracene did not display an absorbance spectrum on our instrument probably due to the low water solubility of anthracene. The only time we were able to

detect anthracene on our UV-Vis spectrophotometer was when one of our polymer samples was present to solubilize the anthracene. Anthracene displays a prominent absorbance peak around 381 nm. Figure 5.10 shows the UV-Vis absorbance spectrum of a MagPolySurfA sample saturated with anthracene. Figures 5.11 and 5.12 show the absorbance spectra of MagPolySurfA and MagPolySurfB samples saturated with anthracene. The magnetic field strength for the MagPolySurfA and MagPolySurfB samples was 0.68 T. The absorbance spectrum images corresponding to some of the experiments are displayed in Appendix B.

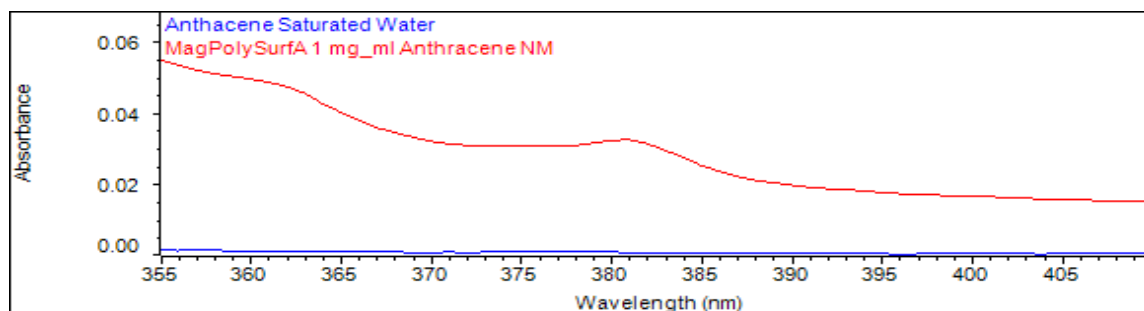


Figure 5.11: The absorbance spectrum of anthracene saturated water (blue line) and MagPolySurfA in water saturated with anthracene (red line)

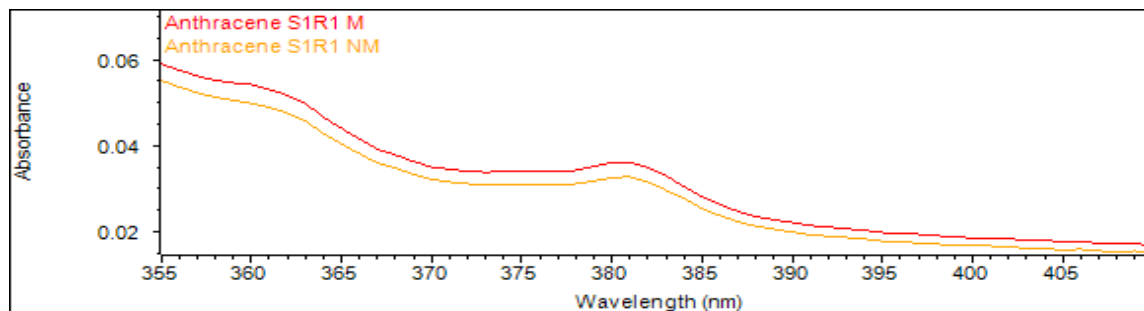


Figure 5.12: The UV-Vis absorbance spectrum of MagPolySurfA samples in water saturated with anthracene. Where “M” represents the sample placed inside of a parallel magnetic field, and “NM” represents the sample placed outside of a parallel magnetic field.

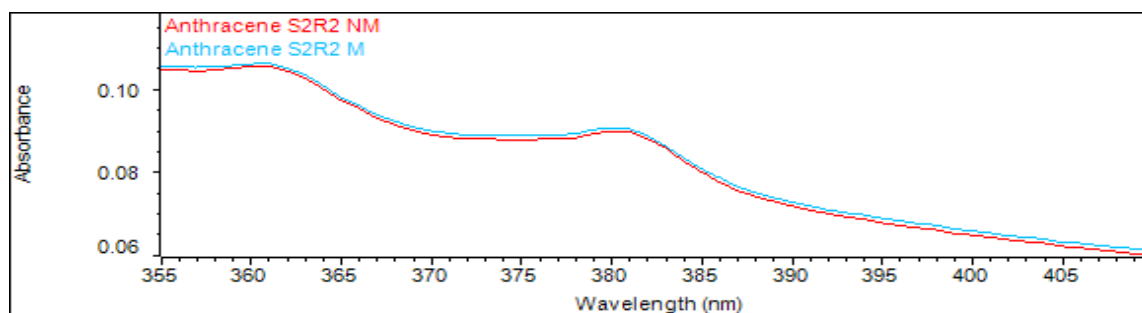


Figure 5.13: The UV-Vis absorbance spectrum of MagPolySurfB samples in water saturated with anthracene. Where “M” represents the sample placed inside of a parallel magnetic field, and “NM” represents the sample placed outside of a parallel magnetic field.

The solubilization results for MagPolySurfA and MagPolySurfB are displayed in Tables 5.6 and 5.7. For MagPolySurfA, the results were: 0 positive runs, 0 negative runs and 6 neutral runs. For MagPolySurfB, the results showed 0 positive runs, 0 negative runs and 6 neutral runs. Overall, these results suggest do not suggest that the presence of the parallel magnetic field may increase the solubilization capacity for anthracene in the polymer aggregates.

Table 5.6: MagPolySurfA Anthracene Solubilization Results

	Run #	Sample	Organic ABS	Baseline ABS	Z	Results
<b>Solution 1</b>	1	M	0.036 ± 0.0021	0.018 ± 0.0021	0.0020 ± 0.0084	Neutral
		NM	0.032 ± 0.0021	0.016 ± 0.0021		
	2	M	0.037 ± 0.0021	0.021 ± 0.0021	0.0000 ± 0.0084	Neutral
		NM	0.03 ± 0.0021	0.014 ± 0.0021		
<b>Solution 2</b>	1	M	0.028 ± 0.0021	0.016 ± 0.0021	0.0000 ± 0.0084	Neutral
		NM	0.029 ± 0.0021	0.017 ± 0.0021		
	2	M	0.028 ± 0.0021	0.017 ± 0.0021	-0.0030 ± 0.0084	Neutral
		NM	0.031 ± 0.0021	0.017 ± 0.0021		
<b>Solution 3</b>	1	M	0.035 ± 0.0021	0.022 ± 0.0021	0.0000 ± 0.0084	Neutral
		NM	0.031 ± 0.0021	0.018 ± 0.0021		
	2	M	0.031 ± 0.0021	0.016 ± 0.0021	0.0020 ± 0.0084	Neutral
		NM	0.029 ± 0.0021	0.016 ± 0.0021		

Table 5.7: MagPolySurfB Anthracene Solubilization Results

	Run #	Sample	Organic ABS		Baseline ABS		Z	Results
<b>Solution 1</b>	1	M	0.088	± 0.0024	0.06	± 0.0022	0.0000 ± 0.0092	Neutral
		NM	0.087	± 0.0023	0.059	± 0.0022		
	2	M	0.093	± 0.0024	0.065	± 0.0023	0.0010 ± 0.0093	Neutral
		NM	0.091	± 0.0024	0.064	± 0.0023		
<b>Solution 2</b>	1	M	0.084	± 0.00234	0.061	± 0.0022	-0.0020 ± 0.0092	Neutral
		NM	0.089	± 0.00236	0.064	± 0.0023		
	2	M	0.09	± 0.00236	0.066	± 0.0023	-0.0010 ± 0.0092	Neutral
		NM	0.09	± 0.00236	0.065	± 0.0023		
<b>Solution 3</b>	1	M	0.095	± 0.00238	0.07	± 0.0023	0.0010 ± 0.0093	Neutral
		NM	0.095	± 0.00238	0.071	± 0.0023		
	2	M	0.093	± 0.00237	0.068	± 0.0023	0.0010 ± 0.0093	Neutral
		NM	0.095	± 0.00238	0.071	± 0.0023		

#### 5.4 Conclusion and Outlook

The results discussed above indicate that the presence of a parallel magnetic field may be increasing the solubilization capacity of the polymer aggregates for naphthalene, but the results do not seem to demonstrate that the magnetic field is having an impact on the solubilization capacity for toluene or anthracene. Relative to the experimental results discussed so far in this work, the naphthalene solubilization experiments are highly encouraging and are worth investigating further, especially with the MagPolySurfB polymer. It may also be a good idea to investigate if a higher concentration of  $Mn^{2+}$  can be coordinated to this polymer.

## CHAPTER VI

### 6 Looking to the Future

#### 6.1 Magnetic Unimeric Surfactants

As discussed in this thesis, the magnetic cationic surfactants that have attracted much attention in the literature appear to not be stable in aqueous solution. This means that for magnetic surfactants to be applicable to low energy separations processes, they should either be anionic with single paramagnetic counterions, or Type II surfactants which possess paramagnetic ions as a constituent part of the surfactant unimer. There is work that is currently in progress on this project to synthesize a paramagnetic Type IIa surfactant.

If a Type II surfactant is successfully synthesized, then it may be redoxable if a suitable transition metal is selected. For example, a redox couple involving  $\text{Mn}^{2+}$  to  $\text{Mn}^{3+}$  could allow for the cationic charge of a surfactant to be increased via an oxidation reaction akin to the ferrocene-based cationic redoxable surfactants discussed in Chapters II and IV. Certain transition metal ions could be inherently paramagnetic assuming that the ligand headgroup does not cause a high degree of crystal field splitting of the metal electronic orbitals. One thing to keep in mind for a surfactant such as this would be auto-oxidation by dissolved oxygen. This has been observed for certain transition metal complexes that are chelated to certain ligand donors, like  $\text{Fe}^{2+}$  coordinated to EDTA.

It may be worth investigating if a cationic magnetic surfactant could be synthesized with

an anionic metal complex (such as MnEDTA) as a counterion. If a divalent metal is selected such as  $Mn^{2+}$  or  $Co^{2+}$ , then a cationic surfactant with two unimers could be synthesized. A drawing of a divalent metal ion coordinated to EDTA is shown in Figure 6.1. The main issue with this reaction would be removing the halide counterion of the cationic surfactants, which is usually  $Br^-$ . If a way to exchange the ions is figured out then the synthesis of the redoxable ferrocene-containing cationic surfactants could be realized if a metal anion is selected with a redox potential that is different enough than ferrocene so a large enough electrochemical operation window can be utilized. Since the redox potential of a lanthanide complex (such as GdEDTA) would be too far away from the redox potential of ferrocene, one could realistically oxidize and reduce the surfactant unimer without oxidizing or reducing the counteranion.

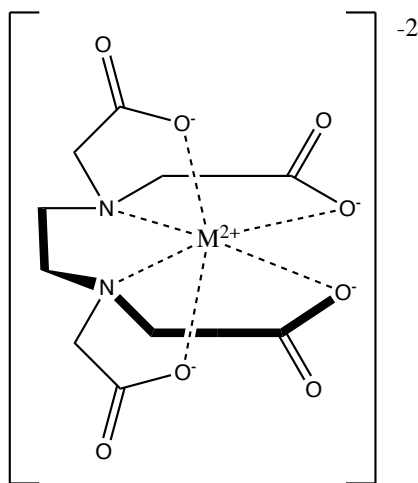


Figure 6.1: A divalent metal coordinated to EDTA forming an anionic complex.

## 6.2 Magnetic Polymeric Surfactants

As discussed in Chapter V of this thesis, there appeared to be no detectable change in solubilization capacity of the magnetic polymeric surfactants in aqueous solution, except for naphthalene. These results are encouraging and merit further investigation. In the future, when performing these experiments, it may be a better choice to use a gas chromatograph (GC) instead

of a UV-Vis. These experiments could be performed by forming a polymer solution with water that has been pre-saturated with an organic contaminant, and then sampling the headspace of the container to measure the amount of organic contaminant in the vapor phase. This experiment depends on the hypothesis that as the solubilization capacity of the polymer aggregates increases, then there would be less organic in the vapor phase as more organic would partition into the micelles.

It also may be worth investigating if the aggregates formed from these polymers in solution can be captured and removed from solution akin to the hypothetical processes involving the unimeric magnetic surfactant micelles. Since the magnetic polymer aggregates in water are larger than typical micelles and can solubilize organic compounds, they may be able to be captured and removed from solution by a high gradient magnetic field separator.

To enhance the magnetic response of the polymer, it would be a good idea to investigate polymer composites containing paramagnetic iron oxide nanoparticles (FeNPs) since the FeNPs should endow the polymer with greater magnetic response than the  $Mn^{2+}$  ions described in Chapter V. A hypothetical process is illustrated in Figure 6.2. The iron oxide particles could be incorporated into a hydrophobic polymeric gel, and the gel inserted into the tubes of a hollow fiber membrane with organic contaminated water on the shell side of the membrane. The organic contaminant could then partition into the polymer gel inside of the tubes. If the module is placed into a parallel magnetic field, the polymer gel may experience an increase in free energy and a magnetically induced higher solubilization capacity causing the gel to absorb extra contaminant. Once the parallel magnetic field is removed, the extra organic contaminant would then be released from the gel and could be captured.

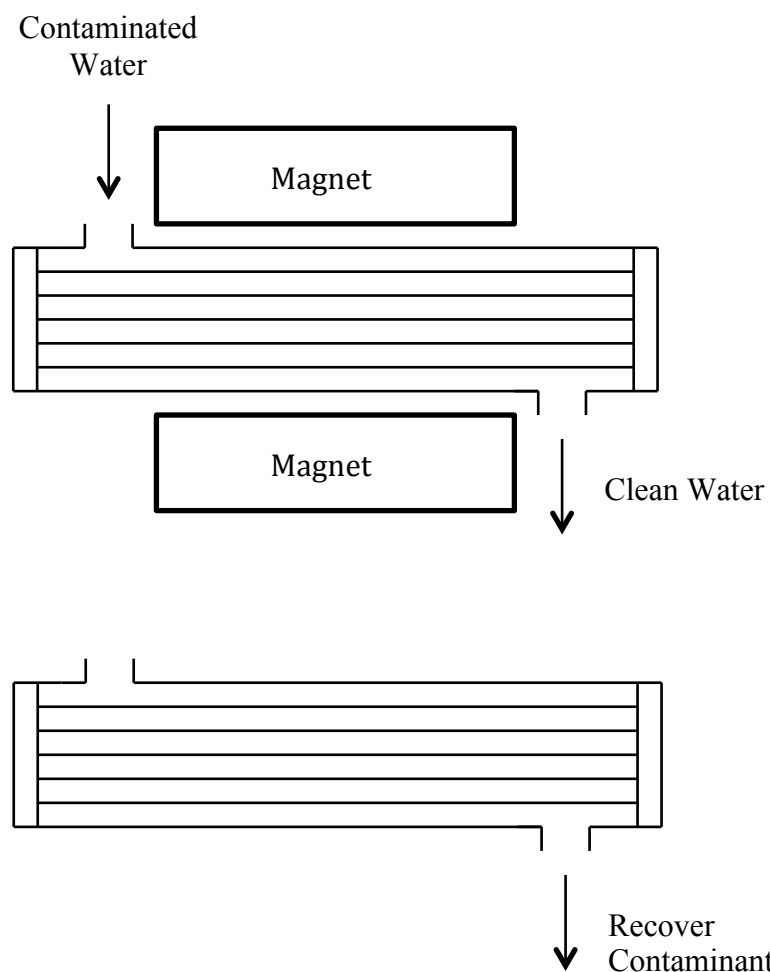


Figure 6.2: (Top) Water contaminated with organic molecules enters on the shell side of the membrane and partitions into the polymer composite contained inside of the tubes. (Bottom) When the magnets are removed, the super saturated polymer composite spits the organic contaminants out.

Another set of experiments that could be performed involving the magnetic polymer samples would be to place an aqueous polymer solution inside of dialysis tubing and then place this solution into a vial containing water with an amount of organic contaminant like naphthalene or toluene below saturation. One vial could be placed inside of a magnetic field and one vial could be placed outside of a field. The water/contaminant solution outside of the tubing could be sampled and run on a UV-VIS for analysis of toluene or naphthalene concentration. If the hypothesis that the magnetic field will induce a greater solubilization capacity of the polymer



aggregates is correct, one should observe a decrease in contaminant concentration in the water outside of the tubing. This experiment would be an improvement upon the experiments described in Chapter V since it would eliminate the polymer UV-VIS signals and perhaps give data that is less noisy.

Appendix C contains standard operating procedures (SOPs) for the light scattering instrument, the tensiometer, and the UV-VIS spectrophotometer, which should help with future work performed on this project.

## LIST OF REFERENCES

- [1] R. D. Noble and R. Agrawal, "Separations research needs for the 21st century," *Ind. Eng. Chem. Res.*, vol. 44, no. 9, pp. 2887–2892, 2005.
- [2] M. Buonomenna and G. Golemme, "Advanced Materials for Membrane Preparation." Bentham Books.
- [3] T. Saji, K. Hoshino, and S. Aoyagui, "Reversible formation and disruption of micelles by control of the redox state of the head group," *J. Am. Chem. Soc.*, vol. 107, no. 24, pp. 6865–6868, 1985.
- [4] A. Y. Zubarev, "To the theory of rheological properties of magnetopolymer suspensions," *Soft Matter*, vol. 9, no. 40, pp. 9709–9713, 2013.
- [5] Milton J. Rosen., *Surfactants and interfacial phenomena*, 3rd ed. John Wiley & Sons, Inc, 2004.
- [6] V. P. Torchilin, "Structure and design of polymeric surfactant-based drug delivery systems," *J. Control. Release*, vol. 73, no. 2–3, pp. 137–172, 2001.
- [7] P. Brown, C. P. Butts, and J. Eastoe, "Stimuli-responsive surfactants," *Soft Matter*, vol. 9, no. 8, pp. 2365–2374, 2013.
- [8] S. Polarz, M. Kunkel, A. Donner, and M. Schlötter, "Added-Value Surfactants," *Chem. - A Eur. J.*, vol. 24, no. 71, pp. 18842–18856, 2018.
- [9] X. Liu and N. L. Abbott, "Spatial and temporal control of surfactant systems," *J. Colloid Interface Sci.*, vol. 339, no. 1, pp. 1–18, 20
- [10] T. Saji, K. Hoshino, Y. Ishii, and M. Goto, "Formation of Organic Thin Films by

- Electrolysis of Surfactants with the Ferrocenyl Moiety,” *J. Am. Chem. Soc.*, vol. 113, no. 2, pp. 450–456, 1991.
- [11] Y. Takahashi, N. Koizumi, and Y. Kondo, “Demulsification of Redox-Active Emulsions by Chemical Oxidation,” *Langmuir*, vol. 32, no. 30, pp. 7556–7563, 2016.
- [12] Y. Takeoka *et al.*, “Electrochemical control of drug release from redox-active micelles,” *J. Control. Release*, vol. 33, no. 1, pp. 79–87, 1995.
- [13] X. Liu and N. L. Abbott, “Lateral transport of solutes in microfluidic channels using electrochemically generated gradients in redox-active surfactants,” *Anal. Chem.*, vol. 83, no. 8, pp. 3033–3041, 2011.
- [14] S. Polarz, S. Landsmann, and A. Kläiber, “Hybrid surfactant systems with inorganic constituents,” *Angew. Chemie - Int. Ed.*, vol. 53, no. 4, pp. 946–954, 2014.
- [15] Scopus\_Search, “‘Magnetic Surfactant’ or ‘Magnetic Surfactants.’” 2019.
- [16] S. Miyamoto, “The effect of metallic ions on surface chemical phenomena. III. Solubility of various metal dodecyl sulfates in water,” *Bull. Chem. Soc. Jpn.*, vol. 33, no. 3, pp. 371–375, 1960.
- [17] A. M. H. Shaikh, S. S. Banerjee, and S. G. Dixit, “Use of magnetic surfactants in the high gradient magnetic separation of essentially nonmagnetic calcite and barite,” *Sep. Technol.*, 1994.
- [18] P. Brown *et al.*, “Magnetic control over liquid surface properties with responsive surfactants,” *Angew. Chemie - Int. Ed.*, vol. 51, no. 10, pp. 2414–2416, 2012.

- [19] P. Brown, A. M. Khan, J. P. K. Armstrong, A. W. Perriman, C. P. Butts, and J. Eastoe, “Magnetizing DNA and proteins using responsive surfactants,” *Adv. Mater.*, vol. 24, no. 46, pp. 6244–6247, 2012.
- [20] P. Brown *et al.*, “Properties of new magnetic surfactants,” *Langmuir*, vol. 29, no. 10, pp. 3246–3251, 2013.
- [21] P. Brown, L. Bromberg, M. I. Rial-Hermida, M. Wasbrough, T. A. Hatton, and C. Alvarez-Lorenzo, “Magnetic Surfactants and Polymers with Gadolinium Counterions for Protein Separations,” *Langmuir*, vol. 32, no. 3, pp. 699–705, 2016.
- [22] L. Xu, L. Feng, S. Dong, and J. Hao, “Magnetic controlling of migration of DNA and proteins using one-step modified gold nanoparticles,” *Chem. Commun.*, vol. 51, no. 45, pp. 9257–9260, 2015.
- [23] P. Brown, C. P. Butts, J. Cheng, J. Eastoe, C. A. Russell, and G. N. Smith, “Magnetic emulsions with responsive surfactants,” *Soft Matter*, vol. 8, no. 29, pp. 7545–7546, 2012.
- [24] BBC News, “‘Magnetic emulsions’ could clean up oil spills,” 2012.
- [25] NBCNEWS, “World’s First Magnetic Soap Could Clean Sticky Messes,” 2012. .
- [26] P. Degen, E. Zwar, M. Paulus, M. Tolan, and H. Rehage, “About the role of surfactants on the magnetic control over liquid interfaces,” *Langmuir*, vol. 30, no. 39, pp. 11563–11566, 2014.
- [27] T. M. McCoy, P. Brown, J. Eastoe, and R. F. Tabor, “Noncovalent magnetic control and reversible recovery of graphene oxide using iron oxide and magnetic surfactants,” *ACS Appl. Mater. Interfaces*, vol. 7, no. 3, pp. 2124–2133, 2015.

- [28] L. Wang, Y. Wang, J. Hao, and S. Dong, “Magnetic Fullerene-DNA/Hyaluronic Acid Nanovehicles with Magnetism/Reduction Dual-Responsive Triggered Release,” *Biomacromolecules*, 2017.
- [29] S. Kim *et al.*, “Nanoparticle-free magnetic mesoporous silica with magneto-responsive surfactants,” *J. Mater. Chem. C*, vol. 1, no. 42, pp. 6930–6934, 2013.
- [30] L. Xu, S. Dong, J. Hao, J. Cui, and H. Hoffmann, “Surfactant-Modified Ultrafine Gold Nanoparticles with Magnetic Responsiveness for Reversible Convergence and Release of Biomacromolecules,” *Langmuir*, vol. 33, no. 12, pp. 3047–3055, 2017.
- [31] C. de la Fuente-Nunez, P. Brown, M. D. T. Torres, J. Cao, and T. K. Lu, “Magnetic Surfactant Ionic Liquids and Polymers With Tetrahaloferrate (III) Anions as Antimicrobial Agents With Low Cytotoxicity,” *Colloids Interface Sci. Commun.*, vol. 22, pp. 11–13, 2018.
- [32] W. Zhao, H. Sun, Y. Wang, J. Eastoe, S. Dong, and J. Hao, “Self-Assembled Magnetic Viruslike Particles for Encapsulation and Delivery of Deoxyribonucleic Acid,” *Langmuir*, vol. 34, no. 24, pp. 7171–7179, 2018.
- [33] W. Zhao, S. Dong, and J. Hao, “Colloidal Wormlike Micelles with Highly Ferromagnetic Properties,” *Langmuir*, vol. 31, no. 41, pp. 11243–11248, 2015.
- [34] P. Brown *et al.*, “Microemulsions as tunable nanomagnets,” *Soft Matter*, vol. 8, no. 46, pp. 11609–11612, 2012.
- [35] P. Brown, T. Alan Hatton, and J. Eastoe, “Magnetic surfactants,” *Curr. Opin. Colloid Interface Sci.*, vol. 20, no. 3, pp. 140–150, 2015.

- [36] L. Wang, S. Dong, and J. Hao, "Recent progress of magnetic surfactants: Self-assembly, properties and functions," *Curr. Opin. Colloid Interface Sci.*, vol. 35, pp. 81–90, 2018.
- [37] J. Le Moigne and J. Simon, "A new type of surfactants. The annelides. Characterization of organized metal ion assemblies obtained by cationic complexation at the micelle subsurface," *J. Phys. Chem.*, vol. 84, no. 2, pp. 170–177, 1980.
- [38] J. P. André, É. Tóth, H. Fischer, A. Seelig, H. R. Mäcke, and A. E. Merbach, "High relaxivity for monomeric Gd(DOTA)-based MRI contrast agents, thanks to micellar self-organization," *Chem. - A Eur. J.*, vol. 5, no. 10, pp. 2977–2983, 1999.
- [39] S. Polarz, C. Bährle, S. Landsmann, and A. Klaiber, "Panoscopic structures by hierarchical cascade self-assembly of inorganic surfactants with magnetic heads containing dysprosium ions," *Angew. Chemie - Int. Ed.*, vol. 52, no. 51, pp. 13665–13670, 2013.
- [40] S. Hermann *et al.*, "Magneto-Adaptive Surfactants Showing Anti-Curie Behavior and Tunable Surface Tension as Porogens for Mesoporous Particles with 12-Fold Symmetry," *Angew. Chemie - Int. Ed.*, vol. 129, no. 20, pp. 5567–5571, 2017.
- [41] S. Landsmann, M. Wessig, M. Schmid, H. Cölfen, and S. Polarz, "Smart inorganic surfactants: More than surface tension," *Angew. Chemie - Int. Ed.*, vol. 51, no. 24, pp. 5995–5999, 2012.
- [42] F. L. Bard AJ, *Electrochemical Methods Fundamentals and Applications*, 2nd ed. Wiley, 2001.
- [43] R. Tilley, *Understanding Solids*, 1st ed. Chichester: John Wiley & Sons Ltd, 2004.

- [44] W. Liu, B. Etschmann, J. Brugger, L. Spiccia, G. Foran, and B. McInnes, "UV-Vis spectrophotometric and XAFS studies of ferric chloride complexes in hyper-saline LiCl solutions at 25-90 °C," *Chem. Geol.*, vol. 231, no. 4, pp. 326–349, 2006.
- [45] R. F. P. Pereira, A. J. M. Valente, and H. D. Burrows, "Thermodynamic analysis of the interaction between trivalent metal ions and sodium dodecyl sulfate: An electrical conductance study," *J. Mol. Liq.*, vol. 156, no. 1, pp. 109–114, 2010.
- [46] C. M. Flynn, "Hydrolysis of Inorganic Iron(III) Salts," *Chem. Rev.*, vol. 84, no. 1, pp. 31–41, 1984.
- [47] L. Wattebled and A. Laschewsky, "New anionic gemini surfactant based on EDTA accessible by convenient synthesis," *Colloid Polym. Sci.*, vol. 285, no. 12, pp. 1387–1393, 2007.
- [48] A. A. Hafiz, "Metallosurfactants of Cu(II) and Fe(III) complexes as catalysts for the destruction of paraoxon," *J. Surfactants Deterg.*, vol. 8, no. 4, pp. 359–363, 2005.
- [49] T. Saji, K. Hoshino, and S. Aoyagui, "Reversible formation and disruption of micelles by control of the redox state of the surfactant tail group," *J. Chem. Soc. Chem. Commun.*, no. 13, pp. 865–866, 1985.



## LIST OF APPENDICES

## Appendix A

### SUPPORTING INFORMATION FOR CHAPTER III

#### A.1 STABILITY OF IONIC MAGNETIC SURFACTANTS IN AQUEOUS SOLUTIONS: MEASUREMENT TECHNIQUES AND IMPACT ON MAGNETIC PROCESSES

##### A.1.1 CMC Characterization

The following data are surface tension vs. concentration measurements of various magnetic and nonmagnetic surfactants in water. The surfactants include C<sub>16</sub>TABr, MnDDS, C<sub>16</sub>TAF<sub>3</sub>Br, C<sub>16</sub>TAG<sub>3</sub>Br and SDS. The CMC values reported in the main body of the manuscript for these compounds were obtained from the surface tension measurements discussed below.

The measurements were obtained from a Sigma 700/701 Biolin Scientific Force Tensiometer using a platinum Du Nouy ring. The Du Nouy ring was cleaned with ethanol and DI water and placed inside a flame until red hot between each measurement. Table A.1 summarizes the data from figures S1-S4.

**Table A.1: CMC values for various surfactants examined in this study**

Surfactant	CMC (mM)
C <sub>16</sub> TABr	1
MnDDS	1.4
C <sub>16</sub> TAF <sub>3</sub> Br	0.6
C <sub>16</sub> TAG <sub>3</sub> Br	0.8
SDS	8.2

C<sub>16</sub>TABr:

The CMC of  $C_{16}TABr$  was found to be 1.0 mM

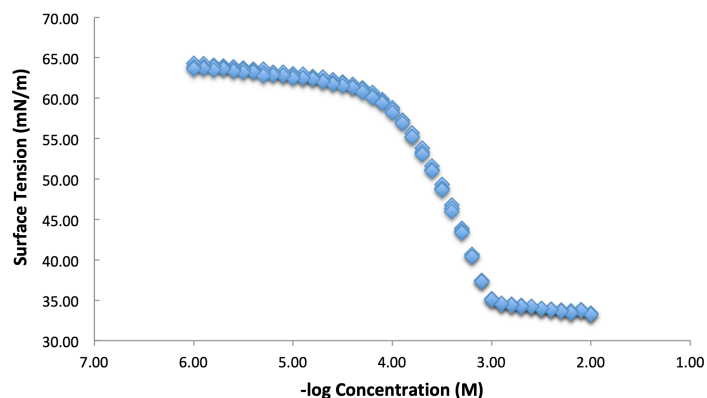


**Figure A.1:** Surface tension vs. concentration measurements of  $C_{16}TABr$  in water.

SDS:

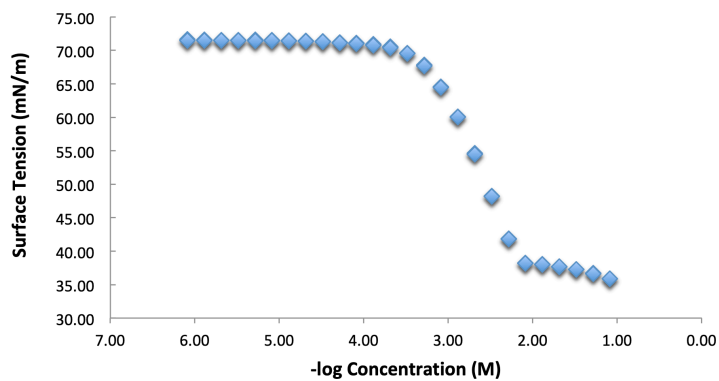


**Figure A.2:** Surface tension vs. concentration measurements of SDS in water.

MnDDS:

The CMC of this surfactant, was determined to be 1.4 mM (Figure A.3), which is in close agreement with a value found in the literature of 1.2 mM

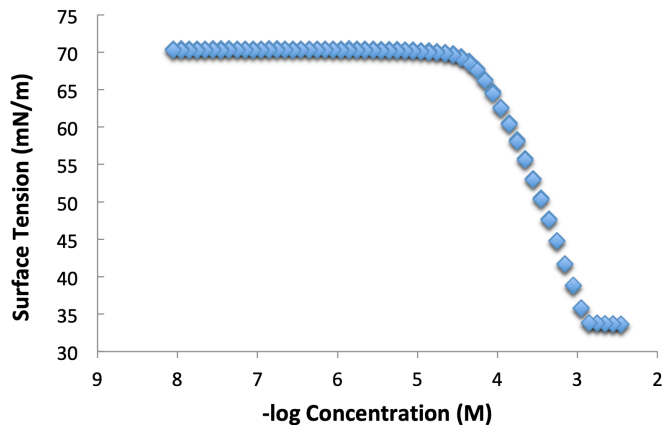


**Figure A.3:** Surface tension vs. concentration measurements of MnDDS in water.

$C_{16}TAF_{e}Cl_{3}Br$ :

The CMC of  $C_{16}TAF_{e}Cl_{3}Br$  was found to be 0.6 mM.

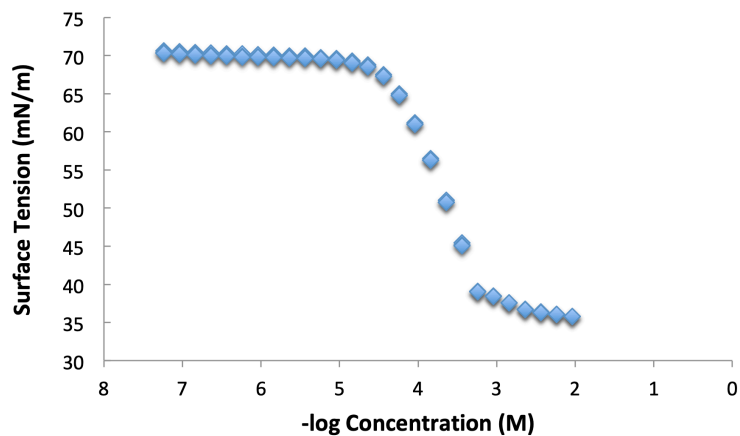


**Figure A.4:** Surface tension vs. concentration measurements of  $C_{16}TAF_{e}Cl_{3}Br$  in water.

$C_{16}TAGdCl_{3}Br$ :

The CMC of  $C_{16}TAGdCl_{3}Br$  was investigated and found to be 0.8 mM

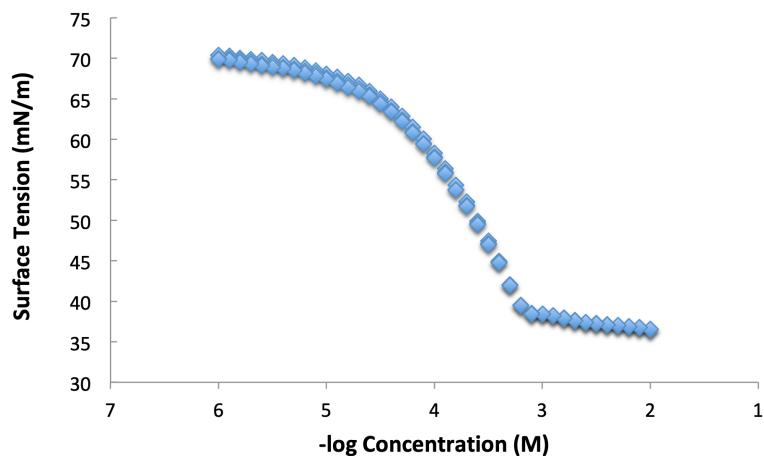


**Figure A.5:** Surface tension vs. concentration measurements of  $C_{16}TAGdCl_3Br$  in water.

### A.1.2 Specific Conductivity Vs. Concentration

This data provides CMC information for MnDDS and  $C_{16}TABr$  for comparison to the CMC data obtained from surface tension measurements. The CMC was taken to be the point in the graph that experienced the greatest change in slope with increasing surfactant concentration. As shown below, this data is in agreement with the surface tension data.

MnDDS:

The CMC was found to be approx. 1.4 mM, which is in agreement with the surface tension measurements of Figure A.6.

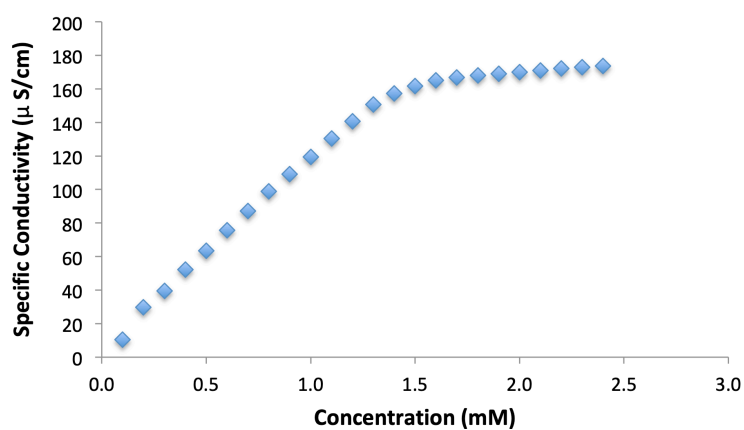


**Figure A.6:** Specific conductivity vs. concentration for MnDDS in water

**C<sub>16</sub>TABr:**

The CMC was found to be approx. 1.0 mM, which is in agreement with the surface tension measurements of Figure A.7.

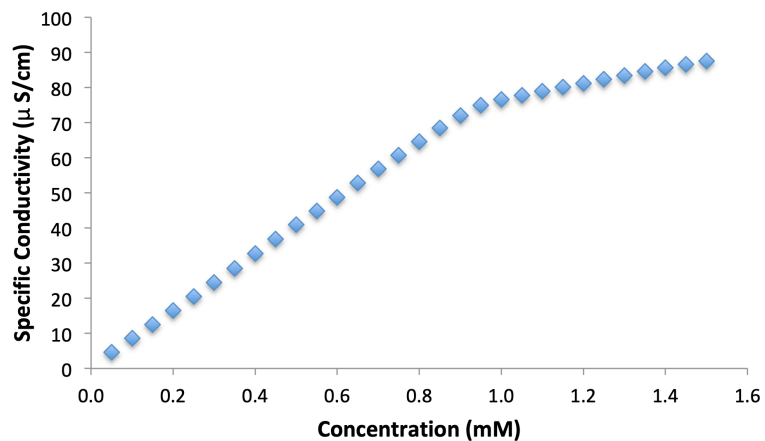


**Figure A.7:** Specific Conductivity vs. concentration for C<sub>16</sub>TABr in water

## Appendix B

### B.1 ORGANIC CONTAMINANT RELATIVE CONCENTRATION CALCULATION

The following are the calculations for the relative concentration of toluene in a saturated magnet and a saturated nonmagnet sample of MagPolySurfA. The instrumentation error provided by the manufacturer is  $0.5 \text{ A} \pm 0.004$ ,  $1.0 \text{ A} \pm 0.006$  and  $2.0 \pm 0.01$ . The following formula was used to calculate the relative concentration of toluene in the samples:

$$(M_1 - NM_1) - Y(M_2 - NM_2) = Z$$

As can be seen in Figure AB.1, which are UV-Vis scans of magnet and nonmagnet MagPolySurfA samples in water saturated with toluene,  $M_1$  and  $M_2$  are the maximum absorbance of toluene and are found at 260 nm. These absorbance values are  $1.276 \pm 0.0071$  and  $0.673 \pm 0.0047$  respectively.  $NM_1$  and  $NM_2$  are the absorbance values of the polymer baseline region and were selected to be at at 310 nm. These absorbance values are  $1.264 \pm 0.0071$  and  $0.672 \pm 0.0047$  respectively.  $Y$  is 0.625 and is found from Figure AB.2, which is a solution of MagPolySurfA in water with no organic contaminant, and is calculated by dividing the absorbance of the polymer at 260 nm (0.471) by the absorbance of the polymer at 310 nm (0.754). Thus,  $Z$  is found to be  $0.0114 \pm 0.0235$ . Since it is inconclusive whether  $Z$  is positive or negative, the results are inconclusive whether there is more or less toluene in the magnet sample.

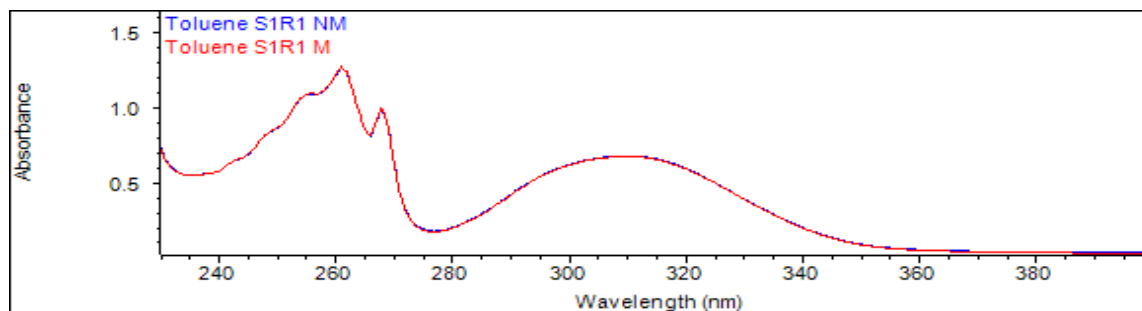


**Figure B.1.** The UV-Vis absorbance spectrum of MagPolySurfA saturated with toluene in water. The red line represents a solution left inside of a parallel magnetic field and the blue line represents a solution left outside of a magnetic field.

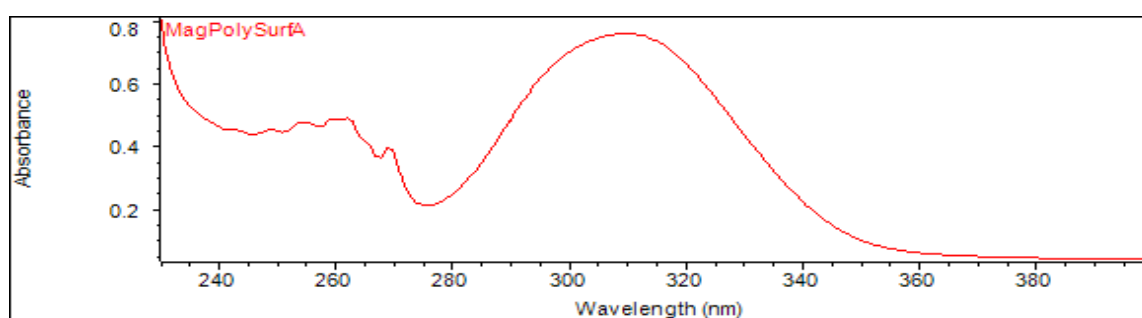


**Figure B.2.** The UV-Vis absorbance spectrum of pure MagPolySurfA in water with no organic contaminant present.



## B.2 UV-VIS Absorbance Spectrums for Other Solubilization Experiments

Note on the terminology: that S1 represents “solution 1” and R1 represents “run 1” etc. Some of the absorbance spectrums are missing, so only the available ones are being shown.

### MagPolySurfA:

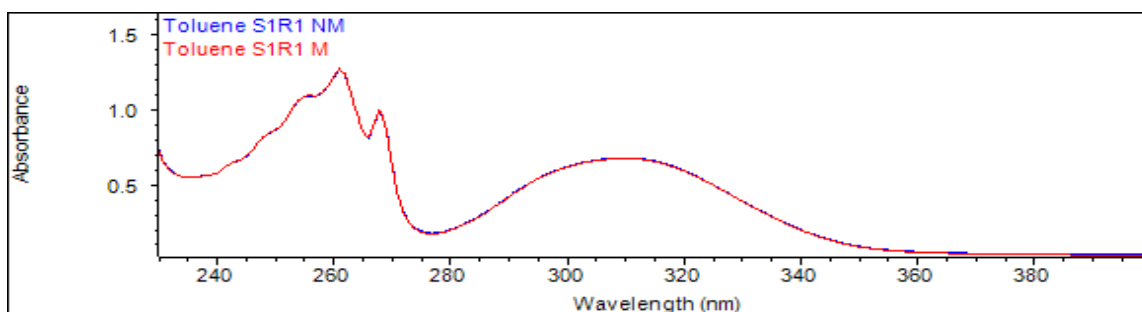


Figure B.3 MagPolySurfA S1R1 saturated with toluene

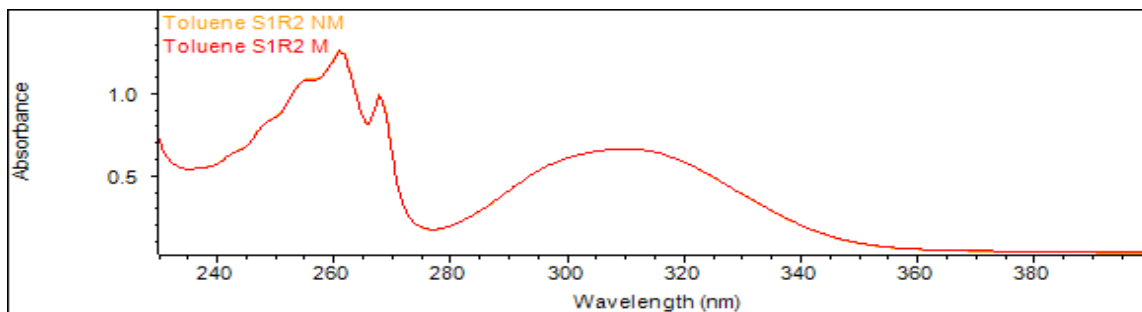


Figure B.4 MagPolySurfA S1R2 saturated with toluene

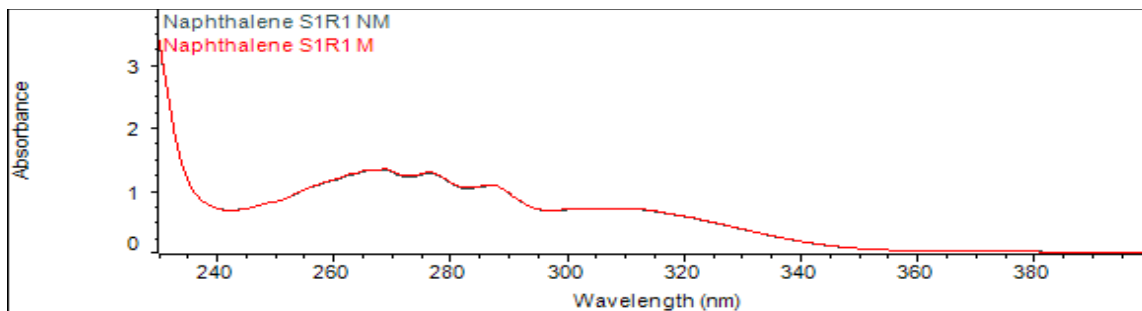
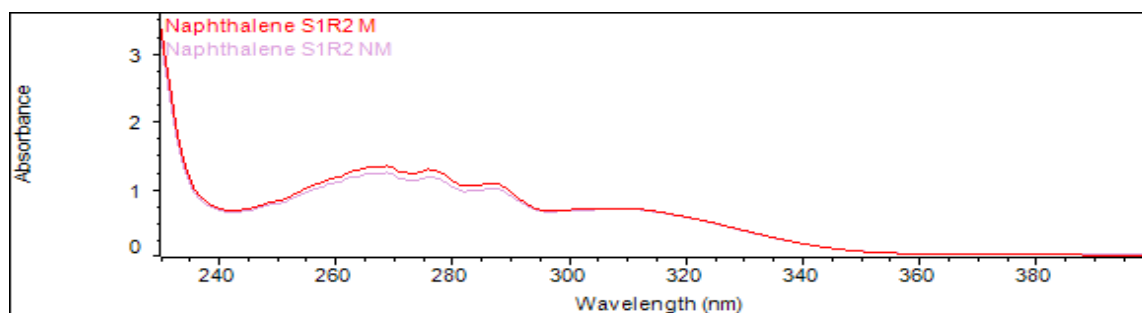
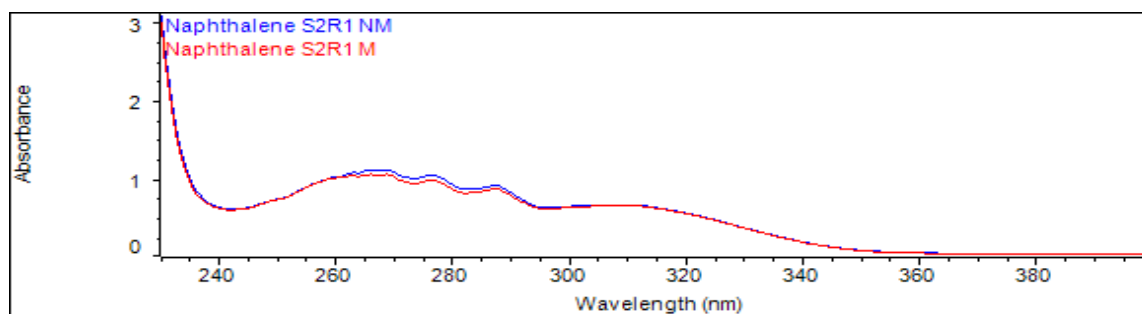


Figure B.5 MagPolySurfA S1R1 saturated with naphthalene



**Figure B.6** MagPolySurfA S1R2 saturated with naphthalene



**Figure B.7** MagPolySurfA S2R1 saturated with naphthalene

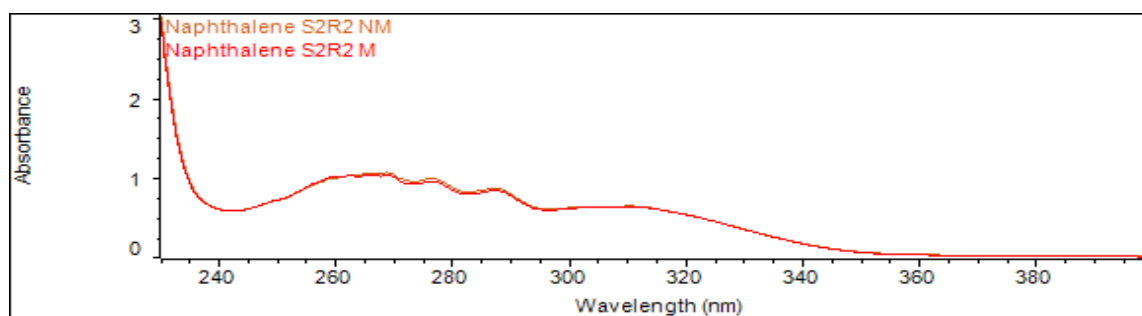


**Figure B.8** MagPolySurfA S2R2 saturated with naphthalene

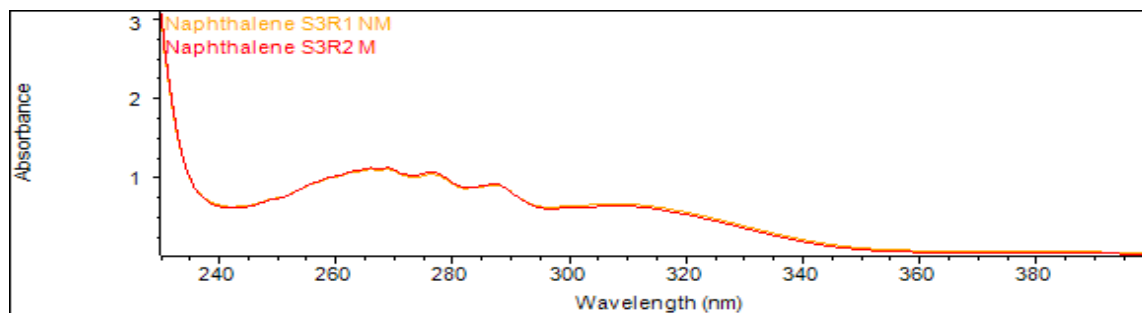


**Figure B.9** MagPolySurfA S3R1 saturated with naphthalene

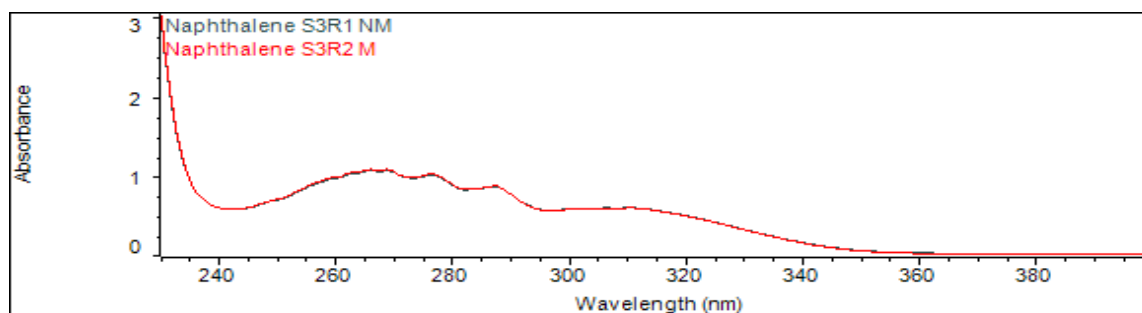


**Figure B.10** MagPolySurfA S3R1 saturated with naphthalene

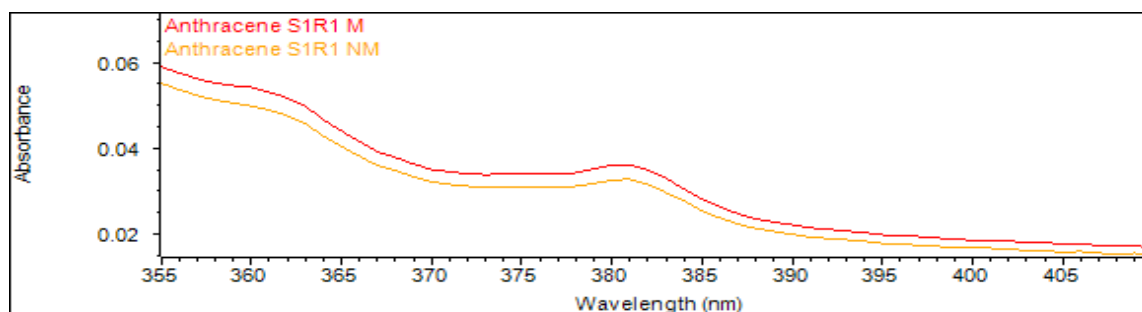


**Figure B.11** MagPolySurfA S1R1 saturated with anthracene

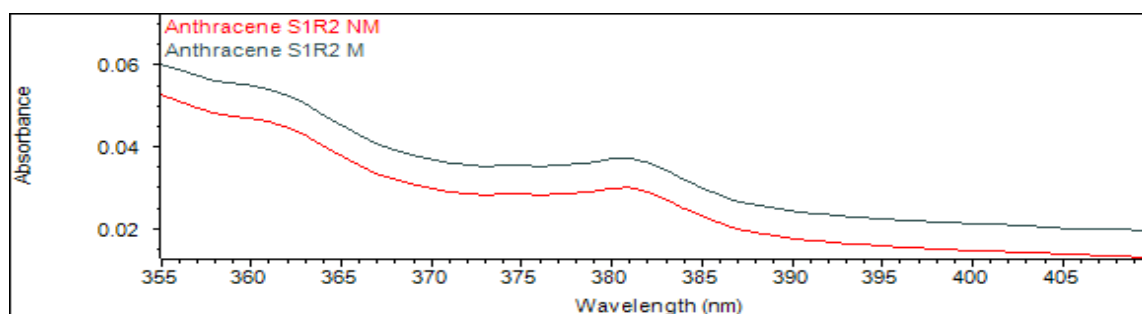


**Figure B.12** MagPolySurfA S1R2 saturated with anthracene

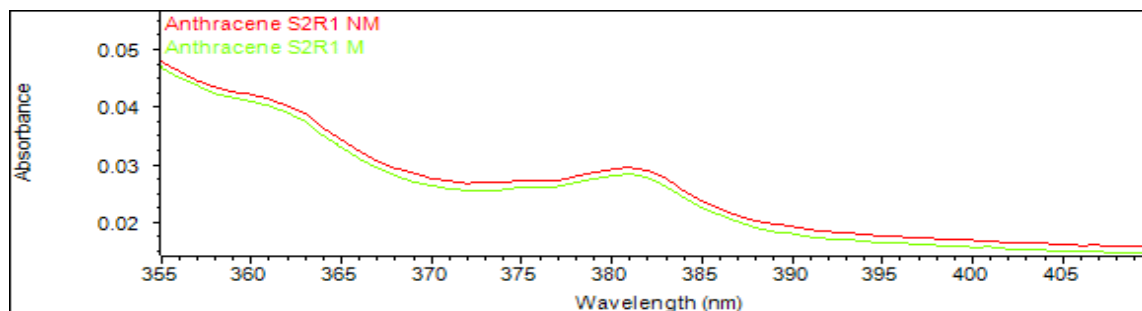


**Figure B.13** MagPolySurfA S2R1 saturated with anthracene

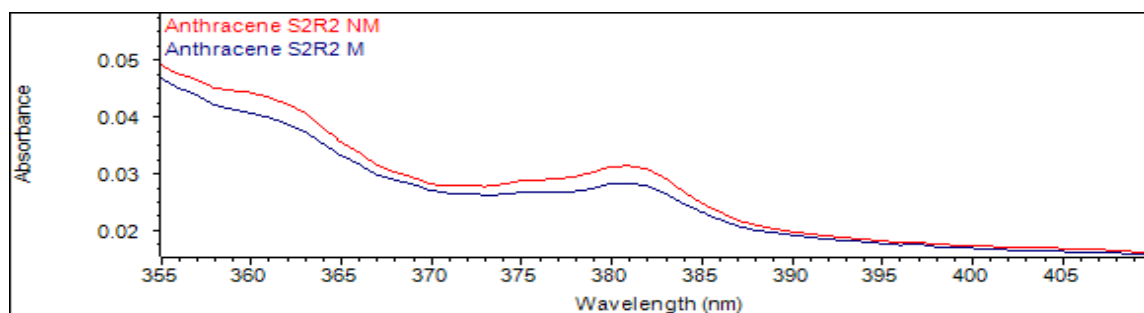


Figure B.14 MagPolySurfA S2R2 saturated with anthracene

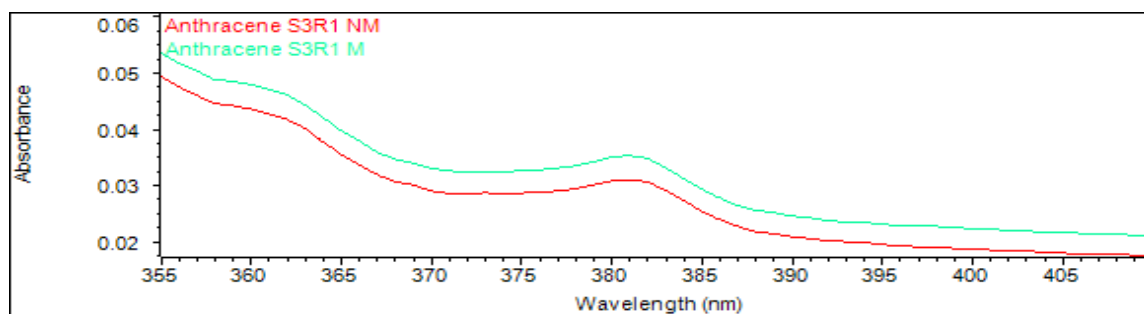


Figure B.15 MagPolySurfA S3R1 saturated with anthracene

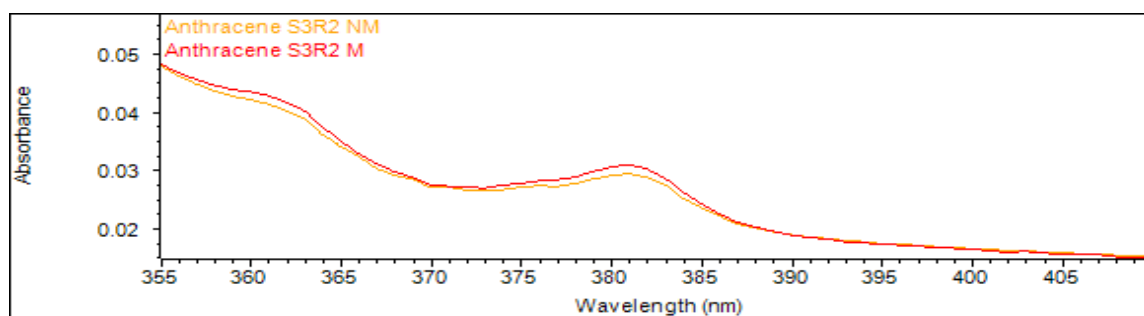


Figure B.16 MagPolySurfA S3R2 saturated with anthracene

### MagPolySurfB:

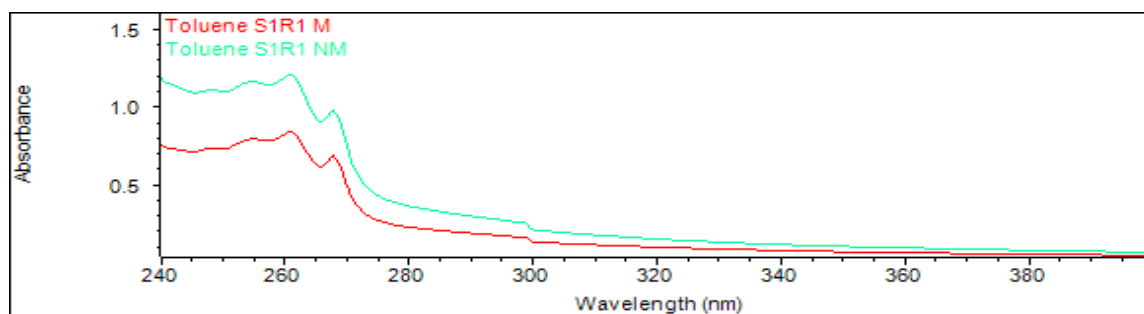
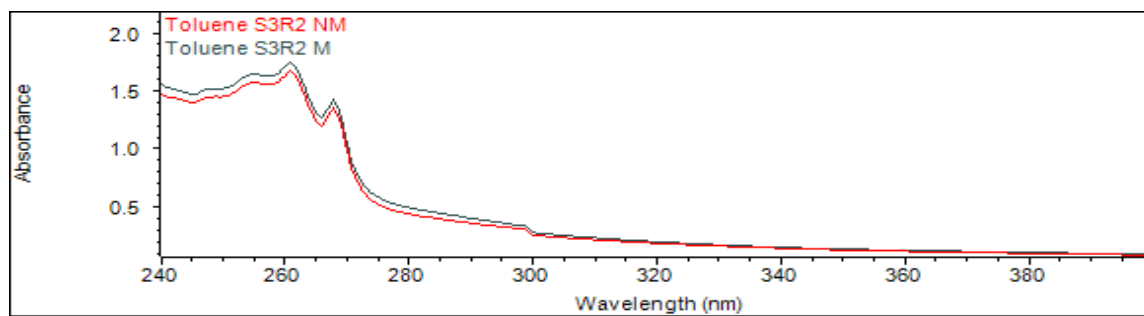
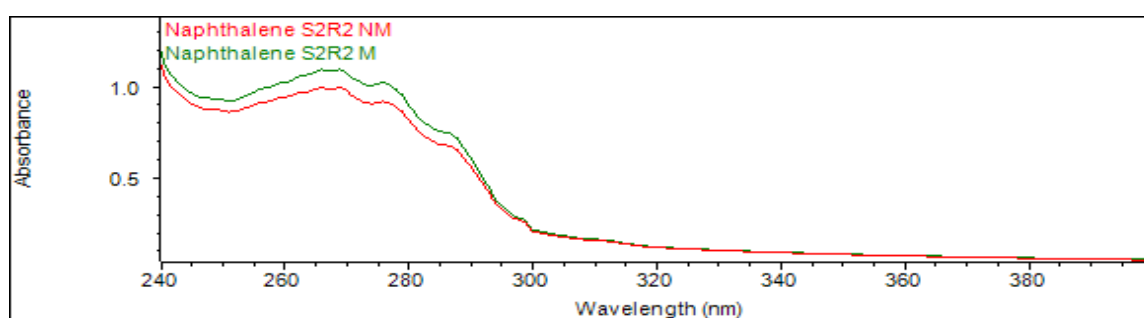


Figure B.17 MagPolySurfB S1R1 saturated with toluene



**Figure B.18** MagPolySurfB S3R2 saturated with toluene



**Figure B.19** MagPolySurfB S2R2 saturated with naphthalene

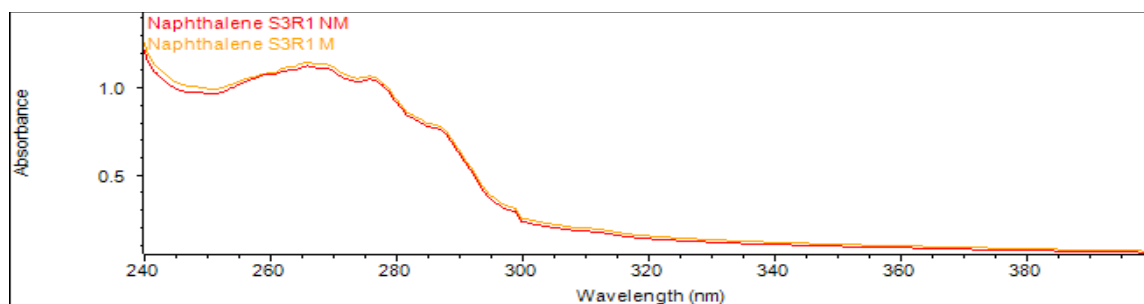


**Figure B.20** MagPolySurfB S3R1 saturated with naphthalene

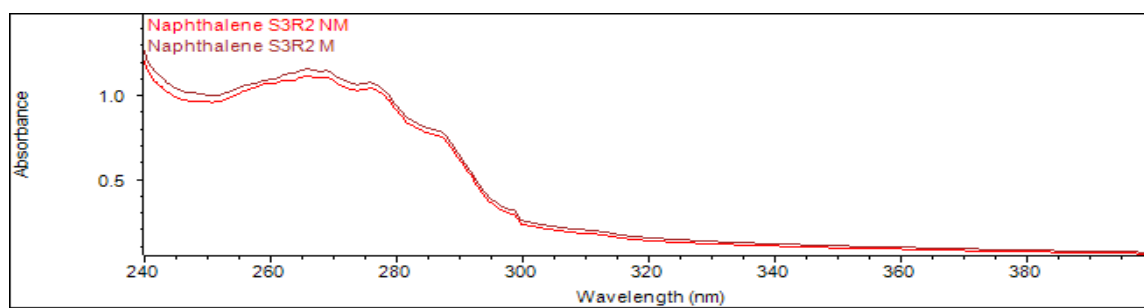


**Figure B.21** MagPolySurfB S3R2 saturated with naphthalene

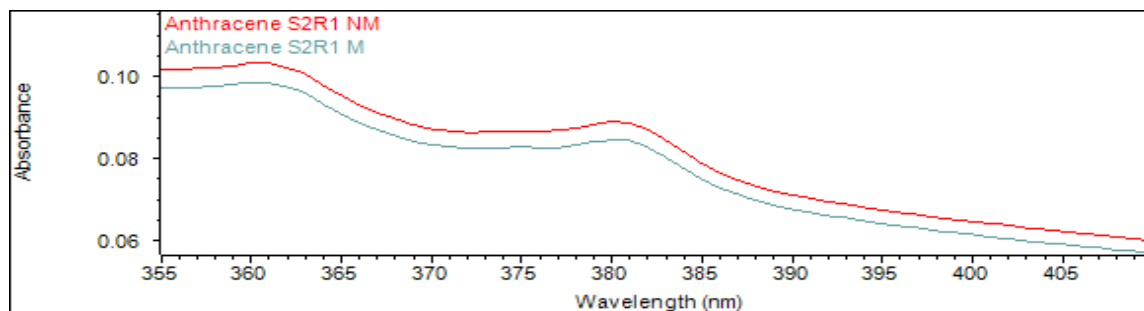


**Figure B.22** MagPolySurfB S2R1 saturated with anthracene

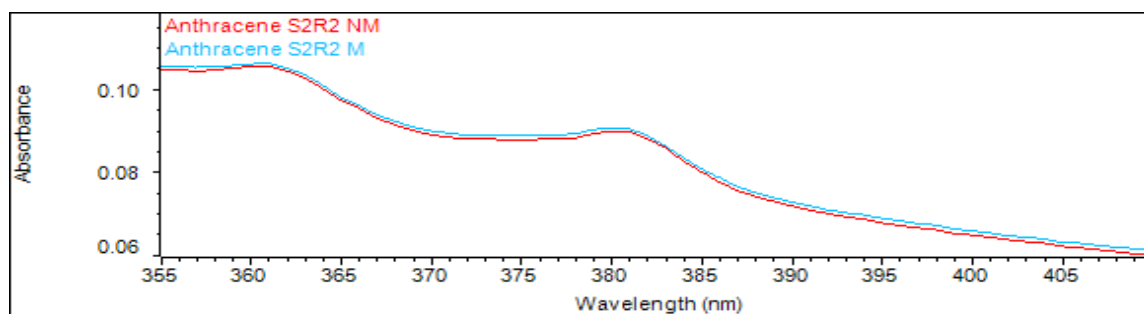


**Figure B.23** MagPolySurfB S2R2 saturated with anthracene

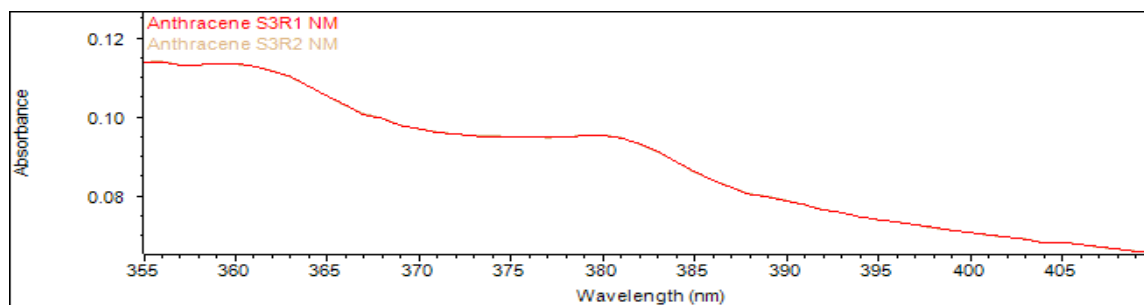


**Figure B.24** MagPolySurfB S3R1 saturated with anthracene

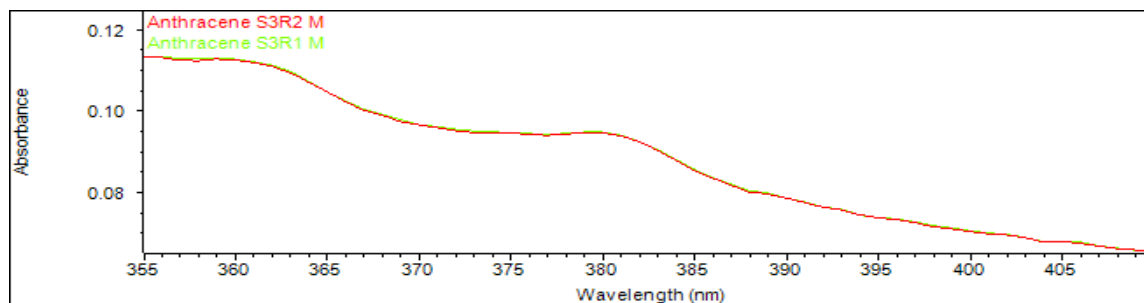


**Figure B.25** MagPolySurfB S3R2 saturated with anthracene

## APPENDIX C

### C.1 SOP For the Light Scattering Instrument

NOTE: The following information assumes that the reader has read the 3D LS Spectrometer Users' Manual in addition to the helpful information found on the LSI website detailing how to prepare samples and operate the 3D LS Spectrometer.

The following describes the sample preparation procedure for the light scattering instrument. This procedure needs to be performed under a clean fume hood. Make several samples over a concentration range. You want to use a sample that is dilute as possible without losing a detection signal. For polymer samples for example, make samples that are 1, 0.5, 0.1 and 0.05 mg/ml.

1. Obtain a cuvette
2. Rinse the cuvette with pure filtered water. Use a 0.1 micrometer syringe filter if possible.
3. Repeat step 2 approx. 4 more times
4. Rinse the cuvette with pure filtered acetone. Use a 0.1 micrometer syringe filter if possible.
5. Repeat step 4 approx. 2 more times.
6. Hang the cuvette upside down inside the fume hood and let the acetone evaporate.
7. Add your colloidal sample to the vial by pushing it through a syringe filter.
8. Cap the cuvette with parafilm (assuming your solvent is not toluene or something that will dissolve parafilm)
9. Insert a cap into the cuvette to seal the solution tightly.

The following describes a step-by-step procedure for performing dynamic light scattering on a colloidal sample. Run each of your samples following a similar script starting with the most concentrated and working your way down to the most dilute. When the particle sizes stop changing with each dilution, you have found the ideal concentration to analyze.

**RULE # 1 OF THE LIGHT SCATTERING INSTRUMENT- THE WORKING AREA OF THE LIGHT SCATTERING INSTRUMENT SHOULD BE KEPT CLEAN AND OBSTRUCTION FREE SO THE GONIATOR ARM DOES NOT BECOME DAMAGED.**

1. Turn on the 3D LS Spectrometer
2. Turn on the Water Bath
3. Pull the LS Program up on the computer and set the temperature if you are operating above 25°C.
4. Wait for the temperature to come to equilibrium.
5. Click “Change Sample” on the Settings tab. A box will pop up. Do not click exit on this box until you have inserted the sample into the instrument.
6. Insert your sample into the instrument. Then exit out of the pop up box.
7. Let your sample come to thermal equilibrium by waiting approx. 10 minutes.
8. Setup an appropriate script. My favorite is to setup a script with a starting angle of 40 degrees and ending at an angle of 140 degrees with a step size of 50 degrees. Select a measurement time of 60-120 seconds. Select an appropriate location to save this file.
9. Set the Scattering intensity manually to 200-400 kHz (this is the ideal range).
10. Select the appropriate solvent. (Water is usually set as the default)
11. Set the scattering geometry to 3D. Set the correlation type to Mod3D, unless your particles are smaller than 20 nm. For small particles (less than 20 nm), select 3D Cross.
12. Go to the measurement tab and click “Start Script”
13. When the script is finished running. Look at the change in intensity with angle under the angle plots tab. If it decreases, this means your samples are either polydisperse or contain different size plots.
14. Set the boundaries on the normalized autocorrelation function vs. lag time plot (see a picture in the user manual for where to place the red line) The decay factor should be set to 0.6 to 0.8 by moving the blue line.
15. Click on perform Contin Analysis.
16. Look at the contin analysis plot. If you see multiple peaks, your have particles consisting of different size plots. If you see only one peak, you have particles consisting of only one size plot, which may be polydisperse or monodisperse.



17. If you detected only one size plot in the Contin Analysis, your particle radius will be the 2<sup>nd</sup> order radius under the “Cumulant Analysis”. (Note: if your normalized autocorrelation function vs. lag time plot looks noisy, use the 3<sup>rd</sup> order radius instead of the 2<sup>nd</sup>.)
18. If you detected multiple size plots in the Contin Analysis, your particles radii are listed in the Contin Analysis table. Note: when possible, rely on the Cumulant Analysis results. (Read the LSI Instruments website for more details on Contin vs. Cumulant Analysis.)

## C.2 SOP For the operating the Tensiometer

For determining the cmc of a surfactant by using the tensiometer, you should formulate a surfactant sample with a volume of at least 30 ml and a concentration approx. 10x above the cmc. Before you begin an experiment, the source jug should be filled completely with DI water, and the waste jug should be empty.

1. Obtain a Du Noy ring. Rinse it thoroughly by gently dunking it into solutions of ethanol and DI Water. Then place it in a flame until red hot. Note: Do not leave it in the flame longer than a few seconds.
2. Place the ring on the tensiometer by hanging it on the hook.
3. Obtain a 70 mm glass dish, a small stir bar and the metal tubes screwed on to the end of the pump lines. Rinse these items thoroughly with ethanol and DI water
4. Place the metal tubes back onto the pump lines and turn on the equipment.
5. Add your solution to the dish and place the dish inside the tensiometer.
6. Pull up the OneAttension program.
7. Select the CMC with ring option.
8. Name the experiment
9. Input the volume of your sample (it must be at least 30 ml)
10. For the Addition option, click the + sign to the left and input the initial concentration of your sample in the “initial concentration” box. For the “Concentration” box, it should be “0.0” if you are diluting your sample with water. Select the appropriate units of the concentration (mg/ml, mol/L etc.)
11. Under the “CMC Parameters” tab, input the concentration of your solution under “Start Conc.”
12. Select the “End Conc.” as the final concentration that you want the solution to be diluted to. (I usually select  $1 \times 10^{-7}$  mol/L)
13. Change the points/ decade to the desired # of data points you want the tensiometer to record. (I usually select 5 or 10.)
14. Change the “Wait after Stir” to 60 seconds.
15. Select the “Use two Dispensers” option.

16. Click the “play button” to start the experiment. (This is the button near the bottom right of the screen with a triangle on it)

### C.3 SOP for the UV-VIS Spectrophotometer

The following contains instructions for performing scans on the UV-VIS spectrophotometer.

1. Turn on the UV-VIS and pull up the UV-VIS program on the computer.
2. Obtain a cuvette.
3. Fill the cuvette at least  $2/3$  of the way full with pure solvent.
4. Select the “Scan” option.
5. Place the cuvette inside of the instrument.
6. Go to the “settings tab” and input the number of samples you wish to run and name them.
7. Select an appropriate scan rate.
8. Select the starting and ending wavelength.
9. Click the “Play” button on the top left corner of the screen. The program will prompt you to run the “blank sample”- this is the pure solvent sample. Click “ok”.
10. When the blank sample has run, the program will prompt you to run an actual sample. Place your sample into the instrument and click “ok”. If you have more samples to run, the program will prompt you to run them in the order you input them into the program.
11. When you are done running your samples, save your results.

## VITA

### Alex Fortenberry

---

<b>Research Interests</b>	Polymeric materials, surfactants, metal/organic hybrid compounds and magnetically responsive materials.	
---------------------------	---	--

---

<b>Education</b>	<b>Master of Science in Engineering Science</b> August 2019 The University of Mississippi, Oxford MS Advisor: Dr. Adam Smith Overall GPA: 3.44
	<b>Bachelor of Science in Chemical Engineering</b> May 2017 The University of Mississippi, Oxford MS Overall GPA: 2.99

---

<b>Research Experience</b>	<b>Graduate Research Assistant</b> May 2017- Present <i>The University of Mississippi, Oxford MS</i>
	<ul style="list-style-type: none"><li>• Performed research under Dr. Adam Smith and Dr. Paul Scovazzo on designing water-stable magnetic single molecule surfactants and magnetic polymeric surfactants, then applying these materials to low energy oil/water separations processes.</li><li>• Gained valuable research experience designing and implementing experiments to synthesize and/or characterize various compounds, as well as to measure their stability in aqueous solution.</li><li>• Gained valuable laboratory skills by being trained in various experimental techniques such as: gel permeation chromatography, dynamic and static light scattering, potentiometry, tensiometry and conductometry.</li></ul>

---

<b>Teaching Assistant</b>	<b>Graduate Student</b> Fall 2017 <i>The University of Mississippi, Oxford MS</i>
	<ul style="list-style-type: none"><li>• Graded student homework assignments for Ch E 451</li></ul>

---

<b>Presentations</b>	<u>Fortenberry, A</u> ; Reed D, Smith, A.E.; Scovazzo, P “Quantifying the Stability of Magnetic Surfactants in Aqueous Solution”, American Institute of Chemical Engineers Annual Meeting, Pittsburgh Pennsylvania, October 29, 2018.
	Reed, D; <u>Fortenberry, A</u> ; Smith, A.E.; Scovazzo, P “Magnetic Surfactant Surface Tension Functionality vs. Magnetic Field Gradient”, American Institute of Chemical Engineers Annual Meeting, Pittsburgh Pennsylvania, October 29, 2018.

---

---

**Publications**

Fortenberry, A; Reed D, Smith, A.E.; Scovazzo, P “Stability of Ionic Magnetic Surfactants in Aqueous Solutions: Measurement Techniques and Impact on Magnetic Processes” *Manuscript in Preparation*

Reed, D; Fortenberry, A; Smith, A.E.; Scovazzo, P “ Magnetic Surfactant Surface Tension Functionality vs. Magnetic Field Gradient” *Manuscript in Preparation*

Chandrasiri, I; Abebe, D.; Sudipta G.; Williams, J.; Rieger, W; Simms, B.; Yaddehige, M.; Noh, Y.; Payne, M.; Fortenberry, A.; Smith, A.E.; Lee, B.; Grayson, S.; Schneider, G.; Watkins, D. L. “Synthesis and Characterization of Polylactide PAMAM “Janus-type” Linear- Dendritic Hybrids” *Journal of Polymer Science Part A: Polymer Chemistry* (2019), 57(13), 1448-1459